Politecnico di Torino

Politecnico di Torino

Corso di Laurea in Ingegneria Matematica

A.a. 2025/2026

Sessione di Laurea Marzo 2026

Analysis of a Network SIRS Epidemic Model

Relatori:

Giacomo Como

Candidati:

Giulia Gatti

Ad una vita normale.

Abstract

The need to describe the dynamics of infectious diseases has motivated the development of mathematical epidemic models. These compartmental models have been extensively studied due to their applications beyond epidemiology. The deterministic SIRS model framework is particularly suited for diseases that allow temporary immunity and its scalar formulation has been deeply investigated. The introduction of network structure on these classical models has provided a way to avoid the assumption of homogeneity, since real-world contacts within populations are quite often highly heterogeneous. In this thesis, we present an SIRS model on a finite, strongly connected network, and we investigate its dynamic behavior. In the scalar case, the model exhibits a transcritical bifurcation when the infection rate exceeds the recovery rate and a stable endemic equilibrium emerges. In the network SIRS model, the epidemic threshold is given by the dominant eigenvalue of the interaction matrix scaled by the recovery rate. We prove the existence and uniqueness of an endemic equilibrium over the threshold, by means of fixed point theory. Moreover, we establish the global asymptotic stability of the disease-free equilibrium below the threshold. For the endemic equilibrium, we derive, through algebraic properties of the Schur complement, a negative upper bound for the real parts of the eigenvalues of the linearized system. This gives us the local asymptotic stability of the endemic equilibrium point above the threshold and provides an estimate of the convergence rate. Two particular network structures are further examined: the out-regular graph and the rank-1 interaction matrix. In the first case the endemic equilibrium can be computed explicitly, while in the latter the matrix structure allows to investigate the region of attraction of this nonzero equilibrium. Finally, we present some numerical results which confirm the theoretical ones and allow us to make conjectures over some open questions.

Acknowledgements

This thesis marks the end of an important chapter of my life, and I would like to take a moment to express my gratitude to the people who supported me along the way.

I would like to express my sincere gratitude to Professor Como for guiding me throughout this work and for constantly encouraging me to ask questions, think critically, and look deeper into the problems I encountered during the development of this thesis.

I am deeply grateful to my family for supporting me throughout all the years of my university journey and for standing by my side, especially during this last year. I know this month is not an easy one for you, but I am glad to reach this milestone now, hoping in some way to rewrite March 2025 with March 2026.

I would also like to thank my boyfriend, who has supported me during these past months and who always managed to calm me down whenever my thoughts started to run too fast.

Finally, I want to thank my friends, the lifelong ones, the poli ones and the circus ones, who know both my weaknesses and my strengths and never turn their backs on me.

This achievement is also theirs.

Table of Contents

List of Figures

Chapter 1

Introduction

Mathematical modeling has long played a central role in the study of infectious disease dynamics. By providing a simplified yet insightful representation of how diseases spread within a population, epidemic models support both theoretical understanding and practical decision-making in public health. Deterministic epidemic models describe the temporal evolution of disease transmission through systems of ordinary differential equations. These models assume that the population is sufficiently large so that stochastic fluctuations can be neglected, and that the dynamics of the epidemic are governed by average rates of interaction and transition between disease states. Despite their simplifying assumptions, deterministic models have proven remarkably effective in capturing key qualitative and quantitative features of real epidemics.

In these models, the total population is divided into a finite number of epidemiological compartments: susceptible (S), infected (I) and recovered (R). Each compartment represents a distinct disease status, and individuals move between compartments according to prescribed transition rates that encode the underlying biological mechanisms of the infection. Owing to their compartmental nature, these models can be conveniently represented by simple flow diagrams, which provide an intuitive description of the disease dynamics. Some well-known deterministic epidemic models, which will be examined in this thesis, are the SI, SIS, SIR, and SIRS. In all these models, susceptible individuals become infected through effective contact with infectious individuals, occurring at an infection rate β. In models that allow recovery, infectious individuals leave the infected compartment

at a recovery rate γ. In the SIRS model, immunity is not permanent, and recovered individuals return to the susceptible compartment at a rate δ. Each compartmental diagram uniquely defines a system of ordinary differential equations describing the temporal evolution of the population fractions in each compartment. The diagrams presented in Figures 1.1 to 1.4 therefore serve as a graphical representation of the mathematical models analyzed in the remainder of this thesis.

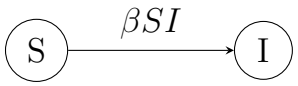

Figure 1.1: Compartmental diagram of the SI model

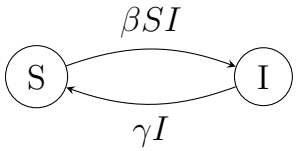

Figure 1.2: Compartmental diagram of the SIS model

Beyond their descriptive power, deterministic epidemic models provide a rigorous mathematical framework for analyzing fundamental concepts such as equilibrium points, stability, threshold conditions, and the basic reproduction number R_0. These analytical tools enable researchers to assess the potential for disease outbreaks, predict long-term behavior, and evaluate the impact of intervention strategies such as vaccination or social distancing.

While classical compartmental models assume homogeneous mixing within the population, real-world contact patterns are often highly heterogeneous and structured. Individuals typically interact through complex networks of social, spatial, or technological connections, which can strongly influence the spread of infectious diseases. Network-based epidemic models provide a natural framework to account for such heterogeneity, allowing the underlying contact structure to be explicitly incorporated into the dynamics. Motivated by these considerations, this thesis investigates epidemic dynamics on networks, with a particular focus on the SIRS model. The results presented in the following chapters aim to highlight how network structure affects the qualitative and quantitative behavior of epidemic processes, extending the classical mean-field description provided by deterministic compartmental

models.

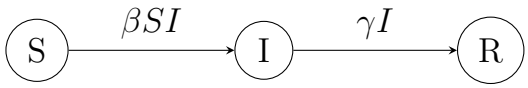

Figure 1.3: Compartmental diagram of the SIR model

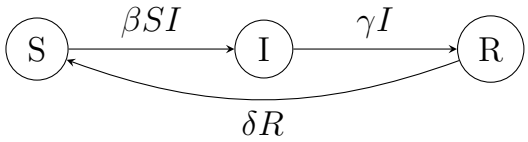

Figure 1.4: Compartmental diagram of the SIRS model

1.1 Some literature

Since the dawn of human civilization, epidemic outbreaks have posed existential threats to societies, prompting both empirical inquiry and theoretical reflection. In parallel with the maturation of calculus and probability theory, mathematicians and epidemiologists began to formalize the spread of infectious diseases. The earliest model can be found in the work of Daniel Bernoulli (1760) [1] on smallpox, where he built a differential equation model to assess the benefits of variolation, anticipating modern concepts of immunization and prevention. In the nineteenth century, William Farr and John Snow [2][3] advanced statistical and spatial analyses of cholera, marking an important step toward a quantitative understanding of epidemic dynamics.

The beginning of the twentieth century marks the birth of scalar epidemic models, that is, compartmental models describing population in aggregate form. In these models, the population is divided into distinct compartments according to disease status: susceptible (S), infected (I) and recovered (R). The interactions among these compartments are expressed through systems of ordinary differential equations that capture the temporal evolution of infection spread.

William Heaton Hamer (1906) [4] was among the first to introduce the so-called *law of mass action*, according to which the rate of new infections is proportional to the product of the numbers of susceptible and infected individuals. Shortly thereafter, Ronald Ross (1911) [5] applied a similar

approach to malaria, formulating the first models for vector-borne diseases and introducing the idea of an epidemic threshold.

The true theoretical foundation of compartmental epidemic modeling was established by William Ogivly Kermack and Anderson Gray McKendrick, who between 1927 and 1933 published their seminal trilogy "A contribution to the Mathematical Theory of Epidemics"[6][7][8]. In these works, they formalized the classical Susceptible-Infected-Recovered model (SIR), providing a mathematical framework for the temporal dynamics of an epidemic and demonstrating how it ceases once the susceptible fraction falls below a critical threshold. The susceptible-infected-recovered model, extensively studied and applied in epidemiology [9],[10], [11], is suitable for infections that provide long-lasting immunity, such as measles or smallpox, and it is described by the following differential equations

$$\begin{cases} \dot{S}(t) = -\beta S(t)I(t) \\ \dot{I}(t) = \beta S(t)I(t) - \gamma I(t) \\ \dot{R}(t) = \gamma I(t) \end{cases} \tag{1.1}$$

For diseases that do not confer lasting immunity and therefore allow for repeated infections, such as gonorrhea and other sexually transmitted infections, the Susceptible–Infected–Susceptible (SIS) model is more appropriate. This modeling framework has been widely studied in the epidemiological literature, particularly in the context of sexually transmitted diseases [12],[13],[14]. In the SIS model, individuals who recover from infection immediately return to the susceptible class, as no immunity is acquired. The population is therefore divided into two compartments only, and the epidemic dynamics are described by the following system of differential equations:

$$\begin{cases} \dot{S}(t) = -\beta S(t)I(t) + \gamma I(t) \\ \dot{I}(t) = \beta S(t)I(t) - \gamma I(t) \end{cases} \tag{1.2}$$

In both these models (1.1),(1.2) the parameters β and γ correspond to the infection and the recovery rate, respectively.

In the 1950s, George Macdonald [15] extended Ross's ideas to vector-host dynamics, laying the foundation of the *Ross–Macdonald model* and

the modern concept of the *basic reproduction number* R_0. Since then, the definition, interpretation, and mathematical properties of R_0 have been extensively investigated in the epidemiological and mathematical biology literature [16],[11],[17],[18],[19],[20],[21],[22].

Classical compartmental epidemic models are based on the assumption of homogeneous mixing, which often fails to represent the heterogeneous contact patterns observed in real populations. Graph theory provides a natural mathematical framework for describing such structured interactions [23],[24]. By representing individuals as nodes and contacts as edges, network-based epidemic models incorporate heterogeneity, clustering, and correlations in contact patterns, leading to a more realistic description of disease transmission and finding widespread application in the study of infectious diseases [25],[26].

More recent contributions, including the reviews by Brauer [27] and Zino and Cao [28], provide a comprehensive overview of the evolution from classical scalar compartmental models to multilayer and network-based approaches. These developments highlight how the scalar compartmental formulation continues to serve as a fundamental framework for analyzing, predicting, and controlling epidemic phenomena.

A first work on the network SIS model was conducted by Lajmanovich ans Yorke in [29], who derived a gonorrhea model for n homogeneous groups as follows

$$\dot{I}_i(t) = \sum_j \beta_{ij} I_i(t)(1 - I_i(t)) - \gamma_i I_i(t) \quad i \in \{1, ..., n\} \tag{1.3}$$

where β_{ij} represents the contact rate of the i-th group's susceptible with the j-th group's infective and γ_i the recovery rate of the i-th group. They used Perron-Frobenius theory about nonnegative and irreducible matrices [30, 31, 32, 33] in order to define a threshold for the existence and stability of the equilibrium point, using La Salle principle [34]. Following the seminal work of Lajmanovich and Yorke [29], several extensions of the multigroup SIS model have been proposed to account for more realistic features of disease dynamics. Aronsson [35] introduced seasonal variations in contact rates to capture periodic fluctuations in transmission. Nallaswamy [36] incorporated spatial diffusion and analyzed the resulting stability properties. Thieme [37] considered short periods of incubation and temporary immunity, providing a more detailed temporal structure of the infection process. Hethcote [38] explored the impact of control interventions on epidemic outcomes, while

Cooke [39] included asymptomatic carriers to better represent undetected transmission. Heterogeneity in transmission was systematically studied by Nold [40], while Lyapunov-based methods for global stability analysis were developed in [41, 42]. Later work extended the SIS framework to complex networks, including higher-order and simplicial interactions [43], coupled epidemic-opinion dynamics [44], awareness-based spreading [45], and competing (bi-virus) epidemics [46, 47]. Analytical approaches for networked epidemics over directed and weighted graphs, using positive systems and Lyapunov techniques, were introduced in [48, 49]. These developments illustrate the evolution from the original scalar and multigroup SIS models to sophisticated network-based formulations, while highlighting the continuing importance of the classical framework for understanding, predicting, and controlling epidemic dynamics.

Graph theory has also been extensively applied to the SIR epidemic model to account for heterogeneous contact structures. Capasso and Serio [50] provided one of the first generalizations of the Kermack–McKendrick deterministic model to networked populations. Since then, numerous studies have explored SIR dynamics on complex networks, including analytical and computational approaches [51],[52], [53],[27].

Extensions have addressed heterogeneous populations and immunization strategies [54], rigorous stability analysis using Lyapunov and spectral methods [41][55][56][57], and the dynamic behavior of SIR epidemics on time-varying or large-scale networks [58]. Together, these contributions demonstrate how network-based formulations of the SIR model provide a more realistic and flexible framework for analyzing, predicting, and controlling epidemic outbreaks in structured populations.

In network epidemic models the reproduction number R_0 represents a threshold for the existence and stability of the equilibrium point. The n-dimensional system is described as a connected graph, where the nodes are interpreted as the individuals or the subpopulations and the edge describes the interaction between the agents. Hence, the interaction matrix is irreducible and nonnegative and this allows to use Perron-Frobenius theory. Therefore, the reproduction number is identified as the dominant eigenvalue of the interaction matrix, since it exists and it is real.

While the classical SIR model assumes that recovered individuals acquire permanent immunity and the SIS model assumes no immunity, many infectious diseases confer only temporary immunity. In such cases, individuals may recover, lose immunity after a finite period, and become susceptible

again, as observed for diseases such as influenza, whooping cough, and certain coronaviruses. To capture this epidemiological feature, the Susceptible–Infected–Recovered–Susceptible (SIRS) model introduces a feedback transition from the recovered compartment to the susceptible compartment, allowing immunity to wane over time. The SIRS model has been extensively investigated to describe recurrent epidemics, seasonal outbreaks, and long-term endemic behavior. Early studies focused on scalar formulations, with particular attention to the role of nonlinear incidence rates in shaping epidemic dynamics. Liu, Levin, and Iwasa [59] analyzed the influence of nonlinear incidence functions on stability and persistence, while further nonlinear effects, including bifurcation phenomena and complex dynamics, were explored in [60].

The scalar SIRS dynamics considered in this work are described by the following system of differential equations:

$$\begin{cases} \dot{S}(t) = -\beta S(t)I(t) + \delta R(t), \\ \dot{I}(t) = \beta S(t)I(t) - \gamma I(t), \\ \dot{R}(t) = \gamma I(t) - \delta R(t), \end{cases} \tag{1.4}$$

where δ denotes the rate at which immunity is lost. In this way, the SIRS model naturally interpolates between the two extremes: it reduces to the classical SIR model when $\delta \to 0$ (permanent immunity) and behaves like an SIS model when $\delta \to \infty$ (no immunity), filling the gap between these limiting cases.

A key aspect in the analysis of SIRS model concerns the global stability of equilibria. In this context, Lyapunov-based techniques have played a central role. Korobeinikov [61] discussed the construction of suitable Lyapunov functions for scalar SIRS systems, providing conditions for global stability. More generally, Vargas-De-León [62] systematically addressed the construction and generalization of Lyapunov functions for SIS, SIR, and SIRS models, including higher-dimensional formulations and variable population sizes, thus offering a framework applicable to multigroup and networked settings. More recent contributions have extended the SIRS framework to structured and network-based populations. Epidemic spreading in heterogeneous complex networks was analyzed in [63] and [64], while layered and multiplex network formulations were proposed in [65] to model interacting

spreading processes. Threshold phenomena and epidemic persistence in network-based SIRS models were investigated in [66], and global stability properties under nonmonotone incidence rates were established in [67]. These works collectively demonstrate the versatility of the SIRS model in capturing realistic epidemic dynamics across both scalar and network-based.

In heterogeneous epidemic models, a classical way to encode structured interactions is the mixing-group approach introduced by Nold [40] and fully explained in [68]. The key assumption of this model is that the rate at which an infected individual belonging to group j makes potentially infectious contacts with individuals of group i is proportional to a group specific activity or exposure level associated with group i, and does not depend explicitly on the infecting group. Under this assumption, contact heterogeneity can be decomposed into two independent components: the relative activity or susceptibility of each group and the total number of infectious contacts generated by an infected individual during the infectious period. As a consequence, the transmission matrix can be written as the outer product of two vectors and therefore it is a rank-1 matrix. In the network-based SIRS models considered in [63, 64, 67], heterogeneity is introduced through the network structure, which is effectively equivalent to assuming that the interaction matrix captures variations in connectivity or activity levels. Within this perspective, restricting the interaction matrix to have rank one corresponds to the simplest nontrivial realization of network heterogeneity. This motivates the study, in this thesis, of a rank-one SIRS model as a natural extension of heterogeneous SIS frameworks to epidemic dynamics with temporary immunity.

1.2 Research Objectives, Methodology, and Thesis Structure

In this thesis, we will present some important result about the network SIRS epidemic model. The reproduction number R_0 refers to the dominant eigenvalue of the network interaction matrix rescaled with the recovering rate. This matrix has the convenience of being an irreducible non-negative matrix, thanks to graph theory. Hence, it is possible to use Perron-Frobenius theory in order to ensure the existence of the dominant eigenvalue and some other properties. In Chapter 2 we present the most known scalar epidemic models

SI, SIS and SIR, reporting the main results obtained about these models: existence, uniqueness and stability of equilibrium points. Furthermore, we put our attention on the analysis of the scalar SIRS model, which is really useful for understanding and predicting the behavior of the same model in the network.

In Chapter 3 we introduce some main results about graph theory, useful in order to explore the network based epidemic models. Then, the SI, SIS and SIR network models are presented, following the same method used in the previous chapter. The analysis of the results derived for these network models establishes a necessary step to study the SIRS network model.

In Chapter 4 the main results of this thesis are presented. Although we were unable to find the endemic equilibrium in explicit form, we proved the existence and uniqueness of the endemic equilibrium above the threshold by means of fixed point theory. This provides a useful algorithm for numerical simulations. The chapter further addresses the local asymptotic stability of the endemic equilibrium, which represents the main contribution of this thesis to the model. To this end, we used a method based on algebraic properties of the Schur complement and derive an upper bound for the real part of the eigenvalues of the linearized system. We also considered the special case of rank-1 interaction matrix, in which we re-derived the quasi-global stability of the endemic equilibrium above threshold, by constructing a Lyapunov function such as in [64], with a different notation.

Finally, in Chapter 5, we present some numerical simulations that confirm our theoretical results and allow us to make conjectures about the region of attraction of the endemic equilibrium.

1.3 Notation

We introduce now the notation that will be used in this thesis. We refer to $\mathbb{R}$, $\mathbb{R}_+$ and $\mathbb{R}_{++}$ the real, nonnegative and positive numbers respectively. We denote with $\mathbf{1}$ and $\mathbf{0}$ the all-1 and all-0 vectors. Given a vector $w \in \mathbb{R}^n$ we use $[w]$ to indicate the diagonal matrix whose diagonal coincides with w. For an irreducible non-negative matrix $W \in \mathbb{R}^{n\times n}$, we denote as λ_W its dominant eigenvalue. Whenever the dominant eigenvalue refers to a product of matrices, we use the notation $\lambda_{\max}$. We use the notation $x < y$ ($x \leq y$) for vectors $x, y \in \mathbb{R}^n$ to indicate that $x_i < y_i$ ($x_i \leq y_i$) for every $i \in \{1, \cdots, n\}$. Similarly, we write $x \lneq y$ if there exists at least one component i such that

$x_i < y_i$ and $x_j \leq y_j$ for every $j \in \{1 \cdots, n\}$. For two matrices $A, B \in \mathbb{R}^{n \times n}$, we denote $A \leq B$ if, for each row i we have $A_i \leq B_i$.

Chapter 2

A Review of Scalar Epidemic Models

The analysis of the scalar models is essential to understand the behavior of the expanded theory on network. We present in this chapter four scalar epidemic models: the SI, SIS, SIR and SIRS. Observe that, in every models, we do not consider population growth or natural death. As we already noticed, these epidemic models are compartmental models (a useful graphical representation could be found in Figures 1.1 to 1.4) where transitions between compartments happen according to some specific rates. In this thesis, we identify β as the infection rate, γ as the recovering rate and δ as the loss of immunity rate and they are taken, reasonably, real and strictly positive. The variables x, y, z correspond to the fraction of susceptible, infected and recovered respectively and therefore it is natural to assume that the state space of these models is the simplex$\mathcal{X}$ defined as:

$$\mathcal{X} = \{(x, y, z) \in \mathbb{R}^3 : x + y + z = 1, x \geq 0, y \geq 0, z \geq 0\} \tag{2.1}$$

In Sections 2.1 to 2.3, we define the systems of ODEs corresponding to the scalar SI, SIS, and SIR models and investigate their dynamical behavior. For all models, the existence and stability of disease-free and endemic equilibria are analyzed, and each model exhibits a threshold governing a qualitative change in the dynamics. Since the simplex $\mathcal{X}$ is positively invariant for every models (it is a simple proof), this allows to reduce the dimension of

the system, since one variable, usually the susceptible fraction x, could be written as $x = 1 - y - z$. For this reason, the models are presented with the dimensional reduction already applied, and $1 - y - z$ is interpreted as the fraction of susceptible individuals. About the SIRS scalar model, we present a more accurate analysis in Section 2.4, necessary to understand the main object of this thesis: the network SIRS model. To do so, we report the proof of the global stability of the disease-free equilibrium under the threshold and the quasi-global stability of the endemic equilibrium over the threshold, since the trial of the analysis of the network SIRS is to find suitable Lyapunov functions to prove stability. Furthermore, we investigate the behavior of trajectories from the classification of equilibria in Section 2.4.3. Finally, in Section 2.5, we highlight the characteristic of the SIRS model of being a tie between the SIS and the SIR model.

2.1 Scalar SI model

In the SI scalar model, a susceptible individual becomes infected when encounters an infected one with an infection rate β. This model does not consider the possibility of recovering, hence there is no transition from infected compartment. This model is useful for those permanent disease and it is described by the following logistic equation:

$$\dot{y}(t) = \beta(1 - y(t))y(t) \tag{2.2}$$

The following result explain the dynamical behavior of the SI scalar model.

Proposition 2.1.1. *For every initial condition $y(0) \in [0,1]$, the solution of the SI scalar model in (2.2) is*

$$y(t) = \frac{y(0)e^{\beta t}}{1 - y(0) + y(0)e^{\beta} t} \tag{2.3}$$

If $y(0) \in (0,1)$, the system is monotonically increasing and converge to the unique endemic equilibrium $y^* = 1$.

Proof. See [69]. □

2.2 Scalar SIS model

The SIS scalar model describes situations where multiple infections are allowed while immunity is neglected. This means that infected individuals return immediately to the susceptible compartment after recovery and the model does not take the recovered class. As in the SI, the susceptible become infected by encountering an infected one at rate β, then they recover and become susceptible again with rate γ. The SIS scalar model is described by the following ODE:

$$\dot{y}(t) = \beta(1 - y(t))y(t) - \gamma y(t) \tag{2.4}$$

Proposition 2.2.1. *The SIS model in (2.4) has the following property:*

- *for $\beta \leq \gamma$ the disease-free equilibrium $y^* = 0$ is globally asymptotically stable (GAS)*
- *for $\beta > \gamma$ the disease-free equilibrium $y^* = 0$ is unstable and there exists the endemic equilibrium $y^* = 1 - \frac{\gamma}{\beta}$ that is locally asymptotically stable with basin of attraction $\mathcal{X}' \setminus \{y = 0\}$.*

Proof. See [70]. □

We can notice that the SIS model presents a transcritical bifurcation when $\frac{\beta}{\gamma} = 1$. A similar behavior will be found also in the SIRS model in Section 2.4, hence this remarks the importance of studying this model on network to understand the SIRS network one.

2.3 Scalar SIR model

The SIR scalar model introduce another compartment: the recovered $z(t)$. This system consider the immunity as permanent, which means that infected individuals that have been recovered cannot become susceptible anymore. We can describe the SIR model with the following system of ODE's:

$$\begin{cases} \dot{x}(t) = -\beta x(t)y(t)\dot{y}(t) = \beta x(t)y(t) - \gamma y(t) \\ \dot{z}(t) = \gamma y(t) \end{cases} \tag{2.5}$$

Despite the previous model, the SIR scalar model does not admit an endemic equilibrium. Indeed, solving the system (2.5), we obtain that

$$\mathcal{X}^* = \{(x^*,0,1-x^*) : x^* \in [0,1]\}$$

is the set of equilibrium point, which always have no infected. In terms of the stability behavior of the equilibrium points, it can be proved (see [71]) the following proposition

Proposition 2.3.1. *The SIR model in eq. (2.5) has the following properties:*

- *the disease-free equilibrium* $(x^*,0,1-x^*)$ *is stable if* $\beta x^* < \gamma$
- $x(t)$ *is monotonically decreasing,* $z(t)$ *is monotonically increasing, while* $y(t)$ *is increasing if and only if* $x(0)\beta > \gamma$
- $y(t)$ *is strictly decreasing if* $\beta x(0) \leq \gamma$*, but in case* $\beta x(0) > \gamma$*, it first increases to a maximum attained when* $x = \frac{\gamma}{\beta}$ *and then decreases to zero.*

2.4 SIRS scalar model

The SIRS (Susceptible–Infectious–Recovered–Susceptible) model describes infectious diseases in which individuals, after recovering from the infection, lose immunity over time and return to the susceptible class. In this sense, immunity is not permanent as in SIR model, and the disease can re-emerge cyclically within the population. In this section, we analyze the scalar version of the SIRS model, which represents one of the simplest compartmental epidemic systems incorporating the loss of immunity. We first introduce the model equations and prove that the epidemiological simplex, representing the biologically meaningful region, is positively invariant. Then, we study the equilibrium points and their stability properties, highlighting the role of the parameters β, γ, and δ. Finally, we show that the system undergoes a transcritical bifurcation as the parameter ratio $R_0 = \beta/\gamma$ crosses the critical threshold $R_0 = 1$, marking the transition between the disease-free and endemic regimes. The scalar SIRS model has been extensively studied in the literature, and analyses closely related to the one presented here can be found in [61] or in these two works [60], [59] which, even if they consider more general nonlinear incidence rates, can be reduced to the bilinear incidence framework adopted in this thesis.

The dynamics of the scalar SIRS model are governed by the following system of ODEs:

$$\begin{cases} \dot{x}(t) = -\beta x(t)y(t) + \delta z(t) \\ \dot{y}(t) = \beta x(t)y(t) - \gamma y(t) \\ \dot{z}(t) = \gamma y(t) - \delta z(t) \end{cases} \tag{2.6}$$

Proposition 2.4.1. *The simplex* $\mathcal{X} = \{(x, y, z) \in \mathbb{R}^3 : x \geq 0, y \geq 0, z \geq 0, x + y + z = 1\}$ *is positively invariant.*

Proof. From the fact that

$$\dot{x}(t) + \dot{y}(t) + \dot{z}(t) = 0 \qquad \forall t \in \mathbb{R}$$

and

$$\dot{y}(t) = y(t)(\beta x(t) - \gamma)$$

we have that the sets $\{(x, y, z) \in \mathbb{R}^3 : x + y + z = 1\}$, $\{(x, y, z) \in \mathbb{R}^3 : y = 0\}$ and $\{(x, y, z) \in \mathbb{R}^3 : y \geq 0\}$ are invariant.
If $y = 0$, we have $\dot{y} = \beta xy - \gamma y = 0$. Hence, trajectories cannot cross this boundary towards $y < 0$. Indeed, any solution satisfying $y(t_0) = 0$ for some $t_0 \in \mathbb{R}$ must satisfy $y(t) = 0$ for all $t \geq t_0$. Therefore, if $y(0) \geq 0$, we have $y(t) \geq 0$ for all $t \geq 0$.
Furthermore, if $z = 0$, then $\dot{z} = \gamma y - \delta z = \gamma y \geq 0$ whenever $y \geq 0$. Thus, on the plane $z = 0$ trajectories can't cross into the region $z < 0$, so, if $z(0) \geq 0$ and $y(0) \geq 0$ we have $z(t) \geq 0$.
Hence, the set $\{y \geq 0,\ z \geq 0\}$ is positively invariant. Using that, if $x = 0$, then $\dot{x} = \delta z \geq 0$ whenever $z \geq 0$. This concludes the proof because we now have that

$$\{(x, y, z) \in \mathbb{R}^3 : x \geq 0, y \geq 0, z \geq 0\}$$

is positively invariant and the set

$$\{(x, y, z) \in \mathbb{R}^3 : x + y + z = 1\}$$

is invariant, so the intersection

$$\mathcal{X} = \{(x, y, z) \in \mathbb{R}^3 : x \geq 0, y \geq 0, z \geq 0\} \cap \{(x, y, z) \in \mathbb{R}^3 : x + y + z = 1\}$$

is positively invariant. □

2.4.1 Equilibrium points and stability

The point (1,0,0) is always a solution of system (2.6). Whenever $\beta > \gamma$, there exists another equilibrium point, known as *endemic equilibrium*:

$$(x^*, y^*, z^*) = \left(\frac{\gamma}{\beta}, \frac{\delta(\beta-\gamma)}{\beta(\delta+\gamma)}, \frac{\gamma(\beta-\gamma)}{\beta(\delta+\gamma)}\right) \tag{2.7}$$

From now on, because $\{x + y + z = 1\}$ is invariant, we consider the system (2.6) in the following form:

$$f(y,z) = (\dot{y}, \dot{z}) = \big(\beta y(t)(1 - y(t) - z(t)) - \gamma y(t), \gamma y(t) - \delta z(t)\big) \tag{2.8}$$

with equilibrium points:

$$(y^*, z^*) = (0,0), \qquad \forall \beta, \gamma > 0 \tag{2.9}$$

$$(y^*, z^*) = \left(\frac{\delta(\beta-\gamma)}{\beta(\delta+\gamma)}, \frac{\gamma(\beta-\gamma)}{\beta(\delta+\gamma)}\right), \qquad \forall \beta > \gamma \tag{2.10}$$

In the following part of this section we will prove the global asymptotical stability of (0,0), whenever $\beta \leq \gamma$. Later, we will discuss the stability of the endemic equilibrium (when $\beta > \gamma$).

Proposition 2.4.2. *For $\beta \leq \gamma$ the origin is globally asymptotically stable.*

Remark 2.4.3. The linearization of the system around the disease-free equilibrium (0,0) shows that it is locally asymptotically stable when $\beta < \gamma$ and unstable when $\beta > \gamma$. Indeed, we should just show the Jacobian matrix of the system (2.8), that is

$$\nabla f(0,0) = \begin{pmatrix} \beta - \gamma & 0 \\ \gamma & -\delta \end{pmatrix} \tag{2.11}$$

However, the case $\beta = \gamma$ requires a more careful analysis.

Proof. When $\beta \leq \gamma$, we can see that, for all $(x(0), y(0), z(0)) \in \mathcal{X}$, it holds:

$$\dot{y}(t) = \beta xy - \gamma y = \beta y(1 - y - z - \frac{\gamma}{\beta}) \leq -\beta y^2$$

hence $y(t) \to 0$, when $t \to \infty$.
Then, from (2.6),

$$z(t) = z(0)e^{-\delta t} + \gamma \int_0^t e^{-\delta(t-s)} y(s) ds \to 0 \quad \text{for} \quad t \to \infty$$

We can conclude that (0,0) is globally asymptotically stable for $\beta \leq \gamma$. □

As we remarked in 2.4.3, in case $\beta > \gamma$, the equilibrium (0,0) is unstable, and there is another equilibrium point, see (2.7). We now want to investigate the stability of this endemic equilibrium.

Proposition 2.4.4. *For $\beta > \gamma$, the endemic equilibrium (y^*, z^*) is locally asymptotically stable, and its basin of attraction is given by $\mathcal{X} \setminus \{y = 0\}$. Moreover, the disease-free equilibrium (0,0) attracts the set $\mathcal{X} \cap \{y = 0\}$.*

Proof. To prove the stability of the endemic equilibrium, we consider the following Lyapunov function:

$$V(t) = y - y^* + y^* \log(\frac{y^*}{y}) + \frac{\beta}{2\gamma}(z - z^*)^2 \tag{2.12}$$

We have that V is of class C^1 on $\mathcal{X} \setminus \{y = 0\}$ and it is positively definite with respect to (y^*, z^*). Indeed,

$$g(y) = y - y^* + y^* \log(\frac{y^*}{y})$$

is strictly convex and has $\min_y g(y) = 0$ reached for $y = y^*$. Furthermore,

$$\begin{aligned}
\dot{V}(t) =& \frac{\partial V}{\partial y}\dot{y} + \frac{\partial V}{\partial z}\dot{z} \\
=& (1 - \frac{y}{y^*})\dot{y} + \frac{\beta}{\gamma}(z - z^*)\dot{z} \\
=& (1 - \frac{y}{y^*})\beta y(1 - y - z - \frac{\gamma}{\beta}) + \frac{\beta}{\gamma}(z - z^*)(\gamma y - \delta z) \\
=& (y - y^*)\beta(1 - y - z - x^*) + \frac{\beta}{\gamma}(z - z^*)\gamma(y - \frac{\delta}{\gamma}z) \\
=& \beta(y - y^*)(1 - y - z - 1 + y^* + z^*) + \beta(z - z^*)(y - \frac{\delta}{\gamma}z) \\
=& -\beta(y - y^*)^2 + \beta(z - z^*)(-y + y^* + y - \frac{\delta}{\gamma}z) \\
=& -\beta(y - y^*)^2 - \frac{\beta\delta}{\gamma}(z - z^*)^2
\end{aligned}$$

So $\dot{V} < 0$ if and only if $(y, z) \neq (y^*, z^*)$ and $y \neq 0$.
Hence, for the first Lyapunov Theorem, the endemic equilibrium is asymptotically stable and, thanks to the invariance principle, we can conclude that the endemic equilibrium (y^*, z^*) attracts the entire set $\mathcal{X} \setminus \{y = 0\}$. Noticing that on $\{y = 0\}$ we have $\dot{z} = -\delta z$, the disease-free equilibrium attracts all the segment $\mathcal{X} \cap \{y = 0\}$. □

In summary, the scalar SIRS model (2.6) exhibits a classical *transcritical bifurcation* at $\beta = \gamma$. When $\beta \leq \gamma$, the disease-free equilibrium (0,0) is globally asymptotically stable: any initial condition in the simplex $\mathcal{X}$ eventually converges to the disease-free state, and the infection cannot invade the population.
When $\beta > \gamma$, the disease-free equilibrium becomes unstable, and an endemic equilibrium (y^*, z^*) emerges, which is locally asymptotically stable. Its basin of attraction is given by $\mathcal{X} \setminus \{y = 0\}$, meaning that all trajectories starting with a positive fraction of infected individuals converge to this endemic state, while trajectories on the boundary $\{y = 0\}$ still converge to the disease-free equilibrium.
Therefore, as the parameter β crosses the threshold γ, the stability of the equilibria exchanges: the disease-free equilibrium loses stability and the

endemic equilibrium appears. This transition clearly illustrates a transcritical bifurcation (see Figure 2.1) and highlights the critical role of the basic reproduction number $R_0 = \beta/\gamma$ in determining whether an infection dies out or becomes endemic.

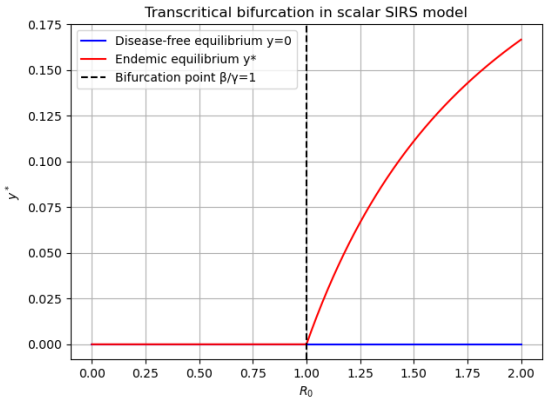

Figure 2.1: Transcritical bifurcation for scalar SIRS model for fixed δ

2.4.2 Interpretation of simulation results

The following figures illustrate the time evolution of the three compartments of the SIRS scalar model: the fraction of susceptible individuals $x(t)$, infected individuals $y(t)$, and recovered individuals $z(t)$, under different parameter configurations. Each subplot corresponds to trajectories starting from distinct initial conditions within the epidemiological simplex $\mathcal{X}$. In the first row of images (see fig. 2.2), we consider the case where $R_0 < 1$, i.e. $\beta < \gamma$. In this regime, only the *disease-free equilibrium* $(x^*, y^*, z^*) = (1, 0, 0)$ exists, and it is globally asymptotically stable. Indeed, regardless of the initial condition, all trajectories in the simplex converge to the disease-free equilibrium, meaning that the infection eventually dies out. In the second row of images((see fig. 2.3), corresponding to the case $R_0 = 1$, the system still preserves global stability of the disease-free equilibrium. The trajectories show that the infection cannot persist and, although transient oscillations may occur depending on the initial state, the system always converges to $(1, 0, 0)$. In the third row of images (see fig. 2.4), where $R_0 > 1$, the behaviour of the system changes qualitatively. The disease-free equilibrium (1,0,0) still exists but becomes unstable, attracting only the subset of the simplex corresponding to the plane $\{y = 0\}$. In particular, the light blue trajectory, which starts with $z \neq 0$

and $x \neq 1$, still converges to the disease-free equilibrium, confirming this partial stability property. However, when $R_0 > 1$, a new *endemic equilibrium* emerges, which attracts all trajectories in the simplex except those lying on the invariant plane $\{y = 0\}$. Hence, for any initial condition with a positive fraction of infected individuals, the system converges to this endemic equilibrium, illustrating the persistence of the disease in the population. Overall, these simulations visually confirm the theoretical results proven in proposition 2.4.2 and proposition 2.4.4: the existence of a transcritical bifurcation at the threshold $R_0 = 1$, where the stability of the disease-free equilibrium is exchanged with that of the endemic equilibrium.

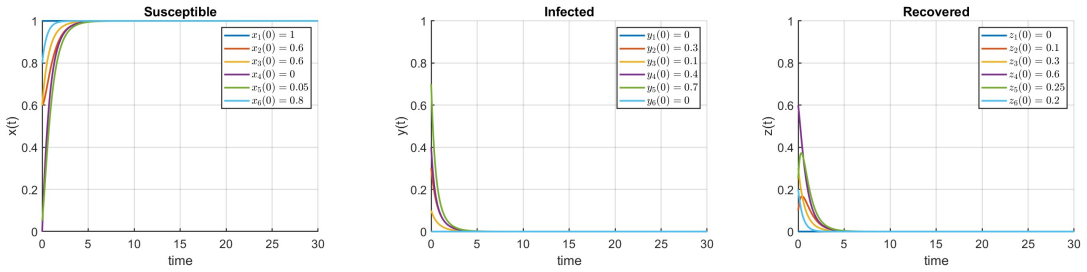

(a) **(b)** **(c)**

Figure 2.2: Trends for $\beta < \gamma$ with different initial conditions. GAS disease-free equilibrium point: $(x^*, y^*, z^*) = (1,0,0)$. Chosen parameter: $\beta = 1; \delta = 2; \gamma = 2$.

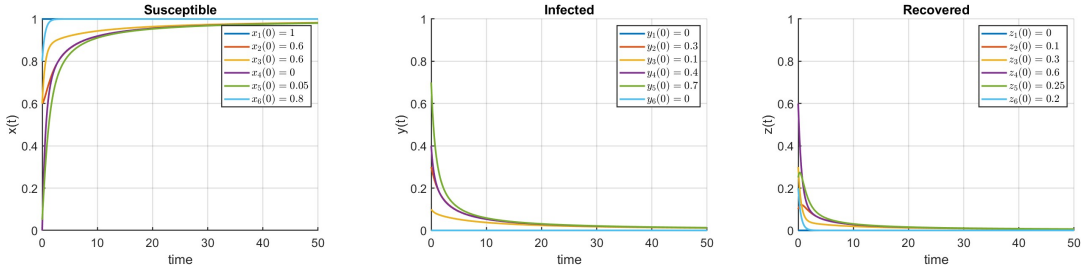

(a) **(b)** **(c)**

Figure 2.3: Trends for $\beta = \gamma$ with different initial conditions. GAS disease-free equilibrium point: $(x^*, y^*, z^*) = (1,0,0)$. Chosen parameter: $\beta = 1; \delta = 2; \gamma = 1$.

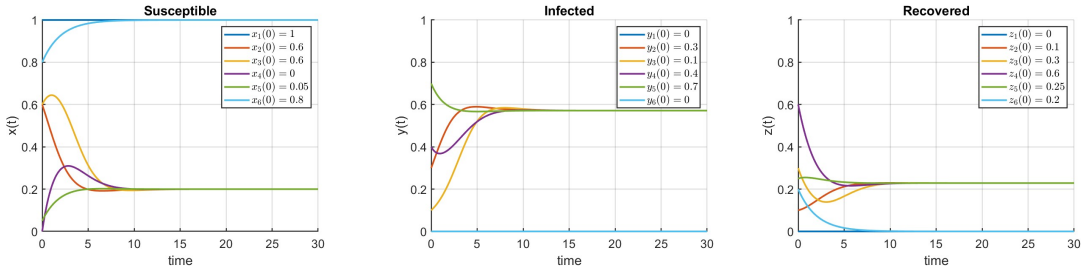

(a) (b) (c)

Figure 2.4: Trends for $\beta > \gamma$ with different initial conditions. LAS endemic equilibrium point: $(x^*, y^*, z^*) = (0.2, 0.57, 0.23)$, unstable disease-free equilibrium $(x^*, y^*, z^*) = (1,0,0)$. Chosen parameter: $\beta = 1; \delta = 0.5; \gamma = 0.2$.

2.4.3 Classification of equilibrium points

In proposition 2.4.2 and proposition 2.4.4 we have proved the stability properties of the scalar SIRS system. We now turn our attention to the classification of the equilibrium points. In general (see [72]), for a linear system such as

$$\dot{x} = Ax$$

the classification is done using the trace τ and the determinant Δ of A. In our case, we need to consider the linearization of the system first around the origin, and then around the endemic equilibrium.
From eq. (2.11), it is clear that the eigenvalue are

$$\lambda_1 = \beta - \gamma \qquad \lambda_2 = -\delta$$

which are both real, so when $\beta < \gamma$, (0,0) is a stable node, while is a unstable node when $\beta > \gamma$.
More interesting is the case of the endemic equilibrium (y^*, z^*). In this case, the Jacobian of system (2.8) evaluated in (y^*, z^*), using the equilibrium equation, is equal to:

$$\nabla f(y^*, z^*) = \begin{pmatrix} \beta(1 - y^* - z^*) - \gamma - \beta y^* & -\beta y^* \\ \gamma & -\delta \end{pmatrix} = \begin{pmatrix} -\beta y^* & -\beta y^* \\ \gamma & -\delta \end{pmatrix} \tag{2.13}$$

Rescaling the system and renaming $\delta' = \delta/\beta$ and $\gamma' = \gamma/\beta$, we can rewrite

$$y^* = \frac{\delta(\beta - \gamma)}{\beta(\gamma + \delta)} = \frac{\delta(1 - \gamma')}{\gamma' + \delta'} \tag{2.14}$$

which exists only for $\gamma' < 1$, and

$$\nabla f(y^*, z^*) = \beta \begin{pmatrix} -y^* & -y^* \\ \gamma' & -\delta' \end{pmatrix} \tag{2.15}$$

Now we need to derive the trace and the determinant of (2.15).

$$\tau = -y^* - \delta' \tag{2.16}$$

$$\Delta = y^*(\delta' + \gamma') \tag{2.17}$$

We want to evaluate the sign of

$$\tau^2 - 4\Delta$$

that is

$$\begin{aligned} \tau^2 - 4\Delta =& (y^* + \delta')^2 - 4y^*(\delta' + \gamma') \\ =& \left(\frac{\delta'(1 - \delta')}{\gamma' + \delta'}\right)^2 - 4\delta'(1 - \gamma') \end{aligned}$$

where we used eq. (2.14). We know from theory of linear system, that if $\tau^2 - 4\Delta > 0$ the equilibrium point is a node, while if $\tau^2 - 4\Delta < 0$ it's a spiral. It's a degenerate node when we have the equality. In fig. 2.5 we can see the classification of the endemic equilibrium point as γ/β varies in interval [0,1) and δ/β in $[0, +\infty)$. The red part corresponds to $\tau^2 - 4\Delta < 0$ that is equal to

$$\delta'(1 - \delta')^2 < 4(1 - \gamma')(\gamma' + \delta')^2$$

while the blue part corresponds to $\tau^2 - 4\Delta > 0$.

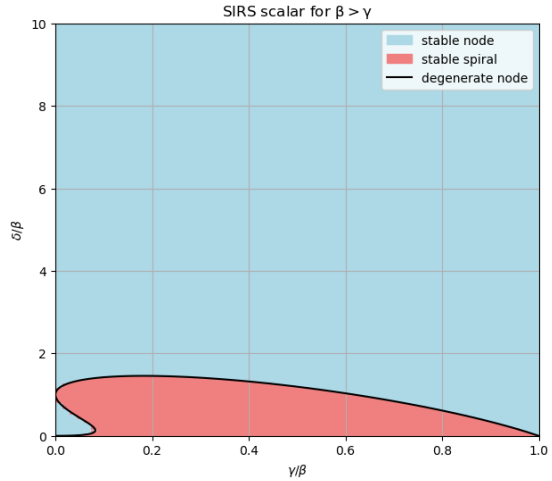

Figure 2.5: Classification of equilibrium point

To better understand the analysis of the equilibrium point classification and the diagram shown in fig. 2.5, Figures 2.6, 2.7, and 2.8 illustrate the phase portraits of the system (2.8) for different parameter configurations.
In fig. 2.6, corresponding to the case $\beta < \gamma$, the only equilibrium point is the disease-free equilibrium $(x^*, y^*, z^*) = (1,0,0)$, which is globally asymptotically stable. All trajectories within the simplex converge to this point, confirming the complete extinction of the infection in this subthreshold regime.
When $\beta > \gamma$, two equilibria coexist: the disease-free equilibrium, which becomes unstable, and an endemic equilibrium that emerges and attracts most trajectories. The qualitative nature of this endemic equilibrium depends on the sign of $\tau^2 - 4\Delta$, as shown in figs. 2.7 and 2.8. Specifically, when $\tau^2 - 4\Delta < 0$, the equilibrium is a *stable spiral* (see fig. 2.7a); when $\tau^2 - 4\Delta > 0$, it becomes a *stable node* (see fig. 2.7b–2.8b). In both cases, the origin acts as an unstable saddle point, and trajectories approach the endemic equilibrium following either oscillatory or monotonic paths depending on parameter values.
This numerical behavior aligns with the analytical classification depicted in fig. 2.5, where the red region corresponds to $\tau^2 - 4\Delta < 0$ (stable spiral), the blue region to $\tau^2 - 4\Delta > 0$ (stable node), and the separating black curve marks the locus of degenerate nodes. These phase portraits thus provide concrete examples of the system's qualitative dynamics in each stability regime and visually confirm the theoretical predictions obtained from the linearization analysis.

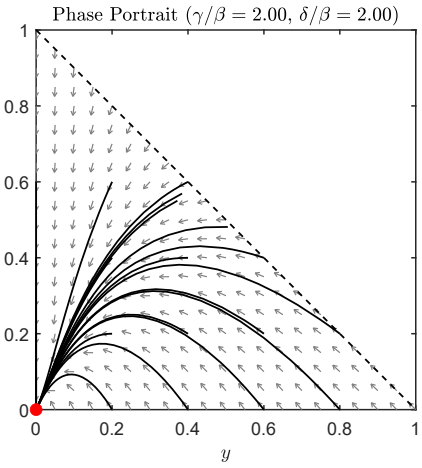

Figure 2.6: Phase portrait in case $\beta < \gamma$. Only one fixed point: origin (stable node).

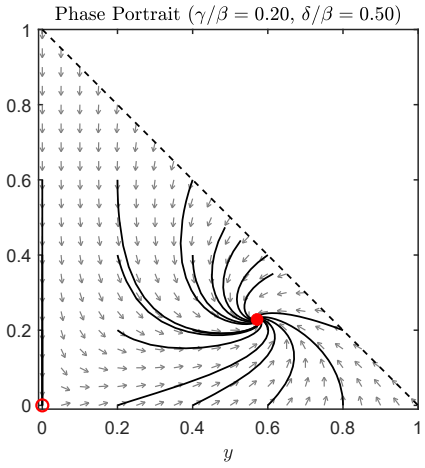

(a) Phase portrait in case $\beta > \gamma$ and $\tau^2 < 4\Delta$. Two fixed points: origin (unstable saddle point) and endemic equilibrium (stable spiral).

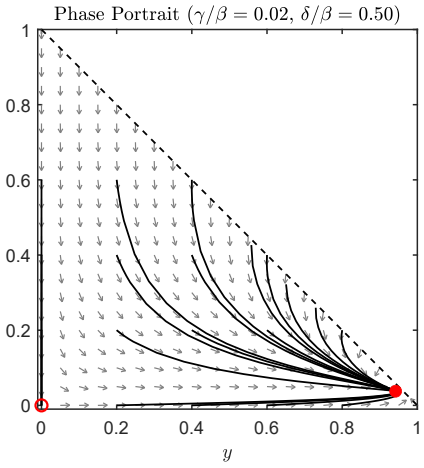

(b) Phase portrait in case $\beta > \gamma$ and $\tau^2 > 4\Delta$. Two fixed points: origin (unstable saddle point) and endemic equilibrium (stable node).

Figure 2.7: Comparison between the two phase portraits for constant parameter $\frac{\delta}{\beta}$ and different $\frac{\gamma}{\beta}$.

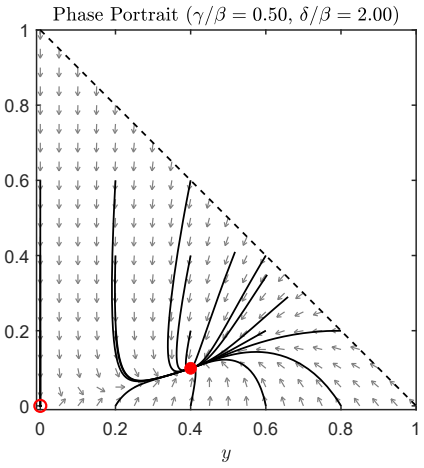

(a) Phase portrait in case $\beta > \gamma$ and $\tau^2 > 4\Delta$. Two fixed points: origin (unstable saddle point) and endemic equilibrium (stable node).

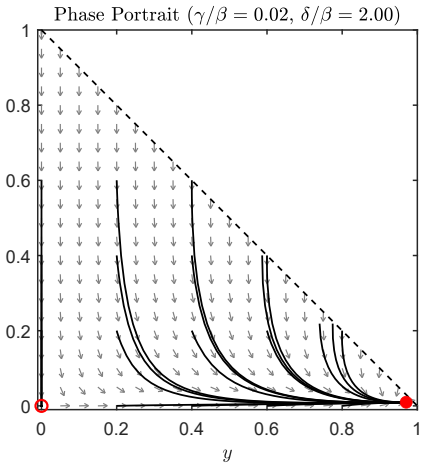

(b) Phase portrait in case $\beta > \gamma$ and $\tau^2 > 4\Delta$. Two fixed points: origin (unstable saddle point) and endemic equilibrium (stable node).

Figure 2.8: Comparison between the two phase portraits for constant parameter $\frac{\delta}{\beta}$ and different $\frac{\gamma}{\beta}$.

2.5 Comparison between SIRS and SIR, SIS model

The SIRS model (2.6) extends the classical SIR and SIS formulations by introducing a finite period of immunity through the parameter $\delta > 0$, which represents the rate at which recovered individuals lose immunity and return to the susceptible compartment. A direct comparison with the SIS and SIR models can be made by analyzing the limiting behavior of system as the immunity-loss rate δ varies.

2.5.1 Limit case for $\delta \to 0$

When δ tends to zero, the loss of immunity becomes negligible. In this regime, individuals who recover from the infection remain immune almost permanently, so that the return flow from z to x vanishes. Formally, taking

$\delta \to 0$ in (2.6) yields

$$\begin{cases} \dot{x} = -\beta xy \\ \dot{y} = \beta xy - \gamma y \\ \dot{z} = \gamma y \end{cases}$$

which is exactly the classical SIR model. Consequently, for small values of δ the system behaves as an SIR dynamics, and the infection eventually dies out. This corresponds to the disease-free equilibrium $(x^*, y^*, z^*) = (x^*, 0, 1-x^*)$, meaning that if the immunity is almost permanent, the epidemic goes extinct. Figure 2.9 illustrates the evolution of the system as the parameter δ approaches zero. In particular, fig. 2.9a shows that, as stated in proposition 2.3.1, the variable $y(t)$ decreases monotonically, while fig. 2.9b highlights that the infection eventually vanishes after an initial growth phase.

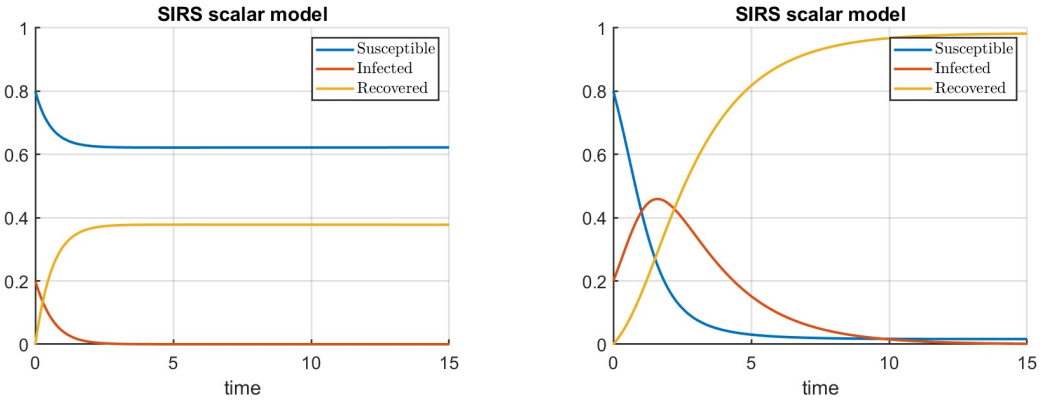

(a) Case $\beta x(0) < \gamma$ **(b)** Case $\beta x(0) > \gamma$

Figure 2.9: Limit case for SIRS scalar model for $\delta \to 0$

2.5.2 Limit case for $\delta \to \infty$

On the other hand, when δ becomes very large, the immunity of recovered individuals is lost almost instantaneously. In this case, the variable $z(t)$ decays much faster than $x(t)$ and $y(t)$, effectively remaining close to zero at all times. Formally, as $\delta \to +\infty$, one obtains $z(t)$ goes to zero very quickly,

and system (2.6) reduces to

$$\begin{cases} \dot{x} = -\beta xy + \gamma y, \\ \dot{y} = \beta xy - \gamma y, \end{cases}$$

which is the classical SIS model, where recovered individuals immediately return to the susceptible class without any lasting immunity. Figure 2.10 illustrates the limiting behavior of the SIRS model as $\delta \to +\infty$, where the system effectively reduces to the SIS dynamics described in (2.4). In this regime, the recovered population $z(t)$ decays almost instantaneously to zero, and the epidemic evolution is fully captured by the interaction between the susceptible and infected compartments. Figure 2.10a shows the sub-threshold case, where $\beta < \gamma$. In accordance with proposition 2.2.1, the disease-free equilibrium $y^* = 0$ is globally asymptotically stable. Consequently, the fraction of infected individuals $y(t)$ decreases monotonically to zero, while the susceptible population $x(t)$ tends to one. This behavior corresponds to the extinction of the infection. In contrast, fig. 2.10b depicts the super-threshold case, where $\beta > \gamma$. As predicted by proposition 2.2.1, the disease-free equilibrium becomes unstable, and the system converges to the endemic equilibrium $y^* = 1 - \frac{\gamma}{\beta}$. In this configuration, the infection persists over time, reaching a nonzero steady state, while the susceptible fraction stabilizes at $x^* = \frac{\gamma}{\beta}$. The numerical trajectories confirm the theoretical predictions, showing convergence toward the endemic equilibrium in the super-threshold regime and toward the disease-free state in the sub-threshold case.

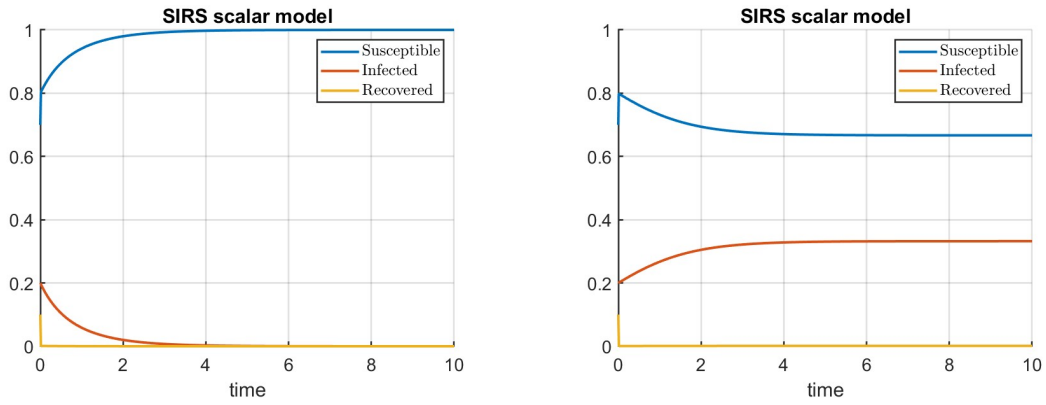

(a) Case $\beta < \gamma$ **(b)** Case $\beta > \gamma$

Figure 2.10: Limit case for SIRS scalar model with $\delta \to \infty$

Chapter 3

A Review of Classical Epidemic Models on Networks

In this chapter we analyze the most known network-based epidemic models. Unlike the corresponding scalar models, admit heterogeneity in the population, allowing for a more accurate description of disease spreading phenomena. A network-based epidemic model is described by a finite weighted directed graph $\mathcal{G}$. The vertices and the edges of the graph represent, respectively, the populations and the links between them. Interactions among populations are then captured by a nonnegative irreducible matrix, which encodes the structure of the network. The number of ODEs describing the model grows linearly in the number of populations, and is equal to the product of the number of compartments times the number of network nodes. In view of these considerations, it is therefore necessary to introduce some basic notions and properties from graph theory, which will be used throughout the chapter to formulate and analyze network-based epidemic models.

3.1 Graph Theory

In this section we introduce some basic notions and properties from graph theory that are necessary to formulate and analyze network-based epidemic models. All results presented in this section can be found in [23, 73].

Definition 3.1.1. A weighted, directed graph is a triple

$$\mathcal{G} = (\mathcal{V}, \mathcal{E}, W),$$

where:

- $\mathcal{V}$ is the finite set of nodes;
- $\mathcal{E} \subseteq \mathcal{V} \times \mathcal{V}$ is the set of links;
- $W \in \mathbb{R}_+^{\mathcal{V}\times\mathcal{V}}$ is the weight matrix, such that $W_{ij} > 0$ if and only if there is a link from i to j, i.e. $(i, j) \in \mathcal{E}$.

Sometimes, in network epidemic models, the graph is assumed to be undirected, where every link is bidirectional, i.e. the interaction matrix W is symmetric.

Definition 3.1.2. For a weighted, directed graph $\mathcal{G} = (\mathcal{V}, \mathcal{E}, W)$ we define:

- the *out-degree* of a node $i \in \mathcal{V}$ as

$$w_i = \sum_{j\in\mathcal{V}} W_{ij};$$

- the *out-degree vector* of the graph $\mathcal{G}$ as

$$w = W\mathbf{1};$$

- the *in-degree* of a node $i \in \mathcal{V}$ as

$$w_i^- = \sum_{j\in\mathcal{V}} W_{ji};$$

- the *in-degree vector* of the graph $\mathcal{G}$ as

$$w^- = W^T\mathbf{1};$$

- the *total degree* of the graph as

$$\sum_{i,j\in\mathcal{V}} W_{ij};$$

- the *average degree* of the graph as

$$\bar{w} = \frac{1}{n}\sum_{i,j\in\mathcal{V}} W_{ij}.$$

A graph $\mathcal{G} = (\mathcal{V}, \mathcal{E}, W)$ is called

- *balanced* if $w_i = w_i^-$ for every node $i \in \mathcal{V}$, i.e. $w = w^-$;
- *out-regular* (*in-regular*) if the out-degree vector w (in-degree vector w^-) is a multiple of the vector $\mathbf{1}$;
- *regular* if $w = w^- = \bar{w}\mathbf{1}$.

Definition 3.1.3. A *walk* from node i to node j is a finite sequence of nodes

$$\Gamma = (i_0, i_1, \ldots, i_\ell)$$

such that $i_0 = i$, $i_\ell = j$, and $(i_{h-1}, i_h) \in \mathcal{E}$ for all $h = 1, \ldots, \ell$. The integer ℓ is defined as the *length* of the walk. A node j is said to be *reachable* from a node i if there exists a walk from i to j.

Definition 3.1.4 (Definition 2.6 [73])**.** A weighted, directed graph $\mathcal{G} = (\mathcal{V}, \mathcal{E}, W)$ is *strongly connected* if for any ordered pair $(i, j) \in \mathcal{E}$ of vertices of $\mathcal{G}$ there exists a walk from node i to node j.

We now introduce a matrix-theoretic notion that is closely related to the connectivity properties of a graph.

Definition 3.1.5. A nonnegative matrix $A \in \mathbb{R}_+^{n\times n}$ is said to be *reducible* if there exists a permutation matrix P such that

$$PAP^T = \begin{pmatrix} A_{11} & A_{12} \\ 0 & A_{22} \end{pmatrix},$$

where A_{11} and A_{22} are square matrices of dimension strictly smaller than n. Otherwise, the matrix A is said to be *irreducible*.

Theorem 3.1.6 (Theorem 2.7 [73]). *A matrix W is irreducible if and only if the associated graph $\mathcal{G} = (\mathcal{V}, \mathcal{E}, W)$ is strongly connected.*

3.1.1 Perron-Frobenius theory

Perron-Frobenius theory [30, 31, 32, 33] gives us some useful properties about nonnegative irreducible matrices. The Perron-Frobenius theorem ensures that, for a nonnegative and irreducible matrix $W \in \mathbb{R}_+^{n\times n}$, there exists a real eigenvalue $\lambda_W > 0$, called the *dominant eigenvalue* of W, which coincides with the spectral radius of W:

$$\lambda_W = \rho(W) = \max\{|\lambda| : \lambda \in \sigma(W)\} \tag{3.1}$$

Moreover, λ_W is simple and there exist two positive eigenvectors $v > 0$ and $\bar{v} > 0$ such that

$$Wv = \lambda_W v, \qquad \bar{v}^T W = \lambda_W \bar{v}^T \tag{3.2}$$

where v and $\bar{v}$ are, respectively, the *right* and *left eigenvectors* associated with λ_W.
We report here a *max-min characterization* of λ_W, also known as *Collatz–Wielandt formula*:

$$\lambda_W = \max_{v>0}\left\{\min_{i\in\mathcal{V}} \frac{(Wv)_i}{v_i}\right\} \tag{3.3}$$

3.2 Dynamic behavior of network epidemic models

We are now ready to analyze the dynamic behavior of some well-known network-based epidemic models. As we anticipate in the beginning of this chapter, an epidemic model on network is described as a system of ODEs which express the interaction between internal population compartments and between populations. We refer to a network of n populations as a

graph $\mathcal{G} = (\mathcal{V}, \mathcal{E}, W)$ where $\mathcal{V} = \{1, \cdots, n\}$ is the finite set of populations, $\mathcal{E} \in \mathcal{V} \times \mathcal{V}$ is the set of links between groups. The nonnegative matrix W expresses the interaction between populations and is taken as irreducible, since we consider a strongly connected graph. In some cases, it is possible to relax this assumption and work on every connected component of the graph.

As in the scalar case, these models retain the compartmental structure. For each population i, the time-dependent variables $x_i(t)$, $y_i(t)$, and $z_i(t)$ denote the fractions of susceptible, infected, and recovered individuals, respectively. Infection spreads through contacts among populations, whose frequency is described by the interaction matrix W. The entries of W satisfy $W_{ij} > 0$ whenever population i is exposed to population j. The strong connectivity of the graph ensures that each population can directly or indirectly influence all others through the network of interactions. In epidemic models, it's common to require the interaction matrix to be irreducible, because it simply reflects that no population is completely isolated from the others. The infecting rate β could be absorbed by the interaction matrix W, while γ_i refers to the recovering rate of the population i. In this analysis, we assume for simplicity that $\gamma_i = \gamma$ for every group i. Similarly to the scalar case, it is natural to assume that the dynamic of network-based models is restricted to the state space $\mathcal{X}$ defined as follows:

$$\mathcal{X} = \{(x_i, y_i, z_i) \in \mathbb{R}^{3n} : x_i, y_i, z_i \geq 0, x_i + y_i + z_i = 1\} \tag{3.4}$$

It is possible to prove that $\mathcal{X}$ is positively invariant for every models considered, hence it is possible to reduce the system dimension using $x_i(t) = 1 - y_i(t) - z_i(t)$ for every $t \geq 0$.

In the rest of the chapter, we analyze, for every model considered, the existence of equilibrium points and the stability behavior of the system. The results presented are adopted from [56].

3.2.1 Network SI model

A SI network model is described by the following ODEs:

$$\begin{cases} \dot{x}_i(t) = -\sum_j x_i(t) W_{ij} y_j(t) \\ \dot{y}_i(t) = \sum_j x_i(t) W_{ij} y_j(t) \end{cases} \tag{3.5}$$

Since the SI model does not consider the recovered compartment, the natural space state (4.2) becomes:

$$\mathcal{X} = \{(x, y) \in \mathbb{R}^{2n}, x_i, y_i \geq 0, x_i + y_i = 1, \forall\, i \in \mathcal{V}\} \tag{3.6}$$

Lemma 3.2.1. *The space state $\mathcal{X}$ in (3.6) is positively invariant for the SI network model (3.5).*

Proof. Since $\{x_i = 0\}$ and $\{y_i = 0\}$ are invariant, $\{x_i \geq 0\}$ and $\{y_i \geq 0\}$ are positively invariant for every node $i \in \mathcal{V}$. Hence, the intersection $\{x_i \geq 0, y_i \geq 0, \forall\, i \in \mathcal{V}\}$ is positively invariant, because intersection of positively invariant sets. From the fact that $\dot{x}_i(t) + \dot{y}_i(t) = 0$ for every $t \in \mathbb{R}$ and for every $i \in \mathcal{V}$, we obtain that the set $\{x_i + y_i = 1, \forall\, i \in \mathcal{V}\}$ is invariant. Therefore, the intersection

$$\mathcal{X} = \{x_i \geq 0, y_i \geq 0, \forall\, i \in \mathcal{V}\} \cap \{x_i + y_i = 1, \forall\, i \in \mathcal{V}\}$$

is positively invariant. □

Remark 3.2.2. Lemma 3.2.1 allows to reduce the dimension of the system (3.5) taking $x_i(t) = 1 - y_i(t)$ for every $t \geq 0$ and for every $i \in \mathcal{V}$. Hence, the network SI model is described by the following ODEs:

$$\dot{y}_i(t) = (1 - y_i(t)) \sum_j W_{ij} y_j, \quad \forall\, i \in \mathcal{V} \tag{3.7}$$

or, in the equivalent vector form

$$\dot{y}(t) = [1 - y(t)] W y(t) \tag{3.8}$$

The following result describes the dynamical behavior of an SI epidemic model as (3.8).

Theorem 3.2.3. *A network SI epidemic model with irreducible interaction matrix W as in (3.8) has the following properties:*

(i) the model presents two equilibrium points: the disease-free $\mathbf{0}$ *and the fully infected* $\mathbf{1}$*,*

(ii) the disease free equilibrium $\mathbf{0}$ *is unstable,*

(iii) the fully infected equilibrium $\mathbf{1}$ *is globally asymptotically stable on* $\mathcal{X} \setminus \{y = \mathbf{0}\}$.

Proof. (i) It is immediate to verify that both $\mathbf{0}$ and $\mathbf{1}$ satisfy the equilibrium equation

$$[1 - y(t)]Wy = 0. \tag{3.9}$$

Assume by contradiction that there exists another equilibrium point $y^* \notin \{\mathbf{0}, \mathbf{1}\}$ solving (3.9). Then, for every $i \in \mathcal{V}$, the i-th component y_i^* satisfies

$$(1 - y_i^*) \sum_{j \in \mathcal{V}} W_{ij} y_j^* = 0.$$

Since $y^* \neq \mathbf{1}$, there exists at least one index $i \in \mathcal{V}$ such that $y_i^* \neq 1$. For such an index, the previous equation reduces to

$$\sum_{j \in \mathcal{V}} W_{ij} y_j^* = 0.$$

Because $W_{ij} \geq 0$ for all i, j, this equality is equivalent to

$$\sum_{j : W_{ij} > 0} W_{ij} y_j^* = 0.$$

Therefore, $y_j^* = 0$ for every j such that $W_{ij} > 0$. Since the graph is strongly connected, or equivalently the matrix W is irreducible, this argument propagates through the network and implies that $y_i^* = 0$ for all $i \in \mathcal{V}$. This contradicts the assumption that $y^* \notin \{\mathbf{0}, \mathbf{1}\}$, and concludes the proof.

(ii) Consider the Jacobian of linearized system around the disease-free equilibrium $\mathbf{0}$:

$$J_{\mathbf{0}} = W$$

From Perron-Frobenius theorem reported in 3.1.1, the dominant eigenvalue of W is $\lambda_W > 0$. Hence the disease-free equilibrium $\mathbf{0}$ is unstable.

(iii) In order to prove the asymptotic stability of the fully infected equilibrium, we take the following Lyapunov function:

$$V(t) = \mathbf{1}^T(\mathbf{1} - y) \tag{3.10}$$

That is a C^1 function and positively definite in respect to $\mathbf{1}$. The time derivative of V is:

$$\dot{V}(t) = -\mathbf{1}^T \dot{y} = -\mathbf{1}^T [1 - y] W y$$

Hence, $\dot{V}(t) \leq 0$ for every $y \in [0,1]^n$ and $\dot{V}(t) = 0$ if and only if $y \in \{\mathbf{0}, \mathbf{1}\}$. For the invariance principle we can conclude that the fully infected equilibrium $\mathbf{1}$ is globally asymptotically stable on $\mathcal{X} \setminus \{y = \mathbf{0}\}$. □

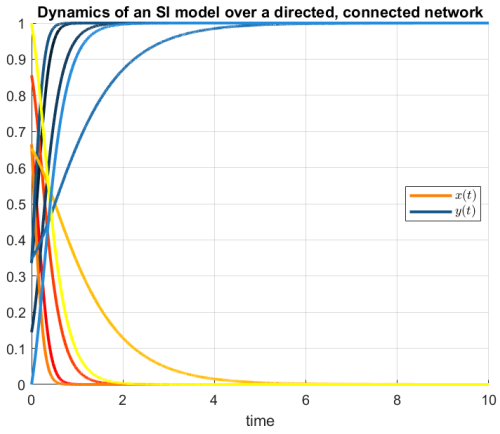

Figure 3.1: Dynamical behavior of an SI network model with $n = 5$ population.

3.2.2 Network SIS model

Unlike the previous model, the SIS network model accounts for the possibility of reinfection. Infected individuals recover from the disease at rate γ and immediately return to the susceptible compartment. This model is therefore appropriate for diseases for which multiple infections are common and no permanent immunity is acquired.
The dynamics of the SIS network model are described by the following system

of ordinary differential equations:

$$\begin{cases} \dot{x}_i(t) = -x_i(t) \sum_j W_{ij} y_j + \gamma y_i(t) \\ \dot{y}_i(t) = x_i(t) \sum_j W_{ij} y_j - \gamma y_i(t) \end{cases} \tag{3.11}$$

Lemma 3.2.4. *The space state $\mathcal{X}$ defined in (3.6) is positively invariant for the SIS network model (3.11). Furthermore, if $y(0) > 0$ then $y(t) > 0$ for every $t > 0$.*

Proof. The proof of the positive invariance of $\mathcal{X}$ follows the same arguments as in Lemma 3.2.1. Moreover, since $\dot{y}_i \geq -\gamma y_i$, it follows that

$$y(t) \geq e^{-\gamma t} y(0) > 0 \quad \forall\, t > 0,$$

which proves positivity of the infected compartment. □

Remark 3.2.5. As we see in the SI network model, we can reduce the dimension of the system using $x_i(t) = 1 - y_i(t)$ for every $t \geq 0$.

$$\dot{y}_i(t) = (1 - y_i(t)) \sum_j W_{ij} y_j(t) - \gamma y_i(t) \quad \forall\, i \in \mathcal{V} \tag{3.12}$$

or, in the equivalent vector form

$$\dot{y}(t) = [\mathbf{1} - y(t)] W y(t) - \gamma y(t) \tag{3.13}$$

Remark 3.2.6. The SIS network model in (3.13) defines a monotone dynamical system. We now recall a property of monotone dynamical systems that will be useful in the sequel.

Proposition 3.2.7. *Let $\varphi : \mathbb{R} \times X \to X$ be a monotone dynamical system on a compact state space X that admits both a minimal element $\underline{x}$ and a maximal element $\overline{x}$, and let $\underline{x}^* = \lim_{t\to\infty} \varphi(t, \underline{x})$ and $\overline{x}^* = \lim_{t\to\infty} \varphi(t, \overline{x})$ be the minimal and maximal equilibrium points, respectively. If $\underline{x}^* = \overline{x}^* = x^*$, then x^* is a globally asymptotically stable equilibrium point.*

The dynamical behavior of the SIS network model is summarized in the following theorem.

Theorem 3.2.8. *Consider the SIS network epidemic model as in (3.13) with irreducible interaction matrix W and recovering rate $\gamma > 0$. Let λ_W be the dominant eigenvalue of W. Then, the following properties hold:*

(i) the disease-free equilibrium $\mathbf{0}$ always exists;

(ii) there exists a unique endemic equilibrium $y^* > 0$ if and only if $\lambda_W > \gamma$;

(iii) if $\lambda_W \leq \gamma$, then the disease-free equilibrium $\mathbf{0}$ is globally asymptotically stable on $\mathcal{X}$;

(iv) if $\lambda_W > \gamma$, the disease-free equilibrium $\mathbf{0}$ is unstable and the endemic equilibrium y^* is globally asymptotically stable on $\mathcal{X} \setminus \{\mathbf{0}\}$.

Proof. (i) It is immediate to verify that $y = \mathbf{0}$ satisfies

$$[1 - y]Wy - \gamma y = 0$$

and therefore the disease-free equilibrium $\mathbf{0}$ always exists.

(ii) the proof of this property could be found in [41].

(iii) Let $\lambda_W \leq \gamma$. Consider the Lyapunov function $V(t) = \bar{v}^T y$, where $\bar{v}$ is the left eigenvector of W correspondent to the dominant eigenvalue λ_W. $V(t)$ is positive definite with respect to 0 on $[0,1]^n$. Moreover,

$$\dot{V}(t) = \bar{v}^T \dot{y} = \bar{v}^T[\mathbf{1} - y]Wy - \gamma \bar{v}^T y \leq \bar{v}^T Wy - \gamma \bar{v}^T y = (\lambda_W - \gamma)V(y) \leq 0$$

For first Lyapunov Theorem, the disease free equilibrium $\mathbf{0}$ is stable. From (ii) $\mathbf{0}$ is the unique equilibrium point, hence, using Proposition 3.2.7, we can conclude that the disease-free equilibrium point is globally asymptotically stable.

(iv) Let $\lambda_W > \gamma$. Consider the Jacobian matrix of the linearized system around $\mathbf{0}$:

$$J_{\mathbf{0}} = W - \gamma I$$

Since we are in case $\lambda_W > \gamma$, it is evident that $\mathbf{0}$ is unstable. Take the right eigenvector v of W associated to λ_W. Let us define $\zeta = \max\{v_i : 1 \leq i \leq n\}$ and $\bar{\varepsilon} = (\lambda_W - \gamma)/\lambda_W \zeta > 0$. For $\varepsilon > 0$, consider the hyper-rectangle

$$H_\varepsilon = \{x \in \mathbb{R}^n : \varepsilon v \leq x \leq \mathbf{1}\}.$$

We now show that H_ε is invariant for every $0 < \varepsilon < \bar{\varepsilon}$. Indeed, for every y in H_ε and $1 \leq i \leq n$ be such that $y_i = \varepsilon v_i$, we have $Wy \geq \varepsilon Wv = \varepsilon \lambda_W v$, so that

$$(Wy)_i \geq \varepsilon \lambda_W v_i = \lambda_W y_i$$

and

$$\dot{y}_i = (1 - y_i)(Wy)_i - \gamma y_i \geq (\lambda_W(1 - \varepsilon v_i) - \gamma) y_i \geq 0.$$

Observe that the invariant set H_ε is compact and contains a minimal element $\underline{y} = \varepsilon v$ and a maximal element $\overline{y} = \mathbf{1}$. By the uniqueness of the endemic equilibrium point proved in (ii), H_ε contains a unique equilibrium point $y^* > \mathbf{0}$. Then, for every $0 < \varepsilon < \bar{\varepsilon}$, we can apply Proposition 3.2.7 to the restricted dynamical system $\varphi : \mathbb{R} \times H_\varepsilon \to H_\varepsilon$, thus concluding that y^* is globally asymptotically stable in H_ε. From the arbitrariness of ε it follows that y^* attracts all points in

$$H = \bigcup_{0<\varepsilon<\bar{\varepsilon}} H_\varepsilon = \{y \in [0,1]^n : x > \mathbf{0}\}.$$

We can then apply Lemma 3.2.4 to conclude that the pandemic equilibrium y^* attracts the whole $[0,1]^n \setminus \{\mathbf{0}\}$.

□

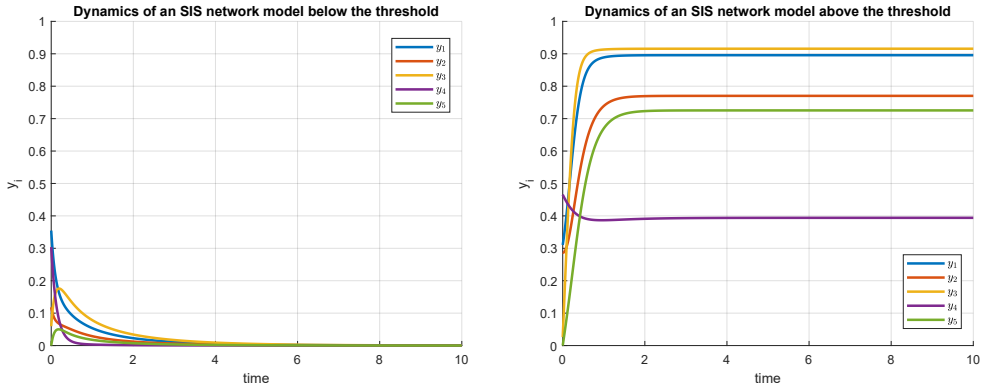

(a) SIS network with $\lambda_W < \gamma$ **(b)** SIS network with $\lambda_W > \gamma$

Figure 3.2: Dynamical behavior of an SIS network model with $n = 5$ population below and above the threshold.

3.2.3 Network SIR model

The Susceptible-Infected-Recovered (SIR) model on network considers permanent immunity. An infected individual recovers from disease at rate γ and remain in the recovered compartment, without possibility of becoming susceptible again. The dynamic of the SIR network model with interaction matrix W and recovery rate $\gamma > 0$ is described by the following ODEs:

$$\begin{cases} \dot{x}_i(t) = -x_i(t) \sum_j W_{ij} y_j(t) \\ \dot{y}_i(t) = x_i(t) \sum_j W_{ij} y_j(t) - \gamma y_i(t) \\ \dot{z}_i(t) = \gamma y_i(t) \end{cases} \tag{3.14}$$

Remark 3.2.9. Since it can be directly determined by (3.14), we can omit the equation for the evolution of the fraction of recovered individuals $z_i(t) = 1 - x_i(t) - y_i(t)$ and the above system becomes:

$$\begin{cases} \dot{x}_i(t) = -x_i(t) \sum_j W_{ij} y_j(t) \\ \dot{y}_i(t) = x_i(t) \sum_j W_{ij} y_j(t) - \gamma y_i(t) \end{cases} \tag{3.15}$$

Lemma 3.2.10. *The set*

$$\mathcal{X} = \{(x, y) \in \mathbb{R}^{2n}, x_i \geq 0, y_i \geq 0, x_i + y_i \leq 1, \forall\, i\}$$

is positively invariant for the SIR network model in (3.15).

Proof. Since $\{x_i = 0\}$ and $\{y_i = 0\}$ are invariant, $\{x_i \geq 0\}$ and $\{y_i \geq 0\}$ are positively invariant for every node $i \in \mathcal{V}$. Hence, the intersection $\{x_i \geq 0, y_i \geq 0, \forall\, i \in \mathcal{V}\}$ is positively invariant, because intersection of positively invariant sets. From the fact that $\dot{x}_i(t) + \dot{y}_i(t) = -\gamma y_i(t) \geq 0$ for every $y_i \geq 0$, we obtain that the set $\{x_i \geq 0, y_i \geq 0, x_i + y_i \leq 1\}$ is positively invariant. □

The SIR network model in (3.15) could be written in the equivalent vector form:

$$\dot{x} = -[x]Wy \qquad \dot{y} = [x]Wy - \gamma y \tag{3.16}$$

The following theorem establishes the dynamic behavior of the SIR network

model in (3.16).

Theorem 3.2.11. *Consider an SIR network model (3.16) with irreducible interaction matrix W and recovery rate $\gamma > 0$. Then, the following hold:*

(i) $\mathcal{X}^* = \{(x^*, \mathbf{0}),\ x^* \in [0,1]^n\}$ *is the set of equilibrium points;*

(ii) an equilibrium point $(x^*, \mathbf{0}) \in \mathcal{X}^*$ *is unstable if and only if* $\lambda_{\max}([x^*]W) > \gamma$

(iii) for every $i \in \{1, \cdots, n\}$, $x_i(t)$ *is nonincreasing for every* $t \geq 0$ *and* $x_i(t) > 0$ *if and only if* $x_i(0) > 0$ *for* $t \geq 0$;

(iv) if $y(0) > \mathbf{0}$, *then* $y(t) > \mathbf{0}$ *for* $t \geq 0$;

(v) there exists $x^* \in [0,1]^n$ *such that* $\mathbf{0} \leq x^* \leq x(0)$ *and*

$$\lim_{t\to\infty} x(t) = x^* \qquad \lim_{t\to\infty} y(t) = \mathbf{0}$$

Proof. (i) The equilibrium equations are

$$\mathbf{0} = -[x^*]Wy^* \qquad \mathbf{0} = [x^*]Wy^* - \gamma y^*$$

Assume by contradiction that there exists a couple (x^*, y^*) with $y^* \neq \mathbf{0}$ which solves the second equilibrium equation, we obtain

$$\mathbf{0} = \gamma y^*$$

And this is possible if and only if $y^* = \mathbf{0}$, hence the equilibrium points must be of the couples $(x^*, \mathbf{0})$ with $x^* \in [0,1]^n$.

(ii) The Jacobian matrix of the linearized system around the equilibrium point $(x^*, \mathbf{0})$ is the following block matrix

$$J_{(x^*,\mathbf{0})} = \begin{pmatrix} 0 & -[x^*]W \\ 0 & [x^*]W - \gamma I \end{pmatrix}$$

Hence, if the dominant eigenvalue of $[x^*]W$ is greater than γ, the equilibrium point is unstable.

(iii) It is evident that $\dot{x}_i = -x_i \sum_j W_{ij} y_j \leq 0$ for every $(x, y) \in \mathcal{X}$, hence x_i is nonincreasing, for every $i \in \{1, \cdots, n\}$. From (3.15),

$$x_i(t) = x(0) e^{-\int_0^t W y(s) ds} > 0 \quad \forall\, t \geq 0$$

for every $x_i(0) > 0$.

(iv) Fix an index i. By continuity of solutions, the function $y_i(t)$ is continuous. Suppose by contradiction that there exists $t_* > 0$ such that $y_i(t_*) = 0$. Define

$$t_0 := \inf\{t > 0 \mid y_i(t) = 0\}.$$

Then $y_i(t) > 0$ for all $t \in [0, t_0)$and $y_i(t_0) = 0$. Evaluating the equation for $\dot{y}_i$ at t_0, we obtain

$$\dot{y}_i(t_0) = x_i(t_0) \sum_j W_{ij} y_j(t_0) - \gamma y_i(t_0) = x_i(t_0) \sum_j W_{ij} y_j(t_0).$$

Since $x_i(t_0) \geq 0$, $W_{ij} \geq 0$, and $y_j(t_0) \geq 0$ for all j, it follows that

$$\dot{y}_i(t_0) \geq 0.$$

Therefore, the trajectory cannot cross the hyperplane $\{y_i = 0\}$ from the positive side. This contradicts the assumption that t_0 is the first time at which $y_i(t)$ vanishes. Hence, $y_i(t) > 0$ for all $t \geq 0$. Since the argument holds for every component i, we conclude that

$$y(t) > \mathbf{0} \quad \text{for all } t \geq 0.$$

(v) Since $\dot{x}(t) \leq \mathbf{0}$ and $x(t) \geq \mathbf{0}$ for every $t \geq 0$, there exists $\lim_{t\to\infty} x(t)$. From the nonincreasing behavior of $x(t)$ we also have that $\lim_{t\to\infty} \dot{x}(t) = \mathbf{0}$ which implies that either $\lim_{t\to\infty} x(t) = \mathbf{0}$ or $\lim_{t\to\infty} y(t) = \mathbf{0}$. If $x(t)$ converges to $\mathbf{0}$, then $\dot{y}(t)$ converges to $-\gamma y(t)$. Hence $y(t) \to y(0)e^{-\gamma t}$ which converges to $\mathbf{0}$. If $x(t)$ converges to some $x^* \in [0,1]^n$, then $y(t)$ still converges to $\mathbf{0}$. □

Remark 3.2.12. Despite the other two models we considered above, the SIR network does not allow the existence of an endemic equilibrium point, hence the disease must disappear.

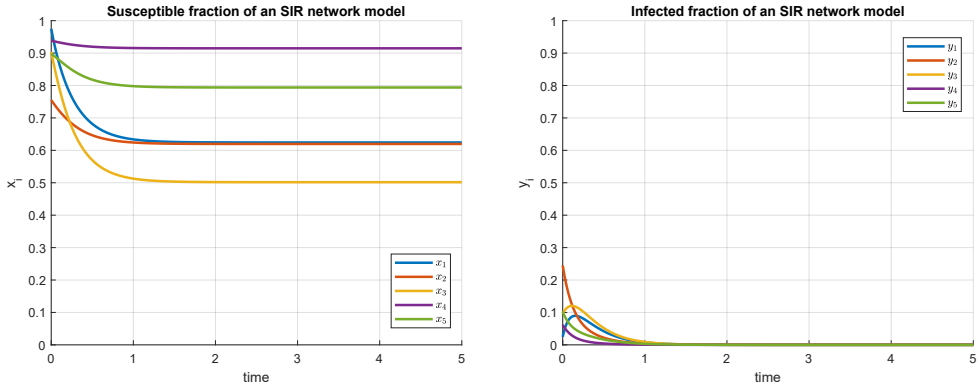

(a) Susceptible fraction **(b)** Infected fraction

Figure 3.3: Dynamical behavior of an SIR network model.

Chapter 4

Dynamical Behavior of a Network SIRS Epidemic Model

In this chapter, we analyze the main objective of this thesis: the network SIRS epidemic model. This model generalizes the corresponding scalar SIRS model discussed in 2.4 by considering interactions within a network. We begin by introducing the model and presenting some preliminary results regarding the well-posedness of the system. In Section 4.2, we focus on the identification of the equilibrium points of the system. Unlike the scalar case, the endemic equilibrium cannot, in general, be expressed explicitly; only in a few special cases is an analytical expression possible. However, we develop an iterative method to approximate it, which proves particularly useful for numerical simulations. In Section 4.3, we analyze the stability of the equilibrium points, when they exist. The main goal of this thesis is to determine the stability properties of the endemic equilibrium above the epidemic threshold. Constructing a suitable Lyapunov function for this purpose is a huge challenge. To overcome this, we employ a method based on Schur complement properties, which allows us not only to establish the local asymptotic stability of the endemic equilibrium but also to derive an upper bound on its convergence rate. Finally, in Section 4.4, we consider the special case of a rank-one interaction matrix. In this scenario, it is possible to

prove the global stability of the endemic equilibrium for all initial conditions with nonzero infection. This special case provides insights into the region of attraction of the endemic equilibrium, which we further explore and validate through the numerical simulations presented in the next chapter.

4.1 Introduction to the model

We consider an SIRS epidemic model defined over a network composed of a finite number of interacting populations. As for the other network-based models seen in Chapter 3, the network is described as a directed, weighted, and strongly connected graph $\mathcal{G} = (\mathcal{V}, \mathcal{E}, W)$, where $\mathcal{V}$ is the finite set of nodes and $\mathcal{E} \subseteq \mathcal{V} \times \mathcal{V}$ is the set of directed edges. The nonnegative irreducible interaction matrix $W \in \mathbb{R}_+^{\mathcal{V}\times\mathcal{V}}$ describes the interactions between populations. Every population i in $\mathcal{V}$ has a specific recovery rate $\gamma_i > 0$ and loss of immunity rate $\delta_i > 0$. In this network setting, the basic reproduction number R_0, which characterizes the epidemic threshold, is defined as

$$R_0 = \lambda_{max}([\gamma]^{-1}W),$$

where $\lambda_{max}(\cdot)$ denotes the dominant eigenvalue.

Definition 4.1.1 (Network SIRS epidemic model)**.** A network SIRS epidemic model with interaction matrix $W \in \mathbb{R}_+^{\mathcal{V}\times\mathcal{V}}$, recovery rate vector $\gamma \in \mathbb{R}_+^{\mathcal{V}}$ and loss of immunity rate vector $\delta \in \mathbb{R}_+^{\mathcal{V}}$, is described by the following ODE system:

$$\begin{cases} \dot{x}_i(t) = -\sum_j W_{ij}\, y_j(t)\, x_i(t) + \delta_i z_i(t) \\ \dot{y}_i(t) = \sum_j W_{ij}\, y_j(t)\, x_i(t) - \gamma_i y_i(t) \\ \dot{z}_i(t) = \gamma_i y_i(t) - \delta_i z_i(t) \end{cases} \tag{4.1}$$

for every i in $\mathcal{V}$.

It is natural to assume that the dynamics of the model evolves in the following state space.

Definition 4.1.2. The state space of the system (4.1) is defined as

$$\mathcal{X} = \{(x, y, z) \in \mathbb{R}_+^{\mathcal{V}} \times \mathbb{R}_+^{\mathcal{V}} \times \mathbb{R}_+^{\mathcal{V}} : x + y + z \leq \mathbf{1}\} \tag{4.2}$$

The following lemma ensures that the dynamics are well defined in the state space $\mathcal{X}$.

Lemma 4.1.3. *Consider the network SIRS epidemic model defined in (4.1) with interaction matrix $W \in \mathbb{R}_+^{\mathcal{V}\times\mathcal{V}}$, recovery rate vector $\gamma \in \mathbb{R}_+^{\mathcal{V}}$ and loss of immunity rate vector $\delta \in \mathbb{R}_+^{\mathcal{V}}$. For every initial condition $(x(0), y(0), z(0)) \in \mathcal{X}$, the system (4.1) admits a unique solution $(x(t), y(t), z(t))$, which remains in $\mathcal{X}$ for all $t \geq 0$.*

Proof. The global existence and uniqueness of solutions follow directly from the Cauchy–Lipschitz theorem, since the vector field in (4.1) is locally Lipschitz.
From the fact that

$$\dot{x}_i(t) + \dot{y}_i(t) + \dot{z}_i(t) = 0, \quad \forall t \in \mathbb{R}, \quad \forall i \in \mathcal{V}$$

we have that the set

$$\{(x, y, z) \in \mathbb{R}^{\mathcal{V}\times\mathcal{V}\times\mathcal{V}} : x_i + y_i + z_i = 1, \forall i \in \mathcal{V}\} \tag{4.3}$$

is invariant. Furthermore, if $y_i(0) = 0 \quad \forall i$, we have from (4.1):

$$\dot{y}_i = \sum_j W_{ij} y_j x_i - \gamma_i y_i = 0 \qquad \forall t \in \mathbb{R}$$

so the set $\{y_i = 0, \forall i \in \mathcal{V}\}$ is invariant. Hence, also the set $\{y_i \geq 0, \forall i \in \mathcal{V}\}$ is invariant. From (4.1), we have that, if $z_i(0) = 0$, then $\dot{z}_i = \gamma y_i \geq 0$ whenever $y_i \geq 0$. Therefore, trajectories on $z_i = 0$ cannot cross into the region $z_i < 0$. So, if $z_i(0) \geq 0$ and $y_i(0) \geq 0$, hence $z_i(t) \geq 0$ for all $t \geq 0$. We can thus conclude that the set $\{\, y_i \geq 0,\ z_i \geq 0,\ \forall i \in \mathcal{V}\}$ is positively invariant, since it is the intersection of two positively invariant sets. To conclude the proof, let us observe that if $x_i(0) = 0$, then $\dot{x}_i = \delta z_i \geq 0$ whenever $z_i \geq 0$. Hence, the set

$$\{(x, y, z) \in \mathbb{R}^{\mathcal{V}\times\mathcal{V}\times\mathcal{V}} : x_i, y_i, z_i \geq 0, \forall i \in \mathcal{V}\}$$

is positively invariant and using (4.3), the intersection

$$\mathcal{X} = \{x_i + y_i + z_i = 1, \forall i\} \cap \{x_i \geq 0, y_i \geq 0, z_i \geq 0, \forall i\}$$

is positively invariant and this concludes the proof. □

Remark 4.1.4. From the fact that $\mathcal{X}$ is positively invariant, it follows that for every admissible triple (x, y, z) in $\mathcal{X}$ there is a unique pair (y, z) satisfying $y, z \geq 0$ and $y + z \leq \mathbf{1}$; the map

$$\Theta : \mathcal{X} \to \mathcal{X}', \qquad \Theta\big((x, y, z)\big) = (y, z),$$

is a bijection with inverse $\Theta^{-1}(y, z) = (1 - y - z, y, z)$. Therefore it is natural and equivalent to describe the dynamics on the reduced state space

$$\mathcal{X}' = \{(y, z) \in \mathbb{R}_+^{\mathcal{V}} \times \mathbb{R}_+^{\mathcal{V}} : \ y + z \leq \mathbf{1}\},$$

obtaining the following equivalent system after substituting $x_i = 1 - y_i - z_i$:

$$\begin{cases} \dot{y}_i = \sum_j W_{ij}\, y_j\, (1 - y_i - z_i) - \gamma_i y_i \\ \dot{z}_i = \gamma_i y_i - \delta_i z_i \end{cases} \tag{4.4}$$

Positive invariance of $\mathcal{X}$ implies positive invariance of $\mathcal{X}'$, so trajectories of (4.4) starting in $\mathcal{X}'$ remain in $\mathcal{X}'$ for all $t \geq 0$.

For the following sections it is useful to write the system (4.4) in the vector form:

$$(\dot{y}, \dot{z}) = f(y, z) = \begin{pmatrix} [1 - y - z]Wy - [\gamma]y \\ [\gamma]y - [\delta]z \end{pmatrix} \tag{4.5}$$

In the following, we will often make use of this reduced form.

From an epidemiological viewpoint, once the infection is introduced in the network, it cannot disappear instantaneously. The following theorem formalizes this intuition by proving that, if the infected fraction is initially strictly positive in at least one node, then the infection remains strictly positive in all nodes for any positive time.

Theorem 4.1.5. *Consider the network SIRS epidemic model defined in* (4.1) *with irreducible interaction matrix* $W \in \mathbb{R}_+^{\mathcal{V}\times\mathcal{V}}$*, positive recovery rate vector* $\gamma \in \mathbb{R}_{++}^{\mathcal{V}}$ *and positive loss of immunity rate vector* $\delta \in \mathbb{R}_{++}^{\mathcal{V}}$*. For every initial*

condition $(x(0), y(0), z(0)) \in \mathcal{X}$ *with* $y(0) \gneq \mathbf{0}$*, then we have that* $y(t) > \mathbf{0}$ *for every* $t > 0$*.*

The proof of the theorem relies on the following technical lemma.

Lemma 4.1.6. *Consider the network SIRS epidemic model defined in (4.1) with irreducible interaction matrix* $W \in \mathbb{R}_+^{\mathcal{V}\times\mathcal{V}}$*, positive recovery rate vector* $\gamma \in \mathbb{R}_{++}^{\mathcal{V}}$ *and positive loss of immunity rate vector* $\delta \in \mathbb{R}_{++}^{\mathcal{V}}$*. Consider an initial condition* $(x(0), y(0), z(0)) \in \mathcal{X}$ *with* $y(0) \gneq \mathbf{0}$ *and let* $j \in \mathcal{V}$ *be such that* $y_j(0) > 0$ *and* $i \in \mathcal{V}$ *such that* $y_i(0) = 0$*. Let* Λ_{ij} *be a path from node* i *to node* j *of minimum length* α_{ij}*. Define*

$$m_{ij} := \Big|\{k \in \Lambda_{ij} : k \neq j, \text{ and } z_k(0) = 1\}\Big|.$$

Then

$$y_i^{(\beta)}(0) \geq 0 \quad \forall \beta = 1, \dots, \alpha_{ij} + m_{ij} - 1,$$

and

$$y_i^{(\alpha_{ij}+m_{ij})}(0) > 0.$$

Proof. We first compute the r-th time derivative of y_i. Since

$$\dot{y}_i = \sum_j W_{ij} y_j (1 - y_i - z_i) - \gamma_i y_i$$

Let $f(t) = \sum_j W_{ij} y_j$ and $g(t) = 1 - y_i - z_i$, for the Leibniz's rule we have the $(r-1)$-th time derivative of $f \cdot g$ is:

$$(fg)^{(r-1)} = \sum_{h=0}^{r-1} \binom{r-1}{h} f^{(h)} g^{(r-1-h)}$$

Hence, the r-th time derivative of y_i is

$$\begin{aligned} y_i^{(r)} =& \dot{y}_i^{(r-1)} \\ =& (fg)^{(r-1)} - \gamma_i y_i^{(r-1)} \\ =& \sum_{h=0}^{r-1} \binom{r-1}{h} f^{(h)} g^{(r-1-h)} - \gamma_i y_i^{(r-1)} \end{aligned}$$

and using the definitions of f and g, we obtain

$$y_i^{(r)} = \sum_{h=0}^{r-1} \binom{r-1}{h} \sum_j W_{ij} y_j^{(h)} (1 - y_i - z_i)^{(r-1-h)} - \gamma_i y_i^{(r-1)} \tag{4.6}$$

Now, we can proceed by induction on the path length α_{ij}.
Take $\alpha_{ij} = 1$: in this case $W_{ij} > 0$ and

$$m_{ij} = \begin{cases} 0, & \text{if } z_i(0) < 1, \\ 1, & \text{if } z_i(0) = 1. \end{cases}$$

If $z_i(0) < 1$, using $y_i(0) = 0$ we obtain

$$\begin{aligned} \dot{y}_i(0) &= \sum_\ell W_{i\ell} y_\ell(0)(1 - y_i(0) - z_i(0)) - \gamma_i y_i(0) \\ &\geq W_{ij} y_j(0)(1 - z_i(0)) > 0 \end{aligned}$$

which proves the claim.

If $z_i(0) = 1$, then $\dot{y}_i(0) = 0$ and we compute the second derivative, using (4.6):

$$\begin{aligned} \ddot{y}_i(0) &= \sum_\ell W_{i\ell} \dot{y}_\ell(0)(1 - y_i(0) - z_i(0)) \\ &\quad + \sum_\ell W_{i\ell} y_\ell(0)(-\dot{y}_i(0) - \dot{z}_i(0)) - \gamma_i \dot{y}_i(0) \\ &\geq -W_{ij} y_j(0) \dot{z}_i(0). \end{aligned}$$

Since $z_i(0) = 1$ and $\dot{z}_i(0) = -\delta_i z_i(0) < 0$, it follows that $\ddot{y}_i(0) > 0$, completing the base case.
Assume that the statement holds for all pairs (k, j) such that $\alpha_{kj} = \alpha$. Let Λ_{ij} be a path of length $\alpha + 1$ and let k be the successor of i in Λ_{ij}, so that $W_{ik} > 0$ and $\alpha_{kj} = \alpha$.
If $z_i(0) < 1$, then $m_{ij} = m_{kj}$. Using (4.6) and evaluating at $t = 0$:

$$y_i^{(\beta)}(0) \geq W_{ik} y_k^{(\beta-1)}(0)(1 - z_i(0))$$

By the inductive hypothesis,

$$y_k^{(r)}(0) \geq 0 \quad \text{for } r \leq \alpha + m_{kj} - 1, \quad y_k^{(\alpha+m_{kj})}(0) > 0.$$

Hence

$$y_i^{(\beta)}(0) \geq 0 \quad \text{for } \beta \leq (\alpha+1) + m_{ij} - 1, \quad y_i^{((\alpha+1)+m_{ij})}(0) > 0.$$

If $z_i(0) = 1$, then $m_{ij} = m_{kj} + 1$. In this case $1 - y_i(0) - z_i(0) = 0$, and the first nonzero contribution arises from the derivative of $(1 - y_i - z_i)$. From (4.6) we obtain

$$y_i^{(\beta)}(0) \geq W_{ik} y_k^{(\beta-2)}(0)(1 - y_i - z_i)'(0).$$

Since $(1 - y_i - z_i)'(0) = -\dot{z}_i(0) = \delta_i z_i(0) > 0$, using the inductive hypothesis we conclude that

$$y_i^{(\beta)}(0) \geq 0 \quad \text{for } \beta \leq (\alpha+1) + m_{ij} - 1, \quad y_i^{((\alpha+1)+m_{ij})}(0) > 0.$$

This completes the inductive step and the proof.

□

We are now ready to prove the theorem.

Proof of Theorem 4.1.5. Using Lemma 4.1.6 we obtain that for every $i \in \mathcal{V}$, there exists $r_i \in \mathbb{N}$ such that

$$y_i^{(r_i)}(0) > 0, \quad \text{and} \quad y_i^{(\beta)}(0) \geq 0 \text{ for all } \beta < r_i \tag{4.7}$$

This means that there exists a right neighborhood $(0, \epsilon_i)$ of the origin with $\epsilon_i > 0$ such that $y_i(t) > 0, \ \forall\, t \in (0, \epsilon_i)$. Let $\epsilon = \min_{i \in \mathcal{V}} \epsilon_i$, so that $y_i(t) > 0$ for all $i \in \mathcal{V}$ and all $t \in (0, \epsilon)$. Since the set $\{y = 0\}$ is invariant for the system, no trajectory starting outside it can reach it in finite time. Hence, $y(t) > 0, \ \forall\, t > 0$. □

4.2 Equilibrium points

In this section we investigate the existence and uniqueness of equilibrium points of the system in Definition 4.1.1. Since $[\gamma]^{-1}W \in \mathbb{R}_+^{\mathcal{V}\times\mathcal{V}}$ is irreducible, for Perron-Frobenius theory (see Section 3.1.1), this matrix admits a dominant eigenvalue

$$\lambda_{max} = \rho([\gamma]^{-1}W)$$

Furthermore there exist two positive eigenvectors $v > \mathbf{0}$ and $\bar{v} > \mathbf{0}$ such that

$$v = \frac{1}{\lambda_{max}}[\gamma]^{-1}Wv \tag{4.8}$$

$$\bar{v}^T = \frac{1}{\lambda_{max}}\bar{v}^T[\gamma]^{-1}W \tag{4.9}$$

and we refer to v and $\bar{v}$ as the right and left eigenvector of $[\gamma]^{-1}W$ associated to the dominant eigenvalue λ_{max}.

It is evident that $(\mathbf{1}, \mathbf{0}, \mathbf{0})$ is always an equilibrium point of the system (4.1); we denote this equilibrium as the disease-free equilibrium. Observe that, if (x^*, y^*, z^*) is an equilibrium such that $y^* \gneq 0$ then, by Lemma 4.1.6, it must be $y^* > 0$. We shall refer to such an equilibrium as to the endemic equilibrium.

The following definitions and properties are useful to investigate the existence and uniqueness of equilibria of system (4.1).

Definition 4.2.1. We define:

$$\begin{aligned} &\psi_i : \mathbb{R}_+ \times \mathbb{R}_+ \to \mathbb{R}_+ \\ &\psi_i(y_i, \alpha_i) = \frac{y_i}{1 + (1+\alpha_i)y_i} \end{aligned} \tag{4.10}$$

$$\begin{aligned} &\Psi : \mathbb{R}_+^{\mathcal{V}} \times \mathbb{R}_+^{\mathcal{V}} \to \mathbb{R}_+^{\mathcal{V}} \\ &(\Psi(y, \alpha))_i = \psi_i(y_i, \alpha_i) \end{aligned} \tag{4.11}$$

$$\begin{aligned} &\Phi : \mathbb{R}_+^{\mathcal{V}} \times \mathbb{R}_+^{\mathcal{V}\times\mathcal{V}} \times \mathbb{R}_+^{\mathcal{V}} \to \mathbb{R}_+^{\mathcal{V}} \\ &\Phi(y, M, \alpha) = \Psi(My, \alpha) \end{aligned} \tag{4.12}$$

The following lemma allows us to reduce the problem of finding equilibria to that of finding fixed points of the function Φ.

Lemma 4.2.2. *Consider the network SIRS epidemic model defined in (4.1) with irreducible interaction matrix $W \in \mathbb{R}_+^{\mathcal{V}\times\mathcal{V}}$, positive recovery rate vector $\gamma \in \mathbb{R}_{++}^{\mathcal{V}}$ and positive loss of immunity rate vector $\delta \in \mathbb{R}_{++}^{\mathcal{V}}$. Then $(x^*, y^*, z^*) \in \mathcal{X}$ is an equilibrium point if and only if*

$$y^* = \Phi(y^*, [\gamma]^{-1}W, [\delta]^{-1}\gamma), \quad z^* = [\gamma][\delta]^{-1}y^*, \quad x^* = 1 - y^* - z^*.$$

Proof. At equilibrium, the system satisfies the following relations:

$$x^* = 1 - y^* - z^* \tag{4.13}$$

$$z^* = [\gamma][\delta]^{-1}y^* \tag{4.14}$$

$$\Big(I - [([\gamma] + [\delta])[\delta]^{-1}y^*]\Big)Wy^* = [\gamma]y^* \tag{4.15}$$

From (4.14), the equilibrium point must be $(1 - y^* - [\gamma][\delta]^{-1}y^*, y^*, [\gamma][\delta]^{-1}y^*)$ for some y^* such that

$$y^* \in \prod_{i\in\mathcal{V}} \left[0, \frac{1}{1 + \frac{\gamma_i}{\delta_i}}\right] \tag{4.16}$$

Consider the equilibrium equation (4.15) componentwise:

$$\frac{1}{\gamma_i}(Wy^*)_i = \frac{y_i^*}{1 - \frac{\gamma_i+\delta_i}{\delta_i}y_i^*} \tag{4.17}$$

We note that the right side coincides with the inverse of $\psi_i\left(y_i^*, \frac{\gamma_i}{\delta_i}\right)$. Hence

$$y_i^* = \Psi_i(([\gamma]^{-1}Wy^*)_i, \frac{\gamma_i}{\delta_i}) = \Phi_i(y^*, [\gamma]^{-1}W, [\delta]^{-1}\gamma)$$

Hence, finding an equilibrium point for the system (4.1) is equivalent to find a fixed point for the equation $\Phi(y, [\gamma]^{-1}W, [\delta]^{-1}\gamma)$. □

Lemma 4.2.3. *Consider the function* Φ *defined in* (4.12)*. Then the following properties hold:*

(i) $\Phi(\mathbf{0}, M, \alpha) = \mathbf{0}$*, for every* M *and* α*,*

(ii) $\Phi(y, M, \alpha)$ *is concave in* y*, for every* M *and* α*,*

(iii) $\Phi(y, M, \alpha) < My$*, for every* $y > 0$ *and irreducible* M*,*

(iv) $\Phi(y, M, \alpha)$ *is:*

(a) nondecreasing in y*, for every fixed* M *and* α

(b) nondecreasing in M*, for every fixed* y *and* α

(c) nonincreasing in α*, for every fixed* y *and* M*.*

(v) $\Phi(y, M, \alpha) < [\mathbf{1} + \alpha]^{-1}\mathbf{1}$ *for every* y *and* M*,*

Proof. (i) It follows directly from the fact that $\psi_i(0, \alpha_i) = 0$.

(ii) Since for every i in $\mathcal{V}$ $\psi_i(y_i, \alpha_i)$ is concave, then $\Psi(y, \alpha)$ is concave. Hence, for every $y, \bar{y} \in \mathcal{V}$, and for every $t \in [0,1]$,

$$\begin{aligned}\Phi(ty + (1-t)\bar{y}, M, \alpha) &= \Psi(tMy + (1-t)M\bar{y}, \alpha) \\ &\geq t\Psi(My, \alpha) + (1-t)\Psi(M\bar{y}, \alpha) \\ &= t\Phi(y, M, \alpha) + (1-t)\Phi(\bar{y}, M, \alpha)\end{aligned}$$

Hence Φ is concave.

(iii) Since, for every i in $\mathcal{V}$, $\psi_i(y_i, \alpha_i) < y_i$ for every $y_i > 0$, then $\Psi(y, \alpha) < y$ for every $y > \mathbf{0}$. Then, by definition of Φ,

$$\Phi(y, M, \alpha) = \Psi(My, \alpha) < My$$

for every $y > \mathbf{0}$ and irreducible M.

(iv) Using the definition of Φ,

$$(\Phi(y, M, \alpha))_i = \psi_i((My)_i, \alpha_i) = \frac{\sum_j M_{ij} y_j}{1 + (1 + \alpha_i) \sum_j M_{ij} y_j}$$

we obtain

$$\frac{\partial(\Phi(y, M, \alpha))_i}{\partial y_j} = \frac{M_{ij}}{(1 + (1 + \alpha_i) \sum_j M_{ij} y_j)^2} \geq 0$$

$$\frac{\partial(\Phi(y, M, \alpha))_i}{\partial M_{ij}} = \frac{y_j}{(1 + (1 + \alpha_i) \sum_j M_{ij} y_j)^2} \geq 0$$

$$\frac{\partial(\Phi(y, M, \alpha))_i}{\partial \alpha_i} = -\frac{(\sum_j M_{ij} y_j)^2}{(1 + (1 + \alpha_i) \sum_j M_{ij} y_j)^2} \leq 0$$

and this concludes the proof.

(v) For every i in $\mathcal{V}$,

$$\lim_{y \to \infty} (\Phi(y, M, \alpha))_i = \frac{1}{1 + \alpha_i}$$

Then, by Lemma 4.2.3(iv)a, $\Phi(y, M, \alpha)$ is upper bounded by the vector $[\mathbf{1} + \alpha]^{-1}\mathbf{1}$.

□

Remark 4.2.4. In the proof of Lemma 4.2.2 we pointed out that the equilibrium y^* of the system (4.1) must be in the compact set defined in (4.16). We define, for every $\alpha \in \mathbb{R}_+^{\mathcal{V}}$, the compact set:

$$\mathcal{Y} = \prod_{i \in \mathcal{V}} \left[0, \frac{1}{1 + \alpha_i}\right] \tag{4.18}$$

Since, from Lemma 4.2.3(v), $Im(\Phi) \subseteq \mathcal{Y}$, we can restrict, for every fixed $M \in \mathbb{R}_+^{\mathcal{V} \times \mathcal{V}}$ and $\alpha \in \mathbb{R}_+^{\mathcal{V}}$, Φ on $\mathcal{Y}$:

$$\Phi : \mathcal{Y} \to \mathcal{Y}$$

Lemma 4.2.5. *For every nonnegative $M \in \mathbb{R}_+^{\mathcal{V} \times \mathcal{V}}$ and nonnegative vector $\alpha \in \mathbb{R}_+^{\mathcal{V}}$. Consider the function $\Phi : \mathcal{Y} \to \mathcal{Y}$ defined in (4.12). Define the*

discrete time

$$y(t) = \Phi^t(y(0)) \quad \forall t \in \mathbb{N} \tag{4.19}$$

with initial condition $y(0) \in \mathcal{Y}$. *Let* $\bar{y}$ *be the maximal element of the compact set* $\mathcal{Y}$ *and consider the discrete time system defined in* (4.19) *with initial condition* $y(0) = \bar{y}$. *Then, there exists*

$$\lim_{t\to\infty} y(t) = \bar{y}^*$$

such that $\bar{y}^* = \Phi(\bar{y}^*)$. *Moreover,* $\bar{y}^* \geq y^*$, *for every* $y^* = \Phi(y^*)$ *fixed point.*

Proof. Since $y(0) = \bar{y}$ is the maximal element of $\mathcal{Y}$ and Φ is nondecreasing in y (see Lemma 4.2.3(iv)a),

$$y(1) = \Phi(y(0)) = \Phi(\bar{y}) \leq \bar{y} = y(0)$$

and

$$y(t+1) = \Phi^t(y(1)) \leq \Phi^t(y(0)) = y(t)$$

Hence $y(t)$, with initial condition $y(0) = \bar{y}$, is nonincreasing. Since $\mathcal{Y}$ is compact, then $y(t)$ must converge to some limit:

$$\bar{y}^* = \lim_{t\to\infty} y(t)$$

But, by the continuity of $\Phi(y)$,

$$\bar{y}^* = \lim_{t\to\infty} y(t) = \lim_{t\to\infty} y(t+1) = \lim_{t\to\infty} \Phi(y(t)) = \Phi(\bar{y}^*)$$

Hence $\bar{y}^*$ is a fixed point. Moreover, for every other fixed point $y^* = \Phi(y^*)$, since the system is monotone, it must be $y^* \leq \bar{y}^*$. □

Theorem 4.2.6. *Let* $M \in \mathbb{R}_+^{\mathcal{V}\times\mathcal{V}}$ *be irreducible. Let* $\lambda_{max} = \rho(M)$ *be the dominant eigenvalue of* M. *Let* $\alpha \in \mathbb{R}_+^{\mathcal{V}}$ *and* $\Phi(y, M, \alpha) = \Phi(y)$. *Consider the discrete time system defined in* (4.19). *Then,*

(i) if $\lambda_{max} \leq 1$, $\mathbf{0}$ *is the unique fixed point of* $\Phi(y)$ *and for every* $y(0) \in \mathcal{Y}$, $\lim_{t\to\infty} y(t) = 0$;

(ii) if $\lambda_{max} > 1$, $\Phi(y)$ *admits two distinct fixed points:* $\mathbf{0}$ *and* $y^* > 0$, *and,*

for every $i \in \mathcal{V}$,

$$\Phi_i(y) > y_i \qquad \textit{if and only if} \qquad 0 < y_i < y_i^*$$

$$\Phi_i(y) < y_i \qquad \textit{if and only if} \qquad y_i > y_i^* > 0$$

Furthermore, for every $y(0) > 0$, $\lim_{t\to\infty} y(t) = y^*$.

Proof. (i) From Lemma 4.2.3(i), $\mathbf{0}$ is a fixed point of $\Phi(y)$ for every M and α. Assume by contradiction that there exists $y > 0$ such that $\Phi(y) = y$. From Lemma 4.2.3(iii)

$$y = \Phi(y) < My$$

This implies that, since $y > 0$,

$$\min_i \frac{(My)_i}{y_i} > 1 \tag{4.20}$$

Consider the characterization of the spectral radius of an irreducible nonnegative matrix reported in Section 3.1.1 :

$$\rho(A) = \max_{x>0} \min_{i\in\mathcal{V}} \frac{(Ax)_i}{x_i}. \tag{4.21}$$

Applying this formula to the irreducible matrix M, (4.20) implies that

$$\lambda_{\max} = \rho(M) > 1,$$

which contradicts the assumption $\lambda_{\max} \leq 1$. Hence, in case $\lambda_{max} \leq 1$, $\mathbf{0}$ is the unique fixed point of $\Phi(y)$. For every $y(0) \in \mathcal{Y}$, we have that $\mathbf{0} \leq y(0) \leq \bar{y}$, where $\bar{y}$ is the maximal element of $\mathcal{Y}$. Since $\mathbf{0}$ is the unique fixed point of Φ, from Lemma 4.2.5 it must be $\bar{y}^* = \mathbf{0}$. Hence, for every $y(0) \in \mathcal{Y}$,

$$\mathbf{0} \leq y(0) \leq \bar{y}$$

and, since Φ is nondecreasing:

$$\mathbf{0} = \Phi^t(0) \leq \Phi^t(y(0)) \leq \Phi^t(\bar{y})$$

hence

$$\mathbf{0} \leq \lim_{t\to\infty} \Phi^t(y(0)) \leq \lim_{t\to\infty} \Phi^t(y(0)) = \bar{y}^*$$

and by comparison theorem it must be

$$\lim_{t\to\infty} y(t) = \mathbf{0}$$

(ii) Assume now that $\lambda_{\max} > 1$. Consider the right eigenvector v associated to the dominant eigenvalue of M as in (4.8). Take $\varepsilon > 0$,

$$\Phi(\varepsilon v) = \Psi(M\varepsilon v) = \Psi(\lambda_{max}\varepsilon v)$$

Observe that

$$\nabla\Phi(0) = \nabla\Psi(0)M = M \tag{4.22}$$

By expanding Φ in a Taylor series around 0 and using (4.22), we obtain

$$\begin{aligned} \Phi(\varepsilon v) =& \Phi(0) + M\varepsilon v + o(\varepsilon) \\ =& \lambda_{\max}\varepsilon v + o(\varepsilon) \quad \text{for } \varepsilon \to 0 \end{aligned} \tag{4.23}$$

Using $\lambda_{max} > 1$ and Lemma 4.2.3(i), there exists $\varepsilon^* > 0$ such that

$$\Phi(\varepsilon^* v) \geq \varepsilon^* v \tag{4.24}$$

By defining $y^0 = \varepsilon^* v$ we can build the sequence

$$y^0 = \varepsilon^* v > \mathbf{0}$$

$$y^{k+1} = \Phi(y^k)$$

From (4.24), $y^1 = \Phi(y^0) \geq y^0$ and from the monotonicity properties of Φ and Lemma 4.2.3(v), the sequence is therefore increasing and bounded:

$$0 < y^0 \leq \cdots \leq y^k \leq y^{k+1} \leq \cdots < (\frac{1}{1+\alpha_1}, \cdots, \frac{1}{1+\alpha_n})$$

Therefore, from the continuity of Φ, the sequence necessarily converges

to some limit $y^* > 0$:

$$\Phi(y^*) = \lim_{k\to\infty} \Phi(y^k) = \lim_{k\to\infty} y^{k+1} = y^*$$

Thus, there exists a positive fixed point $y^* > 0$ of Φ satisfying

$$y^* = \Phi(y^*) \tag{4.25}$$

Once existence has been established, it remains to prove uniqueness. To do so, let us suppose that exist two positive fixed point $y^{**} > 0$ and $y^* > 0$ such that

$$\Phi(y^{**}) = y^{**} \qquad \Phi(y^*) = y^*$$

and assume by contradiction that

$$y^{**} \neq y^*$$

From Lemma 4.2.2 y^{**} and y^* are equilibrium points of the model in (4.1). Without loss of generality we can assume that

$$y_1^* > y_1^{**}, \tag{4.26}$$

and

$$\frac{y_1^*}{y_1^{**}} \geq \frac{y_j^*}{y_j^{**}}, \qquad j \in \mathcal{V}. \tag{4.27}$$

Then, we have

$$\begin{aligned} 0 &= \frac{y_1^{**}}{y_1^*}\left((1-(1+\frac{\gamma_1}{\delta_1})y_1^*)\sum_j W_{1j}y_j^* - \gamma_1 y_1^*\right) \\ &< (1-(1+\frac{\gamma_1}{\delta_1})y_1^{**})\sum_j W_{1j}\frac{y_1^{**}}{y_1^*}y_j^* - \gamma_1 y_1^{**} \\ &\leq (1-(1+\frac{\gamma_1}{\delta_1})y_1^{**})\sum_j W_{1j}y_j^{**} - \gamma_1 y_1^{**} \\ &= 0, \end{aligned}$$

where the first and last equalities follow from the fact that both y^* and y^{**} are equilibrium points, the strict inequality follows from (4.26) while the weak inequality from (4.27). As we have reached a contradiction, we can conclude that $y^* = y^{**}$, hence there exists a unique fixed point of $\Phi(y)$ such that $y^* > 0$.

Let $\zeta_i(y) := \Phi_i(y) - y_i$. The function ζ_i is continuous. Let $0 < y_i < y_i^*$. Since y^* is a fixed point, we have

$$\zeta_i(y^*) = 0.$$

Assume by contradiction that $\Phi_i(y) \leq y_i$, i.e. $\zeta_i(y) \leq 0$. Consider the bounded and increasing sequence $\{y^n\}_{n\in\mathbb{N}}$ we have built above. There exists $k \in \mathbb{N}$ such that $y_i^k < y_i$. By the construction of the sequence, we have $\Phi_i(y^k) \geq y_i^k$, hence $\zeta_i(y^k) \geq 0$.

Therefore, $\zeta_i(y^k) \geq 0$ and $\zeta_i(y) \leq 0$. By continuity of ζ_i, there exists $\tilde{y}$ such that $\tilde{y}_i \in [y_i^k, y_i]$ such that

$$\zeta_i(\tilde{y}) = 0,$$

that is,

$$\Phi_i(\tilde{y}) = \tilde{y}_i \leq y_i < y_i^*.$$

This contradicts the uniqueness of the fixed point $y^* > \mathbf{0}$. Hence $\Phi_i(y) > y_i$ for every $0 < y_i < y_i^*$. The proof of the second relation is equivalent to the one just performed.

Let $y(0) > 0$. For every i in $\mathcal{V}$ such that $y_i(0) < y_i^*$, we have $\Phi_i(y(0)) > y_i(0) > 0$. Hence, since Φ is nondecreasing, the system $\Phi_i^t(y(0))$ is nondecreasing in the compact $\mathcal{Y}$, hence there must exist $\tilde{y}$ such that

$$\lim_{t\to\infty} \Phi_i^t(y(0)) = \tilde{y}_i$$

For every j in $\mathcal{V}$ such that $y_j(0) > y_j^*$, we have $\Phi_j(y(0)) < y_j(0)$. Hence, the system $\Phi_j^t(y(0))$ is nondecreasing in the compact $\mathcal{Y}$, hence there must exist $\hat{y}$ such that

$$\lim_{t\to\infty} \Phi_j^t(y(0)) = \hat{y}_j$$

Observe that, by continuity of Φ, both $\tilde{y}$ and $\hat{y}$ are fixed points of Φ. We also note that, since $y(0) > \mathbf{0}$, hence, by monotonicity of Φ, $\tilde{y} > \mathbf{0}$ and $\hat{y} > \mathbf{0}$. From the fact that, in this case, there exists a unique $y^* > \mathbf{0}$ such that $\Phi(y^*) = y^*$, it must be $y^* = \tilde{y} = \hat{y}$. Hence

$$\lim_{t\to\infty} \Phi^t(y(0)) = y^* \quad \text{for every } y(0) > 0.$$

□

Corollary 4.2.7. *Consider the network SIRS epidemic model defined in (4.1) with irreducible interaction matrix $W \in \mathbb{R}_+^{\mathcal{V}\times\mathcal{V}}$, positive recovery rate vector $\gamma \in \mathbb{R}_{++}^{\mathcal{V}}$ and positive loss of immunity rate vector $\delta \in \mathbb{R}_{++}^{\mathcal{V}}$. Let $\lambda_{max} = \rho([\gamma]^{-1}W)$ be the dominant eigenvalue of $[\gamma]^{-1}W$. Then,*

(i) if $\lambda_{max} \leq 1$, the disease-free equilibrium $\mathbf{0}$ is the unique equilibrium point,

(ii) if $\lambda_{max} > 1$, the system admits the disease-free equilibrium $\mathbf{0}$ and the endemic equilibrium point $y^* > \mathbf{0}$

(iii) $y^*(\cdot)$ is a nondecreasing function of $[\gamma]^{-1}W$ and nonincreasing function of $[\delta]^{-1}\gamma$ whenever exists.

Proof. Using Lemma 4.2.2, (i),(ii) follow directly from Theorem 4.2.6 with $M = [\gamma]^{-1}W$ and $\alpha = [\delta]^{-1}\gamma$.

In order to prove (iii), let $[\gamma]^{-1}W \geq ([\gamma]^{-1}W)'$, where both these matrices have dominant eigenvalue over the threshold. From Theorem 4.2.6 we know

that there exists a unique fixed point $(y^*)' = \Phi((y^*)', ([\gamma]^{-1}W)')$. Since $\Phi(y, \cdot)$ is increasing in $[\gamma]^{-1}W$(Lemma 4.2.3(iv)b, we have

$$(y^*)' = \Phi((y^*)', ([\gamma]^{-1}W)') \leq \Phi((y^*)', ([\gamma]^{-1}W))$$

Hence $(y^*)'$ cannot be the fixed point of the function $H(y, [\gamma]^{-1}W)$ and from Theorem 4.2.6 it must be

$$(y^*)' \leq y^* = \Phi(y^*, [\gamma]^{-1}W)$$

Hence, $y^*([\gamma]^{-1}W)$ is a monotone increasing function provided that $\lambda_{max} > 1$.

Since $\Phi(y, \cdot)$ is decreasing in $[\delta]^{-1}\gamma$, we obtain in an analogous way that $y^*([\delta]^{-1}\gamma)$ is a monotone decreasing function. □

Remark 4.2.8. In Theorem 4.2.6 we proved that, if $\lambda_{max} > 1$, the positive equilibrium point $y^* > 0$ of the monotone discrete system $y(t+1) = \Phi(y(t)), t \in \mathbb{N}$ attracts $\mathcal{Y} \setminus \{\mathbf{0}\}$. Furthermore, this gives us an algorithm convergent to the endemic equilibrium of the network SIRS epidemic model, for every initial condition. Observe that this discrete system is different from the discrete system associated to the network SIRS epidemic model, hence we can only make conjectures from this system. Algorithm 1 formalizes this procedure as a fixed-point iteration, enabling the efficient computation of the endemic equilibrium for a given network and set of model parameters.

Algorithm 1: Fixed-point iteration for computing the endemic equilibrium of the network-based SIRS model

Input: Interaction matrix W, parameters γ, δ, initial condition $y^{(0)} \in \mathcal{Y}$, tolerance ε, maximum number of iterations $k_{\max}$.

Output: Equilibrium values x^*, y^*, z^*.

for $k = 1$ **to** $k_{\max}$ **do**

Compute $Wy^{(k-1)}$;

Set $W_y = [\gamma]^{-1} W y^{(k-1)}$;

Update

$$y^{(k)} = \frac{W_y}{1 + \frac{\delta+\gamma}{\delta} W_y}$$

if $\|y^{(k)} - y^{(k-1)}\|_\infty < \varepsilon$ **then**

break;

Set $y^* = y^{(k)}, \quad z^* = \dfrac{\gamma}{\delta} y^*, \quad x^* = \mathbf{1} - y^* - z^*$;

return (x^*, y^*, z^*);

Example 4.2.9. We now consider a setting in which it is possible to compute the endemic equilibrium.
Define the matrices

$$A = (I + [\gamma][\delta]^{-1}) \tag{4.28}$$

and

$$M = A[\gamma]^{-1} W A^{-1} \tag{4.29}$$

and suppose that

$$M\mathbf{1} = \lambda_M \mathbf{1} \tag{4.30}$$

where λ_M is the dominant eigenvalue of M. Since A is invertible (because positive and diagonal), M is similar to $[\gamma]^{-1}W$. Hence M and $[\gamma]^{-1}W$ share the same spectrum, and in particular their dominant eigenvalues coincide, i.e., $\lambda_{\max} = \lambda_M$.
The equilibrium equation (4.17) for the i-th component, using the matrix

just defined, becomes

$$\sum_j M_{ij}\Big(1+\frac{\gamma_j}{\delta_j}\Big)y_j^* = \frac{\Big(1+\frac{\gamma_i}{\delta_i}\Big)y_i^*}{1-\Big(1+\frac{\gamma_i}{\delta_i}\Big)y_i^*} \quad \forall\, i \in \mathcal{V} \tag{4.31}$$

Consider the following change of variables

$$\tilde{y}_i^* = \Big(1+\frac{\gamma_i}{\delta_i}\Big)y_i^* \quad \forall\ i \in \mathcal{V}$$

Under this transformation, (4.31) takes the form

$$(1-\tilde{y}_i^*)\,(M\tilde{y}^*)_i = \tilde{y}_i^* \tag{4.32}$$

We look for an equilibrium solution of (4.32) of the form $\tilde{y}^* = \tilde{\beta}\,\mathbf{1}$. Substituting this into (4.32) and using (4.30), we obtain

$$(1-\tilde{\beta})\lambda_{\max}\tilde{\beta} = \tilde{\beta}$$

Solving this equation yields

$$\tilde{\beta} = 1 - \frac{1}{\lambda_{\max}} \tag{4.33}$$

Recalling the definition of $\tilde{y}_i^*$, we finally obtain the components of the endemic equilibrium

$$y_i^* = \frac{\delta_i}{\gamma_i+\delta_i}\Big(1-\frac{1}{\lambda_{\max}}\Big),\ \forall\ i \in \mathcal{V} \tag{4.34}$$

Since in Corollary 4.2.7 we proved the uniqueness of the endemic equilibrium if and only if $\lambda_{\max} > 1$, this solution is well defined, positive, and unique.

Remark 4.2.10. If the parameters γ and δ are homogeneous, i.e. $\gamma_i = \bar{\gamma}$ and $\delta_i = \bar{\delta}$ for all i, the matrix M reduces, up to a constant scaling, to $\frac{1}{\bar{\gamma}}W$. In this case, taking M such that (4.30) is satisfied means that the directed graph $\mathcal{G} = (\mathcal{V}, \mathcal{E}, W)$ is an out-regular graph with dominant eigenvalue λ_{max}. Moreover, the endemic equilibrium y^* does not depend on the recovery and

loss of immunity rates:

$$y^* = \frac{\bar{\delta}}{\bar{\gamma} + \bar{\delta}} \left(1 - \frac{1}{\lambda_{max}}\right) \mathbf{1} \tag{4.35}$$

Having an out-regular graph means that every node has the same out-degree, which in epidemiology implies that each population within the system has the same potential to transmit infection to other populations. However, this does not necessarily mean that all populations receive the same number of external influences; therefore, this configuration does not exclude the possibility that some populations are more exposed to infection than others.

Example 4.2.11. We now consider a case in which the problem of finding a fixed point of the function Φ can be reduced to a one dimension problem.

Let W be a rank-1 interaction matrix. Hence there exist $a, b \in \mathbb{R}_+^{\mathcal{V}}$ such that $W = ab^\top$. Let $\gamma, \delta \in \mathbb{R}_{++}^{\mathcal{V}}$ and define

$$h(y) = \sum_{j \in \mathcal{V}} b_j y_j \tag{4.36}$$

Observe that, in this model, W is taken nonnegative and irreducible, hence, the dominant eigenvalue λ_W coincides to the unique nonzero eigenvalue of W $\mu_W = \mathrm{Tr}(W)$ (see Appendix A.2).

In epidemic terms, having such an interaction matrix means that every population i has a specific activity a_i that weighs the susceptibility of the population, and every population j has a factor b_j measuring its relative infectiousness.

Consider the function Φ defined in (4.12). From Lemma 4.2.2, (x^*, y^*, z^*) is an equilibrium of the network SIRS epidemic model with irreducible rank-1 $ab^T \in \mathbb{R}_+^{\mathcal{V} \times \mathcal{V}}$ and $\gamma, \delta \in \mathbb{R}_{++}^{\mathcal{V}}$ if and only if $y^* = \Phi(y^*, ab^T, [\delta]^{-1}\gamma)$.

By definition,

$$\Phi_i(y, ab^T, [\delta]^{-1}\gamma) = \psi_i((ab^T y)_i, \frac{\gamma_i}{\delta_i}) = \frac{a_i h(y)}{1 + (1 + \frac{\gamma_i}{\delta_i}) a_i h(y)}$$

Let (x^*, y^*, z^*) be the equilibrium point of the system and let $h^* = h(y^*)$, then

$$y_i^* = \frac{a_i h^*}{1 + (1 + \frac{\gamma_i}{\delta_i}) a_i h^*}$$

Hence

$$h^* = \sum_i \frac{a_i b_i h^*}{1 + (1 + \frac{\gamma_i}{\delta_i}) a_i h^*}$$

Hence we have to find $h^* \in \mathbb{R}_+$ such that $h^* = \tilde{\Phi}(h^*)$, where, for every fixed a, b, γ, δ

$$\tilde{\Phi} : \mathbb{R}_+ \to \mathbb{R}_+$$

$$\tilde{\Phi}(h) = \sum_i \frac{a_i b_i h}{1 + (1 + \frac{\gamma_i}{\delta_i}) a_i h}$$

The rank-1 case allows us to find the system equilibria as fixed points of a non linear scalar function, which significantly simplifies the problem since finding fixed points of a scalar function is generally easier than dealing with a vector-valued one.

Furthermore, we can investigate the dependence of the endemic equilibrium on the out-degree of the nodes in rank-1 case. Let us assume that two populations i and k have the same recovery and loss of immunity rate

$$\gamma_i = \gamma_k = \tilde{\gamma}, \qquad \delta_i = \delta_k = \tilde{\delta}$$

Consider the equilibrium equation:

$$y_i^* = \frac{a_i h^*}{1 + \frac{\tilde{\gamma} + \tilde{\delta}}{\tilde{\delta}} a_i h^*} \tag{4.37}$$

which is equal to

$$\frac{\tilde{\gamma} + \tilde{\delta}}{\tilde{\delta}} y_i^* = \frac{\frac{\tilde{\gamma} + \tilde{\delta}}{\tilde{\delta}} a_i h^* + 1 - 1}{1 + \frac{\tilde{\gamma} + \tilde{\delta}}{\tilde{\delta}} a_i h^*} = 1 - \frac{1}{1 + \frac{\tilde{\gamma} + \tilde{\delta}}{\tilde{\delta}} a_i h^*} \tag{4.38}$$

If the out-degree of the node i is lower than the one of node k, i.e. $a_i \sum_j b_j < a_k \sum_j b_j$, then the i-th and k-th components of the endemic equilibrium y^*

have the following property:

$$\begin{aligned}\frac{\tilde{\gamma}+\tilde{\delta}}{\tilde{\delta}}y_i^* =& 1-\frac{\tilde{\gamma}}{\frac{\tilde{\gamma}+\tilde{\delta}}{\tilde{\delta}}a_i h^*}\\ <& 1-\frac{\tilde{\gamma}}{\frac{\tilde{\gamma}+\tilde{\delta}}{\tilde{\delta}}a_k h^*}=\frac{\tilde{\gamma}+\tilde{\delta}}{\tilde{\delta}}y_k^*\end{aligned} \tag{4.39}$$

Hence $y_i^* < y_k^*$ whenever $a_i < a_k$.

Remark 4.2.12. Such a dependence on the factor a follows directly from its interpretation as a susceptibility coefficient. Indeed, having $a_i < a_k$ means that the i-th group is less susceptible to infection than the k-one. Hence it is natural to expect that the fraction of infected of the first group would be lower than the other one. We note that the out-degree of a node in such a network is determined by the susceptibility factor a. Hence, for same recovery and loss of immunity rates, a population with higher susceptibility will exhibit a higher fraction of infected.

4.3 Stability analysis

In this section we take in account the stability analysis of the equilibrium points. We manage to derive the global asymptotic stability of the disease-free equilibrium below the threshold $\lambda_{\max} = 1$ and, more relevant, the local asymptotic stability of the endemic equilibrium point over the threshold. We also investigate the region of attraction of the disease-free equilibrium when the endemic equilibrium exists.

4.3.1 Stability of the disease-free equilibrium point

In order to study the stability of the disease free equilibrium $(\mathbf{1}, \mathbf{0}, \mathbf{0})$ we will consider the linearization of the reduced system (4.4). The following technical results are useful to prove the stability properties of the system.

Lemma 4.3.1. *Consider an irreducible nonnegative matrix $W \in \mathbb{R}_+^{\mathcal{V}\times\mathcal{V}}$ and a positive vector $\gamma \in \mathbb{R}_{++}^{\mathcal{V}}$. Let $\lambda_{max} = \rho([\gamma]^{-1}W)$ be the dominant eigenvalue of $[\gamma]^{-1}W$. Then the matrix $W - [\gamma]$ is Metzler stable if and only if $\lambda_{max} < 1$.*

Proof. See Proposition 2.1 in Fall et al. [74] for the proof. □

Let us define the Lyapunov function:

$$V(t) = \bar{w}^T y \tag{4.40}$$

where $\bar{w} = [\gamma]^{-1}\bar{v}$, with $\bar{v}$ the left eigenvector of $[\gamma]^{-1}W$. The time derivative of V is:

$$\begin{aligned}
\dot{V}(t) =& \bar{w}^T \dot{y} \\
=& \bar{w}^T (I - [y+z])Wy - [\gamma]y \\
=& \bar{w}^T Wy - \bar{w}^T [\gamma]y - \bar{w}^T [y+z]Wy \\
=& \bar{v}^T [\gamma]^{-1} Wy - \bar{v}^T [\gamma]^{-1} [\gamma]y - \bar{w}^T [y+z]Wy \\
=& (\lambda_{max} - 1)\bar{v}^T y - \bar{w}^T [y+z]Wy \\
=& (\lambda_{max} - 1)\bar{w}^T [\gamma]y - \bar{w}^T [y+z]Wy
\end{aligned} \tag{4.41}$$

where we used that $\bar{v}$ is the left eigenvector of $[\gamma]W^{-1}$ associated to the dominant eigenvalue $\lambda_{\max}$.

Lemma 4.3.2. *Consider the network SIRS epidemic model defined in (4.1) with irreducible interaction matrix $W \in \mathbb{R}_+^{\mathcal{V}\times\mathcal{V}}$, positive recovery rate vector $\gamma \in \mathbb{R}_{++}^{\mathcal{V}}$ and positive loss of immunity rate vector $\delta \in \mathbb{R}_{++}^{\mathcal{V}}$. Let $\lambda_{max} = \rho([\gamma]^{-1}W)$ be the dominant eigenvalue of $[\gamma]^{-1}W$. Let V be the Lyapunov function defined in (4.40). If $\lambda_{max} = 1$, then the largest invariant subset of $\{\dot{V} = 0\}$ is $\{(y, z) \in \mathcal{X}' : y = 0\}$.*

Proof. In case $\lambda_{max} = 1$, we have from (4.41)

$$\dot{V}(t) = -\bar{w}^T[y + z]Wy$$

Hence, $\dot{V} = 0$ if and only if the intersection $\mathrm{supp}(Wy) \cap \mathrm{supp}(y + z) = \emptyset$. For any (y, z) belonging to an invariant subset of $\{\dot{V} = 0\}$, consider the sets

$$J = \{j : y_j > 0\} \qquad I = \{i : y_i = 0\}$$

and assume by contradiction that $J \neq \emptyset$. Since W is irreducible, there must exist $i \in I$ and $j \in J$ such that $W_{ij} > 0$. Therefore, $i \in \mathrm{supp}(Wy)$ which means that $i \notin \mathrm{supp}(y + z)$ and so $y_i = z_i = 0$. We obtain

$$\dot{y}_i = (1 - y_i - z_i)\sum_k W_{ik}y_k - \gamma_i y_i \geq W_{ij}y_j > 0$$

Therefore $\dot{y}_i > 0$ at the considered state. By continuity, there exists $\varepsilon > 0$ such that for $t \in (0, \varepsilon)$ we have $(Wy)_i(t) > 0$ and $(y + z)_i(t) > 0$. For such small t the term $\bar{w}_i(y_i(t) + z_i(t))(Wy)_i(t)$ is strictly positive, hence

$$\dot{V}(t) = -\sum_i \bar{w}_i(y_i(t) + z_i(t))(Wy)_i(t) < 0.$$

This contradicts the assumption that the trajectory stays in the invariant subset of $\{\dot{V} = 0\}$. Thus no nonzero y can belong to an invariant subset of $\{\dot{V} = 0\}$, and, since we proved in Lemma 4.1.3 that $\{y = 0\}$ is invariant, we can conclude the proof. □

The next theorem establishes the stability properties of the network SIRS epidemic model below the epidemic threshold.

Theorem 4.3.3. *Consider the network SIRS epidemic model defined in (4.1) with irreducible interaction matrix $W \in \mathbb{R}_+^{\mathcal{V}\times\mathcal{V}}$, positive recovery rate*

vector $\gamma \in \mathbb{R}^{\mathcal{V}}_{++}$ *and positive loss of immunity rate vector* $\delta \in \mathbb{R}^{\mathcal{V}}_{++}$. *Let* $\lambda_{max} = \rho([\gamma]^{-1}W)$ *be the dominant eigenvalue of* $[\gamma]^{-1}W$. *If* $\lambda_{max} \leq 1$, *then the disease-free equilibrium point is globally asymptotically stable.*

Proof. Consider the linearization of the reduced system (4.5) around the disease-free equilibrium point (0,0):

$$\nabla f(0,0) = \begin{pmatrix} W - [\gamma] & 0 \\ [\gamma] & -[\delta] \end{pmatrix} \tag{4.42}$$

Since $\nabla f(0,0)$ is a block upper triangular matrix, its eigenvalues coincide with those of the diagonal blocks, namely $W - [\gamma]$ and $-[\delta]$. From Lemma 4.3.1, if $\lambda_{max} < 1$, $W - [\gamma]$ is stable. Then, since the matrix $-[\delta]$ is diagonal, the other eigenvalues of $\nabla f(0,0)$ are going to be $-\delta_1, \cdots, -\delta_n$ which are real and negative. We can conclude that the equilibrium point (0,0) is locally asymptotically stable for $\lambda_{max} < 1$.

Consider the Lyapunov function defined in (4.40), with time derivative as in (4.41). Since both $\bar{v}$ and the coefficients γ_i are positive, then V is positive definite with respect to $y = \mathbf{0}$. Let $\gamma_{\min} = \min_{i \in \mathcal{V}} \gamma_i$, if $\lambda_{max} < 1$, we obtain from (4.41)

$$\dot{V}(t) \leq (\lambda_{max} - 1)\gamma_{\min} V(t) \leq 0 \tag{4.43}$$

and $\dot{V} = 0$ if and only if $y = 0$, since V is a linear combination of y_i with positive coefficient. Using that $\{y = 0\}$ is invariant, in case $\lambda_{max} < 1$ it is the largest invariant set of $\{\dot{V} = 0\}$. When $\lambda_{max} = 1$ we obtain the same result using Lemma 4.3.2.
Therefore, in both cases, using the invariance principle we obtain that

$$y_i(t) \to 0 \text{ for } \quad t \to \infty$$

so, using the dynamic equations of the system (4.4), we have

$$z_i(t) = z_i(0)e^{-\delta_i t} + \gamma_i \int_0^t e^{-\delta_i(t-s)} y_i(s) ds \to 0 \quad \text{for } t \to \infty$$

Hence the disease-free equilibrium point (0,0) is globally asymptotically stable for $\lambda_{max} \leq 1$. □

4.3.2 Stability of the endemic equilibrium point

We now investigate the asymptotic stability of the endemic equilibrium of the SIRS model in the case $\lambda_{max} > 1$ by means of the linearization method.

The following lemma is a useful result in order to prove the stability of the endemic equilibrium point.

Lemma 4.3.4. *Consider the network SIRS epidemic model defined in (4.1) with irreducible interaction matrix $W \in \mathbb{R}_+^{\mathcal{V}\times\mathcal{V}}$, positive recovery rate vector $\gamma \in \mathbb{R}_{++}^{\mathcal{V}}$ and positive loss of immunity rate vector $\delta \in \mathbb{R}_{++}^{\mathcal{V}}$. Let $\lambda_{max} = \rho([\gamma]^{-1}W)$ be the dominant eigenvalue of $[\gamma]^{-1}W$. Let $(1-y^*-z^*, y^*, z^*) \in \mathcal{X}$ be the endemic equilibrium of the system. Let $\lambda \in \mathbb{C}$ and define the matrix*

$$S(\lambda) = [1 - y^* - z^*]W - [Wy^*] - [\gamma] - \lambda I - [\gamma]([\delta] + \lambda I)^{-1}[Wy^*].$$

Let $\eta = \min_{r\in\mathcal{V}} \min((Wy^*)_r, \delta_r)$,
if $\mathrm{Re}(\lambda) > -\eta$, then $S(\lambda)$ is invertible.

Proof. In order to prove Lemma 4.3.4, we consider the matrix

$$M(\lambda) = S(\lambda)[y^*]$$

For every $k \neq j$ we have

$$M_{kj}(\lambda) = (1 - y_k^* - z_k^*)W_{kj}y_j^* \geq 0, \tag{4.44}$$

and, for every k,

$$\begin{aligned} M_{kk}(\lambda) = (1 - y_k^* - z_k^*)W_{kk}y_k^* - \gamma_k y_k^* - (Wy^*)_k y_k^* \\ -\lambda y_k^* - \frac{\gamma_k}{\delta_k + \lambda}(Wy^*)_k y_k^* \end{aligned} \tag{4.45}$$

Defining

$$R_k = \sum_{j\neq k} |M_{kj}(\lambda)| = \sum_{j\neq k}(1 - y_k^* - z_k^*)W_{kj}y_j^* \tag{4.46}$$

$$m_k = (Wy^*)_k y_k^* \tag{4.47}$$

$$g_k(\lambda) = \lambda y_k^* + \frac{\gamma_k}{\delta_k + \lambda}(Wy^*)_k y_k^* \tag{4.48}$$

and, using the equilibrium equation (4.15) componentwise, we obtain that

$$\begin{aligned} 0 =& (1 - y_k^* - z_k^*) \sum_{j=1}^{n} W_{kj} y_j^* - \gamma_k y_k^* \\ =& R_k + (1 - y_k^* - z_k^*) W_{kk} y_k^* - \gamma_k y_k^* \\ =& R_k + M_{kk}(\lambda) + m_k + g_k(\lambda) \end{aligned}$$

thus,

$$M_{kk}(\lambda) = -R_k - m_k - g_k(\lambda) \tag{4.49}$$

Since the endemic equilibrium y^* is strictly positive, and W is assumed irreducible (which implies that for every k there must exists at least one j such that $W_{kj} > 0$), we have $(Wy^*)_k > 0 \ \forall k$, hence $m_k > 0$. Moreover, m_k does not depend on λ. We also note that, if $Re(\lambda) > -\lambda_{\min}$,

$$\begin{aligned} Re(g_k(\lambda)) =& Re(\lambda) y_k^* + \frac{\gamma_k m_k (\delta_k + Re(\lambda))}{(\delta_k + Re(\lambda))^2 + Im(\lambda)^2} \\ >& -\eta y_k^* \\ &+ \frac{\gamma_k m_k (\delta_k - \eta)}{(\delta_k + Re(\lambda))^2 + Im(\lambda)^2} \\ \geq& -(Wy^*)_k y_k^* \\ =& -m_k \end{aligned}$$

where, by definition, η is a lower bound for both $(Wy^*)_k$ and δ_k, for every $k \in \mathcal{V}$. Thanks to these considerations, we can conclude that, for every k, the real part of the diagonal term M_{kk} satisfies:

$$Re(M_{kk}(\lambda)) = -R_k - m_k - Re(g_k(\lambda)) < -R_k \tag{4.50}$$

whenever $Re(\lambda) > -\eta$. Therefore, every Gershgorin disk $B_{R_k}(M_{kk}(\lambda)) \subseteq \{\mu \in \mathbb{C} : Re(\mu) \leq -m_k\}$. By Gershgorin Theorem (see A.3) all eigenvalues

of $M(\lambda)$ belong to

$$\bigcup_{k=1}^{n} B_{R_k}(M_{kk}(\lambda))$$

hence, for every λ such that $Re(\lambda) > -\eta$,

$$\sigma(M(\lambda)) \subseteq \{\mu \in \mathbb{C} : Re(\mu) \leq -\min_k m_k\} \tag{4.51}$$

Since $m_k > 0$, for every k, all eigenvalues of $M(\lambda)$ have negative real part, so that $\forall \lambda : Re(\lambda) > -\eta$, $\det(M(\lambda)) \neq 0$.
Noticing that, from $y_i^* > 0 \, \forall i$, the diagonal matrix $[y^*]$ is invertible, we can conclude the proof because $S(\lambda) = M(\lambda)[y^*]^{-1}$ is non singular. □

The following theorem establishes the stability behavior of an SIRS network model above the threshold $\lambda_{\max} = 1$.

Theorem 4.3.5. *Consider the network SIRS epidemic model defined in (4.1) with irreducible interaction matrix $W \in \mathbb{R}_+^{\mathcal{V}\times\mathcal{V}}$, positive recovery rate vector $\gamma \in \mathbb{R}_{++}^{\mathcal{V}}$ and positive loss of immunity rate vector $\delta \in \mathbb{R}_{++}^{\mathcal{V}}$. Let $\lambda_{max} = \rho([\gamma]^{-1}W)$ be the dominant eigenvalue of $[\gamma]^{-1}W$. If $\lambda_{max} > 1$, then the disease-free equilibrium point $(\mathbf{1}, \mathbf{0}, \mathbf{0})$ is unstable and the endemic equilibrium point (x^*, y^*, z^*) is locally asymptotically stable.*

Proof. From Lemma 4.3.1, when $\lambda_{max} > 1$ the disease-free equilibrium point is unstable.
For the proof of the local asymptotic stability of the endemic equilibrium point, consider the Jacobian matrix of the linearization of the reduced system (4.4) around the endemic equilibrium (y^*, z^*)

$$\nabla f(y^*, z^*) = \begin{pmatrix} [1 - y^* - z^*]W - [Wy^*] - [\gamma] & -[Wy^*] \\ [\gamma] & -[\delta] \end{pmatrix} \tag{4.52}$$

We want to prove that every eigenvalue of $\nabla f(y^*, z^*)$ has real part less than $-\eta$. That is, in terms of characteristic equation,

$$\text{if } Re(\lambda) > -\eta \text{ then } \det(\nabla f(y^*, z^*) - \lambda I) \neq 0 \tag{4.53}$$

and we consider the matrix $\nabla f(y^*, z^*) - \lambda I$:

$$\begin{pmatrix} [1 - y^* - z^*]W - [Wy^*] - [\gamma] - \lambda I & -[Wy^*] \\ [\gamma] & -([\delta] + \lambda I) \end{pmatrix} \tag{4.54}$$

For every λ such that $Re(\lambda) > -\eta$, the matrix $-([\delta] + \lambda I)$ is invertible (as $\lambda \neq -\delta_i \quad \forall i$ obviously), therefore we can use the Schur complement $S(\lambda)$, whose expression is:

$$S(\lambda) = [1 - y^* - z^*]W - [Wy^*] - [\gamma] - \lambda I - [\gamma]([\delta] + \lambda I)^{-1}[Wy^*] \tag{4.55}$$

Using Proposition A.1.2 (see Appendix A.1) about the Schur complement, we achieve

$$\begin{aligned} &\det(\nabla f(y^*, z^*) - \lambda I) \\ &= \det(-([\delta] + \lambda I)) \det(S(\lambda)) \\ &= (-1)^n \prod_i (\delta_i + \lambda) \det(S(\lambda)) \end{aligned}$$

Hence, proving (4.53) is equivalent to prove that for every λ with real part grater than $-\eta$, $\det(S(\lambda)) \neq 0$. We now use Lemma 4.3.4 and we can conclude the proof. □

4.3.3 Disease-free equilibrium region of attraction

When $\lambda_{\max} \leq 1$ Theorem 4.3.3 ensures the global attractiveness of the disease free equilibrium point. In case $\lambda_{\max} > 1$, Corollary 4.2.7 ensures the existence of an endemic equilibrium point which is locally asymptotical stable as proved in Theorem 4.3.5. The following theorem ensures that, if $\lambda_{max} > 1$, the disease free equilibrium point $(\mathbf{1}, \mathbf{0}, \mathbf{0})$ attracts only the hyperplane $\{y = \mathbf{0}\}$.

Theorem 4.3.6. *Consider the network SIRS epidemic model defined in (4.1) with irreducible interaction matrix $W \in \mathbb{R}_+^{\mathcal{V}\times\mathcal{V}}$, positive recovery rate vector $\gamma \in \mathbb{R}_{++}^{\mathcal{V}}$ and positive loss of immunity rate vector $\delta \in \mathbb{R}_{++}^{\mathcal{V}}$. Let $\lambda_{max} = \rho([\gamma]^{-1}W)$ be the dominant eigenvalue of $[\gamma]^{-1}W$. If $\lambda_{max} > 1$, then*

$$\mathcal{A}((\mathbf{0}, \mathbf{0})) = \{y = \mathbf{0}\}$$

Proof. Observe that, for every $z(0)$, if $y = 0$, we have $\dot{y} = 0$ and $\dot{z} = -[\delta]z < 0$. Hence, for every initial condition $(y(0), z(0)) = (0, z(0))$, the system converge to the disease-free equilibrium point (0,0). So the region of attraction $\mathcal{A}((0,0))$ of the disease-free equilibrium must contain the hyperplane $\{y = 0\}$. We now want to prove that $\mathcal{A}((0,0))$ coincides with the hyperplane $\{y = 0\}$. Take $\epsilon > 0$ such that

$$(1 - \epsilon)\lambda_{\max} - 1 > 0 \tag{4.56}$$

For every initial condition $(y(0), z(0))$ such that $y(0) \neq 0$ we know from Theorem 4.1.5 that $y(t) > 0, \quad \forall\, t > 0$. By contradiction, assume that $(y(t), z(t))$ converge to (0,0). Then, there exists $T > 0$ such that $y_i(t)+z_i(t) \leq \epsilon, \quad \forall\, i \in \mathcal{V}, \forall\, t \geq T$. Let $V(t) = \bar{w}^T y$, with $\bar{w} = [\gamma]^{-1}\bar{v}$, where $\bar{v}$ is the left eigenvector of $[\gamma]^{-1}W$. Hence, $\forall t \geq T$ we have that

$$\begin{aligned}
\dot{V}(t) &= \sum_i \bar{w}_i \dot{y}_i \\
&\geq (1 - \epsilon) \sum_i \bar{w}_i \sum_j W_{ij} y_j - \sum_i \gamma_i \bar{w}_i y_i \\
&= (1 - \epsilon)\lambda_{\max} \sum_j \bar{v}_j y_j - \sum_i \bar{v}_i y_i \\
&\geq \gamma_{\min}((1 - \epsilon)\lambda_{\max} - 1)V(t) \\
&> 0
\end{aligned} \tag{4.57}$$

Here, the first inequality follows from the fact that $y_i(t) + z_i(t) \leq \epsilon$, which implies $\dot{y}_i \geq (1 - \epsilon) \sum_j W_{ij} y_j - \gamma_i y_i$. The subsequent equality uses the definition $\bar{v}_i = \gamma_i \bar{w}_i$ together with the spectral property of $\lambda_{\max}$. The second inequality then follows from $\gamma_i \geq \gamma_{\min}$ for all $i \in \mathcal{V}$, and the final inequality holds by choosing ϵ according to (4.56).
This contradicts the hypothesis and the system cannot converge to the disease-free equilibrium. Hence

$$\mathcal{A}((0,0)) = \{y = 0\} \tag{4.58}$$

□

Remark 4.3.7. Although this theorem does not provide a theoretical result over the region of attraction of the endemic equilibrium, however it ensures that it will be a subset of $\mathcal{X} \setminus \{y = 0\}$. It is reasonable to conjecture that, as

in the scalar case, the endemic equilibrium attracts the entire state space $\mathcal{X}$, except for the hyperplane $\{y = 0\}$. We will prove this result in case where the interaction matrix W has rank 1, by means of a Lyapunov function in Section 4.4. In Chapter 5 will be shown some numerical results consistent with this theoretical conjecture.

4.4 Stability analysis of the endemic equilibrium point with rank-1 interaction matrix and homogeneous recovery rate

Consider a network SIRS epidemic model with rank-1 interaction matrix $W = ab^T$, introduced in Example 4.2.11.

From Theorem 4.3.5 we have the local asymptotic stability of the endemic equilibrium (x^*, y^*, z^*) for a general nonnegative irreducible matrix W. In case W has rank-1, it is possible to derive a theoretical result over the basin of attraction of the endemic equilibrium.

Theorem 4.4.1. *Consider the network SIRS epidemic model defined in (4.1) with irreducible and rank-1 $W \in \mathbb{R}_+^{\mathcal{V}\times\mathcal{V}}$, $\delta \in \mathbb{R}_{++}^{\mathcal{V}}$ and homogeneous $\gamma = \bar{\gamma}\mathbf{1}$ with $\bar{\gamma} > 0$. Let $\lambda_{max} = \rho([\gamma]^{-1}W)$ be the dominant eigenvalue of $[\gamma]^{-1}W$. If $\lambda_{\max} > 1$, the endemic equilibrium (x^*, y^*, z^*) is locally asymptotically stable and its basin of attraction is the subset $\mathcal{X} \setminus \{y = \mathbf{0}\}$.*

Proof. From Theorem 4.3.5 we have the local asymptotic stability. From Theorem 4.3.6, $\{y = \mathbf{0}\}$ is the basin of attraction of the disease free equilibrium point when $\lambda_{max} > 1$, hence we investigate the attractiveness of the endemic equilibrium in the subset $\mathcal{X} \setminus \{y = \mathbf{0}\}$.

Consider the function h defined in Equation (4.36) and let $h^* = h(y^*)$. Define, for every $y \geq \mathbf{0}$, the following functions:

$$V_1(t) = \frac{1}{2}\sum_i \frac{b_i}{x_i^*}(x_i - x_i^*)^2 \tag{4.59}$$

$$V_2(t) = \frac{1}{2}\sum_i \frac{\delta_i b_i}{\bar{\gamma} x_i^*}(z_i - z_i^*)^2 \tag{4.60}$$

$$V_3(t) = h(y) - h^* + h^* \ln\left(\frac{h^*}{h(y)}\right) \tag{4.61}$$

Take the Lyapunov function:

$$V(t) = V_1(t) + V_2(t) + V_3(t) \tag{4.62}$$

V is positive definite with respect to the endemic equilibrium (x^*, y^*, z^*).

$$\begin{aligned}
\dot{V}_1 =& \sum_i \frac{b_i}{x_i^*}(x_i - x_i^*)\dot{x}_i \\
=& \sum_i \{\frac{b_i}{x_i^*}(x_i - x_i^*)(-a_i h x_i + \delta_i z_i)\} \\
=& \sum_i \{\frac{b_i}{x_i^*}(x_i - x_i^*)(-a_i h(x_i - x_i^*) - a_i x_i^*(h - h^*) + \delta_i(z_i - z_i^*))\} \\
=& -\sum_i \frac{b_i}{x_i^*} a_i h (x_i - x_i^*)^2 - (h - h^*)\sum_i b_i a_i (x_i - x_i^*) \\
&+ \sum_i \frac{b_i}{x_i^*}\delta_i (x_i - x_i^*)(z_i - z_i^*)
\end{aligned} \tag{4.63}$$

$$\begin{aligned}
\dot{V}_2 =& \sum_i \{\frac{\delta_i}{\bar{\gamma}}\frac{b_i}{x_i^*}(z_i - z_i^*)\dot{z}_i\} \\
=& \sum_i \{\frac{\delta_i}{\bar{\gamma}}\frac{b_i}{x_i^*}(z_i - z_i^*)(\bar{\gamma} y_i + \delta_i z_i)\} \\
=& \sum_i \{\frac{\delta_i}{\bar{\gamma}}\frac{b_i}{x_i^*}(z_i - z_i^*)(\bar{\gamma} - \bar{\gamma} x_i - (\bar{\gamma} + \delta_i) z_i)\} \\
=& \sum_i \{\frac{\delta_i}{\bar{\gamma}}\frac{b_i}{x_i^*}(z_i - z_i^*)(\bar{\gamma}(x_i^* - x_i) + (\bar{\gamma} + \delta_i)(z_i^* - z_i))\} \\
=& -\sum_i \{\delta_i \frac{b_i}{x_i^*}(z_i - z_i^*)(x_i - x_i^*)\} - \sum_i \{\frac{\delta_i}{\bar{\gamma}}\frac{b_i}{x_i^*}(\bar{\gamma} + \delta_i)(z_i - z_i^*)^2\}
\end{aligned} \tag{4.64}$$

Using that, since $\sum_i a_i b_i x_i^* = \bar{\gamma}$,

$$\begin{aligned}\dot{h} &= \sum_i b_i \dot{y}_i = \sum_i b_i [a_i h x_i - \bar{\gamma} y_i] = \sum_i b_i a_i h x_i - \sum_i b_i \bar{\gamma} y_i \\ &= h(\sum_i b_i a_i x_i - \bar{\gamma}) = h(\sum_i b_i a_i x_i - \sum_i b_i a_i x_i^*) = h\Big(\sum_i b_i a_i (x_i - x_i^*)\Big)\end{aligned}$$

we obtain

$$\dot{V}_3 = \frac{h - h^*}{h}\dot{h} = (h - h^*)\sum_i b_i a_i (x_i - x_i^*) \tag{4.65}$$

Using (4.63)(4.64)(4.65), the time derivative of V is :

$$\dot{V} = \dot{V}_1 + \dot{V}_2 + \dot{V}_3 = \sum_i \left\{ -\frac{b_i a_i h}{x_i^*}(x_i - x_i^*)^2 - \frac{\delta_i b_i (\bar{\gamma} + \delta_i)}{\bar{\gamma} x_i^*}(z_i - z_i^*)^2 \right\} \tag{4.66}$$

Hence $\dot{V} \leq 0$ and $\dot{V} = 0$ if and only if the couple $(x, z) \neq (x^*, z^*)$, that is $(x, y, z) \neq (x^*, y^*, z^*)$. According to the invariance principle, the endemic equilibrium is globally asymptotically stable on $\mathcal{X} \setminus \{y = \mathbf{0}\}$. □

Remark 4.4.2. The proof of Theorem 4.4.1 is almost identical to the proof given in [63].

4.5 Convergence rate

4.5.1 Case $\lambda_{\max} < 1$

Let $\lambda_{\max} < 1$. Consider the left eigenvector $\bar{v}$ of $[\gamma]^{-1}W$ associated with $\lambda_{\max}$ and define the weighted norm

$$||x|| = \sum_i |x_i| \bar{v}_i \tag{4.67}$$

From (4.43), it follows that

$$||y(t)|| \leq ||y(0)|| e^{-(1-\lambda_{\max})\gamma_{\min} t} \tag{4.68}$$

This inequality provides an explicit estimate of the exponential convergence rate toward the disease-free equilibrium.

4.5.2 Case $\lambda_{\max} > 1$

In the case $\lambda_{\max} > 1$, from Theorem 4.3.5 it follows that all eigenvalues of the Jacobian matrix obtained by linearization around the endemic equilibrium have strictly negative real parts. As a consequence, the endemic equilibrium is locally exponentially stable and the following estimate holds:

$$\|(x(t), y(t), z(t)) - (x^*, y^*, z^*)\|_\infty \leq C(0)\, e^{-\eta t}, \tag{4.69}$$

where $C(0)$ denotes the norm of the initial deviation from the endemic equilibrium, measured in the ℓ_∞-norm. Numerical simulations reported in Chapter 5 show that the observed bound over the convergence rate is consistent with the theoretical one derived from the stability analysis.

Chapter 5

Numerical simulations

In this chapter we provide some numerical results which confirm the theoretical obtained in Chapter 4 and which allows us to make conjecture over some open question.

5.1 Dynamic behavior of a 5 population network SIRS model

We analyse the dynamical behavior of the model on a strongly connected network of $n = 5$ populations. Two different cases are explored, corresponding to different values of the parameter λ_{max}. In both cases, we discuss how the network structure influences the transient behavior and the stability of the resulting equilibrium. The interaction matrix used in all simulations is

$$W = \begin{bmatrix} 1.5 & 3.0 & 2.0 & 0.5 & 4.0 \\ 0.2 & 0.8 & 2.0 & 0.0 & 1.0 \\ 3.0 & 2.1 & 4.2 & 3.0 & 2.1 \\ 0.3 & 0.0 & 0.0 & 0.6 & 0.2 \\ 2.0 & 0.0 & 0.0 & 0.5 & 0.9 \end{bmatrix},$$

The loss of immunity rate is fixed in both cases as

$$\delta = \begin{bmatrix} 0.3 & 0.4 & 0.2 & 0.1 & 0.6 \end{bmatrix}$$

5.1.1 Case $\lambda_{\max} < 1$

Taking the recovery rate:

$$\gamma = \begin{bmatrix} 5 & 20 & 15 & 5 & 7 \end{bmatrix}$$

so that the matrix $[\gamma]^{-1}W$ is

$$[\gamma]^{-1}W = \begin{bmatrix} 0.3000 & 0.6000 & 0.4000 & 0.1000 & 0.8000 \\ 0.0100 & 0.0400 & 0.1000 & 0 & 0.0500 \\ 0.2000 & 0.1400 & 0.2800 & 0.2000 & 0.1400 \\ 0.0600 & 0 & 0 & 0.1200 & 0.0400 \\ 0.2857 & 0 & 0 & 0.0714 & 0.1286 \end{bmatrix}$$

whose dominant eigenvalue is $\lambda_{max} = 0.8743 < 1$, hence, from Theorem 4.3.3, we know that the disease-free equilibrium is globally asymptotically stable.

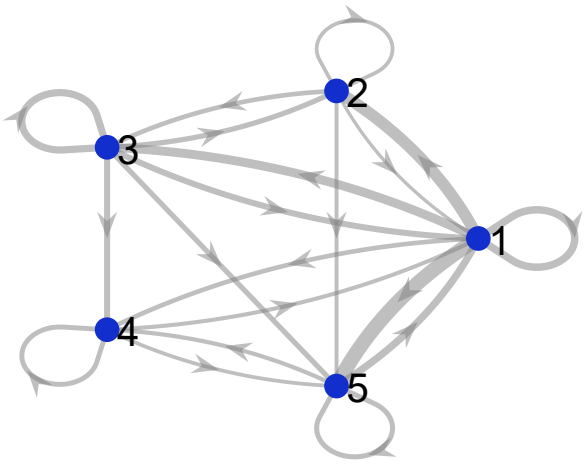

Figure 5.1: Interaction graph associated with the matrix $[\gamma]^{-1}W$, where W encodes the contact structure of the population and $[\gamma]^{-1}$ scales each node by its recovery rate.

The structure of the graph in Figure 5.1 highlights the heterogeneity of the effective transmission pathways induced by the matrix $[\gamma]^{-1}W$. Nodes associated with smaller recovery rates (i.e., larger entries in $[\gamma]^{-1}$) exert a proportionally stronger influence on their neighbors, resulting in highly asymmetric edge weights.
In this case, all the simulations are initialized from distinct initial condition for each population. Specifically, the initial infected and recovered fractions are given by

$$y(0) = (0.4,\, 0.2,\, 0.1,\, 0.5,\, 0.3),$$
$$z(0) = (0.1,\, 0.4,\, 0.2,\, 0.15,\, 0.2),$$

while the initial susceptible fractions are determined by the normalization condition

$$x(0) = \mathbf{1} - y(0) - z(0),$$

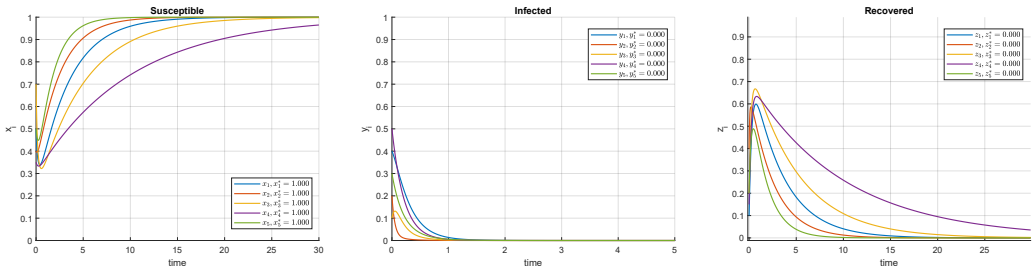

(a) Susceptible **(b)** Infected **(c)** Recovered

Figure 5.2: Time evolution of the susceptible, infected and recovered individuals for an SIRS model on a connected network composed of $n = 5$ populations in the case $\lambda_{\max} < 1$.

Figures 5.2a to 5.2c show that, independently of the initial conditions, the trajectories of all populations converge asymptotically to the disease-free equilibrium point $(x^*, y^*, z^*)_i = (1,0,0)$. This behavior indicates that the disease dies out in all nodes of the network. These observations are consistent with the theoretical analysis and confirm the global asymptotic stability of the disease-free equilibrium when $\lambda_{\max} < 1$, as established in Theorem 4.3.3. Figures 5.3a and 5.3b depict the temporal evolution of $\|y(t)\|$ for 20 different initial conditions, compared with the theoretical upper bound in (4.68). The semilogarithmic representation highlights the exponential convergence of the trajectories toward the bound.

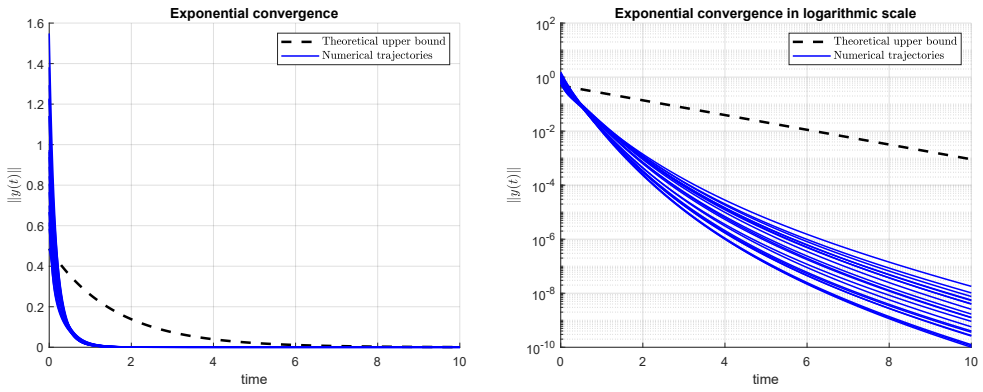

(a) Linear scale **(b)** Semilogarithmic scale.

Figure 5.3: Exponential decay of $\|y(t)\|$ for 20 initial conditions compared with the theoretical upper bound.

5.1.2 Case $\lambda_{\max} > 1$

In this case we consider the recovery rate vector:

$$\gamma = \begin{bmatrix} 0.5 & 2 & 1.5 & 0.5 & 0.7 \end{bmatrix}$$

so the matrix $[\gamma]^{-1}W$ is

$$[\gamma]^{-1}W = \begin{bmatrix} 3.0000 & 6.0000 & 4.0000 & 1.0000 & 8.0000 \\ 0.1000 & 0.4000 & 1.0000 & 0 & 0.5000 \\ 2.0000 & 1.4000 & 2.8000 & 2.0000 & 1.4000 \\ 0.6000 & 0 & 0 & 1.2000 & 0.4000 \\ 2.8571 & 0 & 0 & 0.7143 & 1.2857 \end{bmatrix}$$

whose dominant eigenvalue is $\lambda_{max} = 8.7434 > 1$, hence we are in case over threshold and from Corollary 4.2.7 we know that a unique endemic equilibrium exists. Since γ is chosen as γ in the previous section divided by 10, the structure of the interaction graph associated with $[\gamma]^{-1}W$ is just a rescaling of the one presented in fig. 5.1.

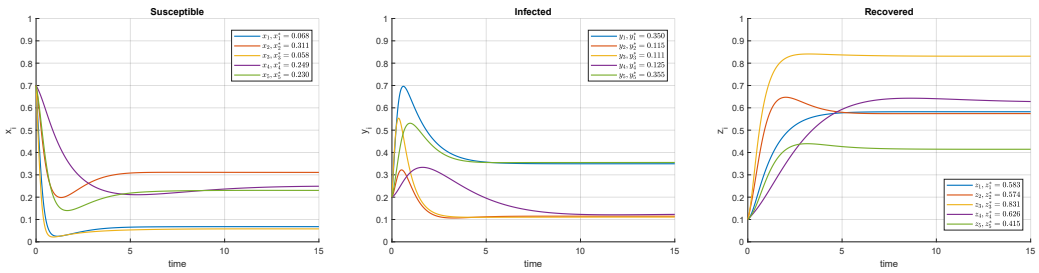

(a) Susceptible **(b)** Infected **(c)** Recovered

Figure 5.4: Time evolution of the susceptible, infected and recovered individuals for a SIRS model on a network composed of $n = 5$ populations in the case $\lambda_{\max} > 1$.

Figures 5.4a to 5.4c illustrate the behavior of the entire system when $\lambda_{\max} > 1$. All populations within the network were assigned the same initial conditions:

$$(x_i(0), y_i(0), z_i(0)) = (0.2, 0.1, 0.7) \quad \forall i$$

It can be observed that the reached equilibrium points depend on the interaction matrix W and the parameters vector γ and δ (which are specific to each population). For example, we can note that for the lowest parameters of δ (populations 3 and 4), the recovered fraction is higher at equilibrium, while population 1 and 5 that has the highest influences from the others, report the biggest number of infected. This behavior is not as simple as seems here, but it reflects the theoretical monotonicity investigated in Corollary 4.2.7.

In Figures 5.5a to 5.5c we performed six simulations and highlight the behavior of one single population. We can see that, for every initial condition in $\mathcal{X} \setminus \{y = \mathbf{0}\}$, the trajectories converge to the endemic equilibrium. Furthermore, we can notice that, if $(x(0), y(0), z(0)) \in \{y = \mathbf{0}\}$, than the trajectories converge to the disease free equilibrium, as expected from Theorem 4.3.6.

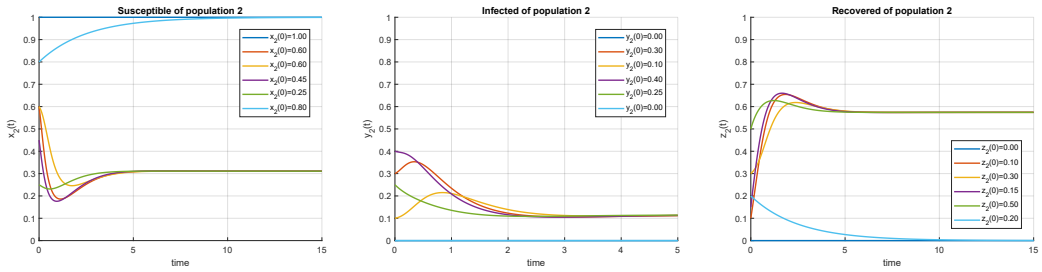

(a) Susceptible **(b)** Infected **(c)** Recovered

Figure 5.5: Time evolution of the susceptible, infected and recovered individuals in the second population for 6 different initial conditions. The blue and light blue curves correspond to initial condition in $\{y = \mathbf{0}\}$.

In figs. 5.6a to 5.6c every populations has initial condition

$$(x_i(0), y_i(0), z_i(0)) = (1,0,0)$$

except for the first one, whose initial condition is set to (0.99,0.01,0). We observe that even if the majority of the network populations are initially in a disease-free state, the interaction with a single infected population causes the others to transition out of the disease-free regime. As proved in Theorem 4.1.5, if a small fraction of infected individuals is present in one population, then, due to the connectivity of the system, every other population will reach a nonzero infected fraction. From the simulations, we can see that, in case $\lambda_{\max} > 1$, even if the system starts arbitrarily close to

the disease-free equilibrium $(\mathbf{1}, 0{,}0)$, its trajectories converge to the endemic equilibrium. These numerical results provide strong evidence in support of our theoretical conjecture about the quasi-global attractiveness of the endemic equilibrium point stated in Remark 4.3.7.

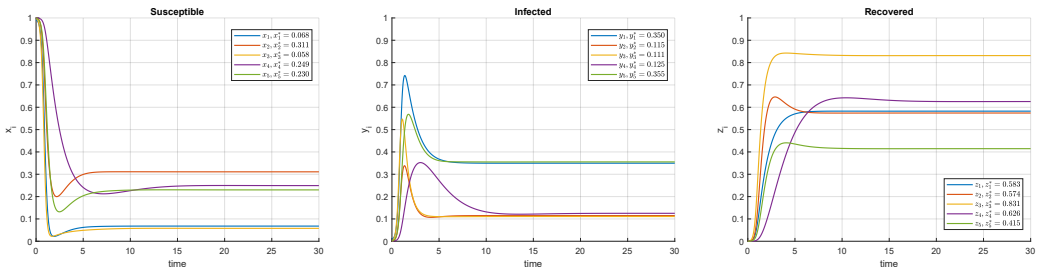

(a) Susceptible **(b)** Infected **(c)** Recovered

Figure 5.6: Time evolution of the susceptible 5.6a, infected 5.6b and recovered 5.6c individuals across the entire network in case $(x_1, y_1, z_1)(0) = (0.99{,}0.01{,}0)$ and $(x_i, y_i, z_i)(0) = (1{,}0{,}0)$ $\forall i \neq 1$.

Figures 5.7a and 5.7b, show the error decay behavior, evaluated as (4.69), discussed in Section 4.5. Simulations are obtain from 20 different initial conditions and the dotted line represents the upper bound derived from the proof of Theorem 4.3.5: the curve $Ce^{-\eta t}$.

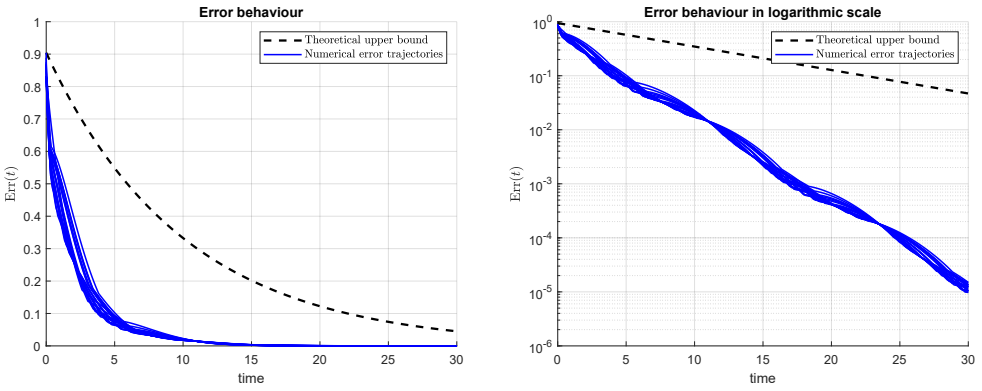

(a) Error decay for 20 different initial conditions.

(b) Logarithmic error decay for 20 different initial conditions.

Figure 5.7

5.2 Out-regular graph

In Example 4.2.9 we managed to find an explicit form for the endemic equilibrium taking assumption of the regularity of the graph. We now consider the special case in which the recovery and loss of immunity rates γ and δ are homogeneous within the populations. In this case, every subpopulations of the out-regular network admits the same equilibrium point (x^*, y^*, z^*).

$$W = \begin{bmatrix} 2.0000 & 2.1000 & 0 & 0 & 3.6000 \\ 0.3000 & 2.0000 & 0 & 0 & 5.4000 \\ 0 & 0 & 5.0050 & 0.3850 & 2.3100 \\ 3.0395 & 1.8237 & 0 & 2.8368 & 0 \\ 0 & 0 & 0.3500 & 1.0500 & 6.3000 \end{bmatrix} \tag{5.1}$$

$$\gamma = 2 \cdot \mathbf{1} \qquad \delta = 0.3 \cdot \mathbf{1} \tag{5.2}$$

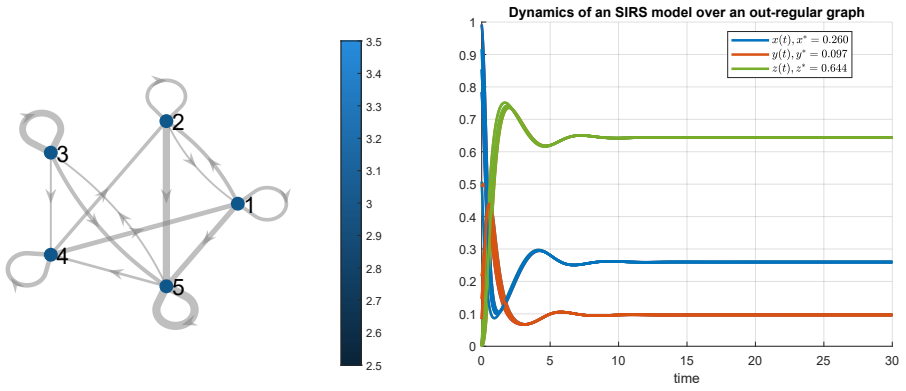

(a) Out-regular graph representation **(b)** Susceptible, Infected and Recovered individuals

Figure 5.8: Dynamics of an SIRS network model over an out-regular network of $n = 5$ populations with homogeneous recovery and loss of immunity rates, starting from different initial fraction of infected.

Figure 5.8a give us a graphical representation of the out-regular graph described by the interaction matrix W in (5.1). We can see that every node has the same color, meaning that the out-degree is the same for every

nodes. Assuming an out-regular contact network ensures that each node contributes equally to disease transmission in terms of outgoing contacts, thereby eliminating structural superspreading effects. This assumption over the network implies that, over threshold, the equilibrium point is homogeneous within the populations, such as in (4.35). This behavior is highlighted by Figure 5.8b, which shows the dynamical trajectories of susceptible, infected and recovered fractions of every populations starting from different initial fraction of infected.

We know that in case of an out-regular graph with homogeneous rates γ and δ, the endemic equilibrium point is homogeneous and it depends only on the dominant eigenvalue λ_W as in (4.35). We now consider three out-regular network with same $\lambda_W = 2$ described by the following matrices. In Figure 5.9 there is a representation of these graphs.

$$W_{comp} = \begin{pmatrix} 1 & \frac{1}{5} & \frac{1}{5} & \frac{1}{5} & \frac{1}{5} & \frac{1}{5} \\ \frac{1}{5} & 1 & \frac{1}{5} & \frac{1}{5} & \frac{1}{5} & \frac{1}{5} \\ \frac{1}{5} & \frac{1}{5} & 1 & \frac{1}{5} & \frac{1}{5} & \frac{1}{5} \\ \frac{1}{5} & \frac{1}{5} & \frac{1}{5} & 1 & \frac{1}{5} & \frac{1}{5} \\ \frac{1}{5} & \frac{1}{5} & \frac{1}{5} & \frac{1}{5} & 1 & \frac{1}{5} \\ \frac{1}{5} & \frac{1}{5} & \frac{1}{5} & \frac{1}{5} & \frac{1}{5} & 1 \end{pmatrix}, \quad W_{ring} = \begin{pmatrix} 1 & \frac{1}{2} & 0 & 0 & 0 & \frac{1}{2} \\ \frac{1}{2} & 1 & \frac{1}{2} & 0 & 0 & 0 \\ 0 & \frac{1}{2} & 1 & \frac{1}{2} & 0 & 0 \\ 0 & 0 & \frac{1}{2} & 1 & \frac{1}{2} & 0 \\ 0 & 0 & 0 & \frac{1}{2} & 1 & \frac{1}{2} \\ \frac{1}{2} & 0 & 0 & 0 & \frac{1}{2} & 1 \end{pmatrix} \tag{5.3}$$

$$W_{out} = \begin{pmatrix} 1 & 0.3 & 0 & 0 & 0 & 0.7 \\ 0.8 & 1 & 0.2 & 0 & 0 & 0 \\ 0 & 0 & 1 & 0 & 1 & 0 \\ 1 & 0 & 0 & 1 & 0 & 0 \\ 0 & 0 & 0 & 1 & 1 & 0 \\ 0.4 & 0 & 0.6 & 0 & 0 & 1 \end{pmatrix} \tag{5.4}$$

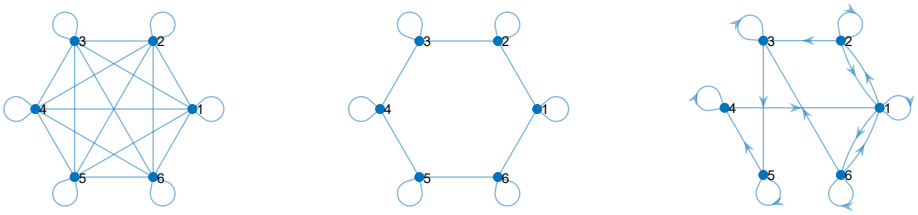

(a) Complete graph **(b)** Ring graph **(c)** Out-regular digraph

Figure 5.9: Representation of a 6 populations complete graph, ring graph and a generic out-regular digraph associated to the interaction matrix in (5.3),(5.4). 5.9a,5.9b are symmetrical graphs, while 5.9c is a directed graph.

Even if every system converges to the endemic equilibrium $y^* = \frac{\delta}{\delta+\gamma}\left(1 - \frac{1}{\lambda_{max}}\right)\mathbf{1}$, we note that the convergence happens in different ways. This behavior is shown both from the trajectories as in Figure 5.10 than from the trend of the norm-2 distance from the equilibrium point as in Figures 5.11 and 5.12.

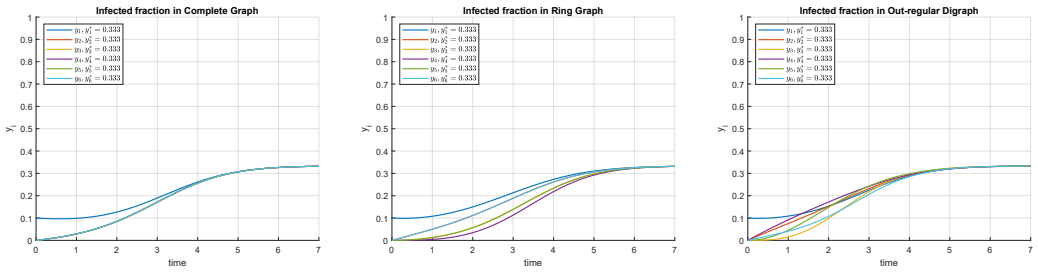

(a) Complete graph **(b)** Ring graph **(c)** Out-regular digraph

Figure 5.10: Infected fraction trajectories for three different out-regular network composed by $n = 6$ populations starting from the same initial condition $y_1(0) = 0.1$, $y_j(0) = 0$, for $j \in \{2, \cdots, 6\}$, $z_i(0) = 0$, for $i \in \{1, \cdots, 6\}$.

Convergence time for each population

5.9024	6.0074	6.0054
5.8384	5.9454	6.0254
5.9694	5.9534	6.0354
5.8334	5.9144	5.9534
5.8694	5.7934	5.8284
5.8364	5.8824	5.9814

Figure 5.11: Convergence time for each population to the endemic equilibrium point. Rows indicate nodes, while columns represent different outregular graph $W_{comp}, W_{ring}, W_{out}$ as in (5.3),(5.4). Threshold is fixed as 10^{-4}.

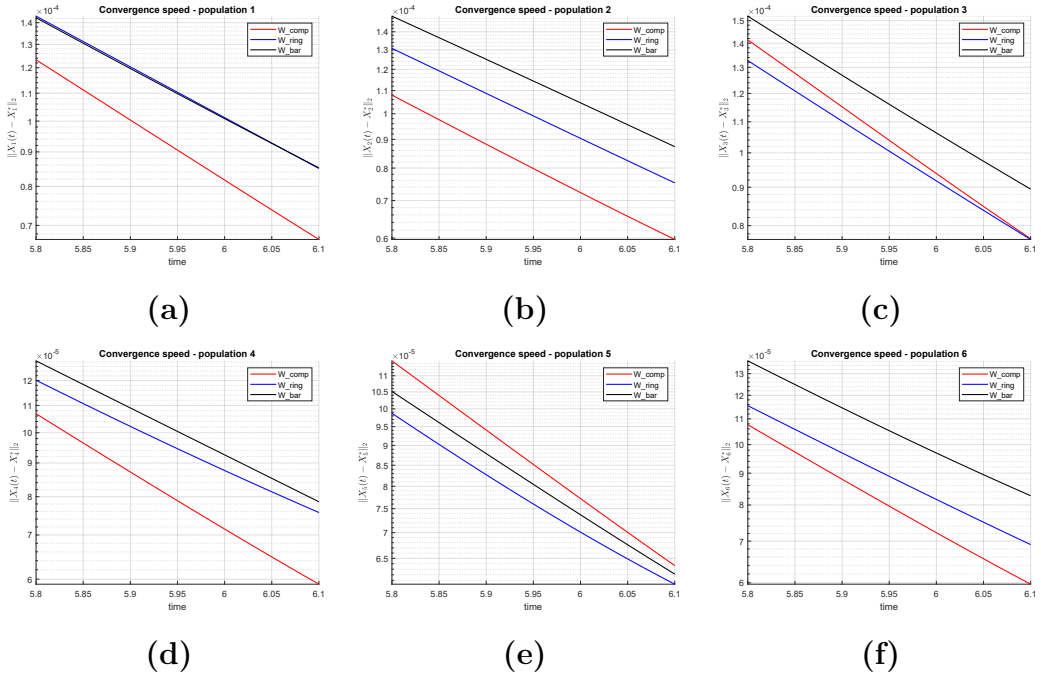

Figure 5.12: Euclidian norm $\|(x(t_k), y(t_k), z(t_k)) - (x^*, y^*, z^*)\|_2$ near the convergence time for each population. The convergence times correspond to those listed in Figure 5.11. In each panel the curves follow the same convergence order reported in Figure 5.11.

5.3 Dependence of the endemic equilibrium on W

Consider two graphs which share the same dominant eigenvalue λ_{max} associated to the matrices:

$$A = \begin{pmatrix} 1 & 1 & 0 & 0 \\ 0 & 1 & 2 & 0 \\ 0 & 0 & 1 & 3 \\ 4 & 0 & 0 & 1 \end{pmatrix} \qquad B = \begin{pmatrix} 1 & 2 & 0 & 0 \\ 0 & 1 & 3 & 0 \\ 0 & 0 & 1 & 12 \\ 4 & 0 & 0 & 1 \end{pmatrix} \tag{5.5}$$

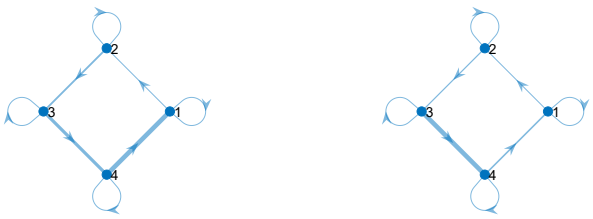

(a) **(b)**

Figure 5.13: Representation of the graphs associated with matrices A and B in (5.5). The two matrices share the dominant eigenvalue, but exhibit a different row distributions. This difference is visually reflected in the edge thickness, which is proportional to the (i, j)-entry of each matrix for every i and j nodes.

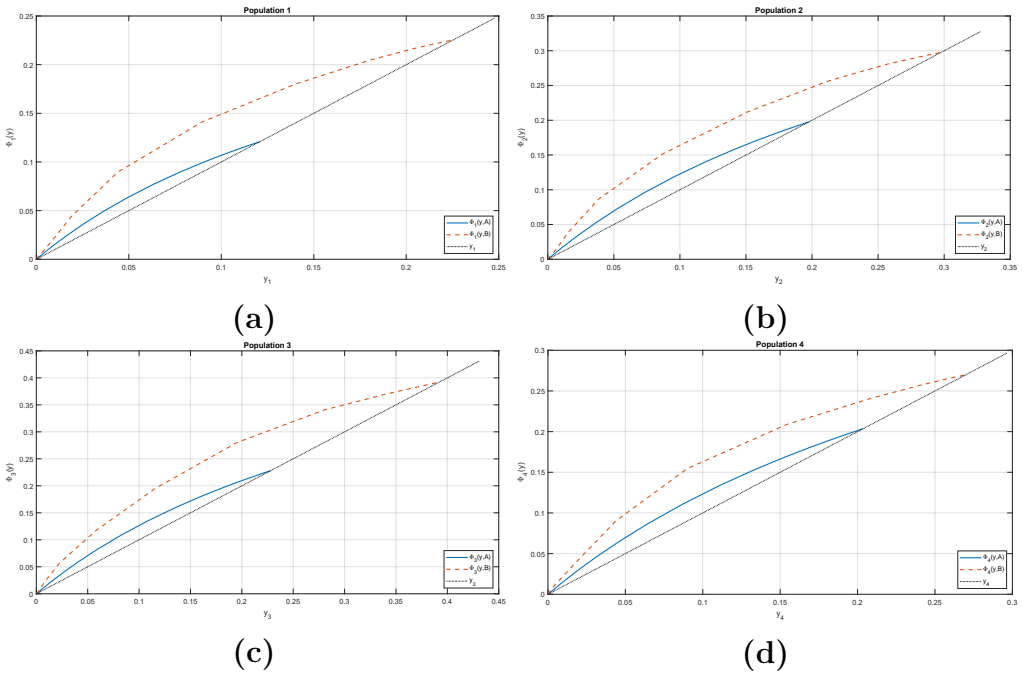

Figure 5.14: Plots of the components of $\Phi(y, [\gamma]^{-1}W)$ for different values of the rows of $[\gamma]^{-1}W$ and for each population. The fixed point is given by the intersection with the line y. As one row of $[\gamma]^{-1}W$ increases, the correspondent entry of the fixed point shifts to higher values, confirming the monotone dependence on $[\gamma]^{-1}W$ established in Corollary 4.2.7. This behavior is consistently observed across all populations.

5.4 Dependence of the endemic equilibrium on γ and δ.

Let A and B be two different graph matrices. Consider the ratio:

$$[\delta_A]^{-1}\gamma_A = \begin{pmatrix} 1 & \frac{1}{2} & \frac{3}{2} & \frac{1}{2} \end{pmatrix} \qquad [\delta_B]^{-1}\gamma_B = \begin{pmatrix} \frac{3}{2} & 1 & 2 & \frac{1}{2} \end{pmatrix} \tag{5.6}$$

The $[\gamma]^{-1}W$ matrices in this case are:

$$[\gamma]_A^{-1}A = [\gamma]_B^{-1}B = \begin{pmatrix} \frac{1}{2} & 1 & 0 & 0 \\ 0 & 2 & 1 & 3 \\ \frac{1}{3} & 0 & \frac{1}{3} & 0 \\ 3 & 0 & 0 & 1 \end{pmatrix} \tag{5.7}$$

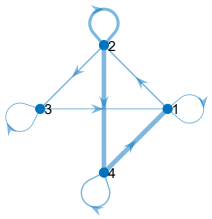

Figure 5.15: Representation of the interaction matrix in (5.7).

As shown in Corollary 4.2.7, the fixed point of the equation

$$\Phi(y, [\delta]^{-1}\gamma) = y$$

is monotonically decreasing with respect to the parameter $[\delta]^{-1}\gamma$. In particular, larger values of $[\gamma][\delta]^{-1}$ yield a lower equilibrium value y^*.

This behavior is confirmed by the numerical simulations reported in Figure 5.15. The plots of the components of H clearly show that the trajectories converge to lower fixed-point values as $[\delta]^{-1}\gamma$ increases, consistently with the analytical result established in Corollary 4.2.7.

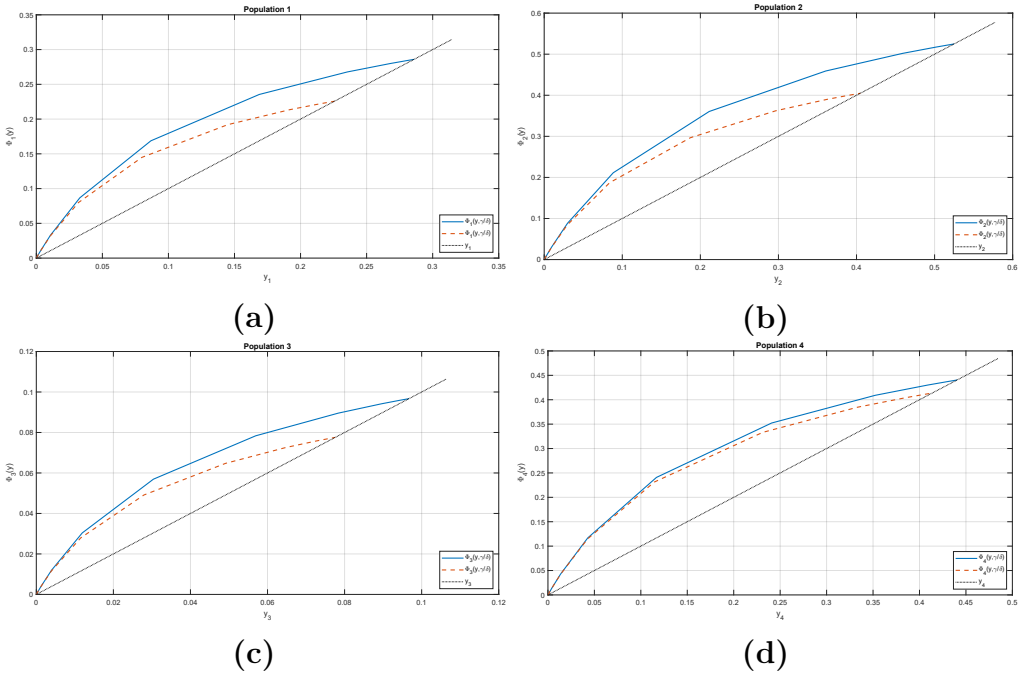

Figure 5.16: Plots of the components of $\Phi(y, [\delta]^{-1}\gamma)$ for different values of the parameter $[\delta]^{-1}\gamma$ and for each population. The fixed point is given by the intersection with the line y. As $[\delta]^{-1}\gamma$ increases, the fixed point shifts to lower values, confirming the monotone dependence on $[\delta]^{-1}\gamma$ established in Corollary 4.2.7. This behavior is consistently observed across all populations.

Conclusion

In this thesis, we have provided a rigorous dynamical analysis of the SIRS epidemic model defined on finite, strongly connected networks. Building upon the foundational material on classical compartmental models presented in Chapter 2 and the formulation of network-based epidemic models in Chapter 3, we focused on the network SIRS model as the central object of study in Chapter 4.

We first identified the epidemic threshold in terms of the basic reproduction number R_0, defined as the dominant eigenvalue of the rescaled interaction matrix. Above this threshold, we proved the existence and uniqueness of an endemic equilibrium $y^* > 0$ using fixed point theory in Theorem 4.2.6. Below the threshold, we established the global asymptotic stability of the disease-free equilibrium in Theorem 4.3.3, thereby extending classical epidemic results to the structured network setting.

The main contribution of this work is the analysis of the stability of the endemic equilibrium above threshold. Using algebraic properties of the Schur complement, we derived a negative upper bound for the real parts of the eigenvalues of the Jacobian at the endemic equilibrium in Theorem 4.3.5, which yields its local asymptotic stability and provides an explicit estimate for the exponential convergence rate. Over the threshold, we proved that the disease-free equilibrium is unstable and its basin of attraction coincides with the hyperplane $\{y = 0\}$. In Chapter 5 we perform some simulations which allows us to make a conjecture over the basin of attraction of the endemic equilibrium point. We shown in these numerical simulations that the trajectories starting out from the hyperplane $\{y = 0\}$ converge to the endemic equilibrium. Even if we could not manage to find a suitable Lyapunov function proving this conjecture, this behavior is the same as the one presented in the scalar case.

We explored also two special network structures: the out-regular graph

and the rank-1 graph. In the first case, the assumption that every node has the same out-degree, which in epidemiological field means that every population has the same possibility of being infected, allowed us to explicitly express the endemic equilibrium. In the case of a rank-1 interaction matrix, we revisited the quasi-global stability result obtained in [63] constructing a suitable Lyapunov function. This offers additional insight into the basin of attraction of the endemic equilibrium in the general case.

In Chapter 5 we performed some numerical results which confirm the theoretical analysis made before. We also pointed out that, in the out-regular case, even if the trajectories converge to the same equilibrium point, different graphs with same dominant eigenvalues show different transient. Furthermore, we presented in this section a confirm of the dependence of the endemic equilibrium on the interaction matrix and on the recovery and loss of immunity rates.

Several open questions remain. A primary theoretical challenge is to prove analytically that the basin of attraction of the endemic equilibrium indeed comprises the entire state space, excluding only the invariant hyperplane $\{y = \mathbf{0}\}$. Another important direction is to investigate the effects of an external forcing term, which, epidemiologically, models the continuous introduction of infections from outside the network, and to characterize how such a forcing influences threshold dynamics and stability properties.

In summary, this thesis deepens the understanding of SIRS epidemic dynamics on networks by integrating rigorous analysis with computational evidence. The findings not only extend classical scalar epidemic theory to heterogeneous contact structures but also provide a solid foundation for future analytical and applied research on network-based infectious disease models.

Appendix A

Appendix A

A.1 Schur complement

Definition A.1.1. For a block matrix A

$$A = \begin{pmatrix} A_{11} & A_{12} \\ A_{21} & A_{22} \end{pmatrix}$$

with A_{22} invertible, the Schur complement of the block A_{22} is

$$S = A_{11} - A_{12}A_{22}^{-1}A_{21} \tag{A.1}$$

Proposition A.1.2. *For a block matrix A, the Schur complement $S(A)$ has the following property:*

$$\det(A) = \det(A_{22})\det(S) \tag{A.2}$$

A.2 Spectral properties of rank-1 matrix

In general, a square matrix $W \in \mathbb{R}^{n\times n}$ has $\operatorname{rank}(W) = 1$ if and only if $W = ab^\top$ for some nonzero vectors $a, b \in \mathbb{R}^n$.

Proposition A.2.1. *Let $W = ab^\top$ be a square non-negative matrix with $a, b \in \mathbb{R}^n$, $a \neq 0$, $b \neq 0$. Then W has a unique nonzero eigenvalue $\mu_W =$*

$\mathrm{Tr}(W) = b^\top a$, *and the corresponding eigenvector is* a.

Proof. Since $\mathrm{rank}(W) = 1$, the matrix W has exactly one nonzero eigenvalue, with algebraic multiplicity one, while 0 has multiplicity $n-1$. Moreover,

$$Wa = ab^\top a = (b^\top a)\, a = \mathrm{Tr}(W)\, a. \tag{A.3}$$

Therefore, a is an eigenvector associated with the unique nonzero eigenvalue $\mu_W = \mathrm{Tr}(W)$. □

A.3 Gershgorin Theorem

Theorem A.3.1 (Gershgorin)**.** *([75], Theorem 6.1.1) Let* $A \in \mathbb{C}^{nxn}$*, let*

$$R_k(A) = \sum_{j \neq k} |a_{kj}|, \qquad k = 1, \cdots, n \tag{A.4}$$

denote the deleted absolute row sums of A*, and consider the* n *Gersgorin discs*

$$B_{R_k} = \{z \in \mathbb{C} : |z - a_{kk}| \leq R_k(A)\} \quad k = 1, \cdots, n$$

The eigenvalues of A *are in the union of Gersgorin discs:*

$$G(A) = \bigcup_{k=1}^{n} B_{R_k} = \bigcup_{k=1}^{n} \{z \in \mathbb{C} : |z - a_{kk}| \leq R_k(A)\} \tag{A.5}$$

Bibliography

[1] Daniel Bernoulli. «Essai d'une nouvelle analyse de la mortalité causée par la petite vérole, et des avantages de l'inoculation pour la prévenir». In: *Mém. Math. Phys. Acad. Roy. Sci. Paris* (1760) (cit. on p. 3).

[2] William Farr. «Influence of Elevation on the Fatality of Cholera». In: *Quarterly Journal of the Statistical Society of London* 15 (1852), pp. 155–183. DOI: 10.2307/2338305 (cit. on p. 3).

[3] John Snow. *On the Mode of Communication of Cholera*. 2nd. London: John Churchill, 1855 (cit. on p. 3).

[4] William Heaton Hamer. «The Milroy Lectures on Epidemic Diseases in England: The Evidence of Variability and Persistency of Type». In: *The Lancet* (1906) (cit. on p. 3).

[5] Ronald Ross. *The Prevention of Malaria*. John Murray, 1911 (cit. on p. 3).

[6] W. O. Kermack and A. G. McKendrick. «A contribution to the mathematical theory of epidemics». In: *Proceedings of the Royal Society of London. Series A* 115.772 (1927), pp. 700–721 (cit. on p. 4).

[7] William O. Kermack and Anderson G. McKendrick. «Contributions to the Mathematical Theory of Epidemics. II. The Problem of Endemicity». In: *Proceedings of the Royal Society A* 138 (1932), pp. 55–83 (cit. on p. 4).

[8] William O. Kermack and Anderson G. McKendrick. «Contributions to the Mathematical Theory of Epidemics. III. Further Studies of the Problem of Endemicity». In: *Proceedings of the Royal Society A* 141 (1933), pp. 94–122 (cit. on p. 4).

[9] Roy M. Anderson and Robert M. May. *Infectious Diseases of Humans: Dynamics and Control*. Oxford: Oxford University Press, 1991. ISBN: 978-0198540403 (cit. on p. 4).

[10] B. T. Grenfell. «Chance and Chaos in Measles Dynamics». In: *Journal of the Royal Statistical Society: Series B (Methodological)* 54.2 (1992), pp. 383–398. URL: https://doi.org/10.1111/j.2517-6161.1992.tb01888.x (cit. on p. 4).

[11] O. Diekmann and J. A. P. Heesterbeek. *Mathematical Epidemiology of Infectious Diseases: Model Building, Analysis and Interpretation*. Wiley, 2000 (cit. on pp. 4, 5).

[12] Kenneth L Cooke and James A Yorke. «Some equations modelling growth processes and gonorrhea epidemics». In: *Mathematical Biosciences* 16.1-2 (1973), pp. 75–101 (cit. on p. 4).

[13] Herbert W Hethcote. «Asymptotic behavior in a deterministic epidemic model». In: *Bulletin of Mathematical Biology* 35 (1973), pp. 607–614 (cit. on p. 4).

[14] Geoffrey P. Garnett and Roy M. Anderson. «Sexually Transmitted Diseases And Sexual Behavior: Insights From Mathematical Models». In: *The Journal of Infectious Diseases* 174.Supplement$_2$ (Oct. 1996), S150–S161. ISSN: 0022-1899. DOI: 10.1093/infdis/174.Supplement_2.S150. URL: https://doi.org/10.1093/infdis/174.Supplement_2.S150 (cit. on p. 4).

[15] George Macdonald. *The Epidemiology and Control of Malaria*. Oxford University Press, 1957 (cit. on p. 4).

[16] Odo Diekmann, Johan Andre Peter Heesterbeek, and Johan Anton Jacob Metz. «On the definition and the computation of the basic reproduction ratio R 0 in models for infectious diseases in heterogeneous populations». In: *Journal of mathematical biology* 28.4 (1990), pp. 365–382 (cit. on p. 5).

[17] Klaus Dietz. «The estimation of the basic reproduction number for infectious diseases». In: *Statistical methods in medical research* 2.1 (1993), pp. 23–41 (cit. on p. 5).

[18] JAP Heesterbeek and Klaus Dietz. «The concept of Ro in epidemic theory». In: *Statistica neerlandica* 50.1 (1996), pp. 89–110 (cit. on p. 5).

[19] Johan Andre Peter Heesterbeek. «A brief history of R 0 and a recipe for its calculation». In: *Acta biotheoretica* 50.3 (2002), pp. 189–204 (cit. on p. 5).

[20] John A Jacquez, Carl P Simon, and JS Koopman. «The reproduction number in deterministic models of contagious diseases». In: *Comment. Theor. Biol* 2 (1991) (cit. on p. 5).

[21] Horst R Thieme. *Mathematics in population biology*. Princeton University Press, 2018 (cit. on p. 5).

[22] Pauline Van den Driessche and James Watmough. «Reproduction numbers and sub-threshold endemic equilibria for compartmental models of disease transmission». In: *Mathematical biosciences* 180.1-2 (2002), pp. 29–48 (cit. on p. 5).

[23] Béla Bollobás. *Graph theory*. Vol. 1. Elsevier, 1982 (cit. on pp. 5, 30).

[24] Frank Harary. *Graph Theory*. Reading, MA: Addison-Wesley, 1969 (cit. on p. 5).

[25] Håkan Andersson. «Epidemic models and social networks». In: *Mathematical Scientist* 24.2 (1999), pp. 128–147 (cit. on p. 5).

[26] Leon Danon, Ashley P. Ford, Thomas House, Chris P. Jewell, Matt J. Keeling, Gareth O. Roberts, Joshua V. Ross, and Matthew C. Vernon. «Networks and the epidemiology of infectious disease». In: *Interdisciplinary Perspectives on Infectious Diseases* 2011 (2011), pp. 1–28. DOI: 10.1155/2011/284909 (cit. on p. 5).

[27] Fred Brauer. «Mathematical epidemiology: Past, present, and future». In: *Infectious Disease Modelling* 2.2 (2017), pp. 113–127. DOI: 10.1016/j.idm.2017.02.001 (cit. on pp. 5, 6).

[28] Lorenzo Zino and Ming Cao. «Analysis, Prediction, and Control of Epidemics: A Survey from Scalar to Dynamic Network Models». In: *IEEE Circuits and Systems Magazine* 21.2 (2021), pp. 4–24. DOI: 10.1109/MCAS.2021.3074055 (cit. on p. 5).

[29] A. Lajmanovich and J. A. Yorke. «A deterministic model for gonorrhea in a nonhomogeneous population». In: *Mathematical Biosciences* 28.3-4 (1976), pp. 221–236 (cit. on p. 5).

[30] Oskar Perron. «Zur theorie der matrices». In: *Mathematische Annalen* 64.2 (1907), pp. 248–263 (cit. on pp. 5, 32).

[31] Georg Frobenius. «Über Matrizen aus positiven Elementen». In: *Sitzungsberichte der Königlich Preussischen Akademie der Wissenschaften* 1 (1908), pp. 471–476 (cit. on pp. 5, 32).

[32] Georg Frobenius. «Über Matrizen aus positiven Elementen, 2». In: *Sitzungsberichte der Königlich Preussischen Akademie der Wissenschaften* 2 (1909), pp. 514–518 (cit. on pp. 5, 32).

[33] Georg Frobenius. «Über Matrizen aus nicht negativen Elementen». In: *Sitzungsberichte der Königlich Preussischen Akademie der Wissenschaften* (1912), pp. 456–477 (cit. on pp. 5, 32).

[34] Joseph P. LaSalle. *The Stability of Dynamical Systems*. Philadelphia: Society for Industrial and Applied Mathematics, 1976. ISBN: 978-0898711857 (cit. on p. 5).

[35] Gunnar Aronsson and Ingvar Mellander. «A deterministic model in biomathematics. Asymptotic behavior and threshold conditions». In: *Mathematical Biosciences* 49.3-4 (1980), pp. 207–222 (cit. on p. 5).

[36] R Nallaswamy and JB Shukla. «Effects of dispersal on the stability of a gonorrhea endemic model». In: *Mathematical Biosciences* 61.1 (1982), pp. 63–72 (cit. on p. 5).

[37] Horst R Thieme. «Global asymptotic stability in epidemic models». In: *Equadiff 82: Proceedings of the international conference held in Würzburg, FRG, August 23–28, 1982*. Springer. 2006, pp. 608–615 (cit. on p. 5).

[38] Herbert W Hethcote, James A Yorke, and Annett Nold. «Gonorrhea modeling: a comparison of control methods». In: *Mathematical Biosciences* 58.1 (1982), pp. 93–109 (cit. on p. 5).

[39] Kenneth L Cooke. «Models for endemic infections with asymptomatic cases. I. One group». In: *Mathematical Modelling* 3.1 (1982), pp. 1–15 (cit. on p. 6).

[40] Annett Nold. «Heterogeneity in disease-transmission modeling». In: *Mathematical biosciences* 52.3-4 (1980), pp. 227–240 (cit. on pp. 6, 8).

[41] A. Fall, A. Iggidr, G. Sallet, and J. J. Tewa. «Epidemiological Models and Lyapunov Functions». In: *Mathematical Modelling of Natural Phenomena* 2.1 (2007), pp. 62–83. DOI: 10.1051/mmnp:2008011 (cit. on pp. 6, 38).

[42] Zhisheng Shuai and P. van den Driessche. «Global Stability of Infectious Disease Models Using Lyapunov Functions». In: *SIAM Journal on Applied Mathematics* 73.4 (2013), pp. 1513–1532. DOI: 10.1137/120876642. URL: https://doi.org/10.1137/120876642 (cit. on p. 6).

[43] P. Cisneros-Velarde and F. Bullo. «Multigroup SIS Epidemics with Simplicial and Higher Order Interactions». In: *IEEE Transactions on Control of Network Systems* 9.2 (2021), pp. 695–705 (cit. on p. 6).

[44] W. Xuan, R. Ren, P. E. Paré, M. Ye, S. F. Ruf, and J. Liu. «On a Network SIS Model with Opinion Dynamics». In: *IFAC-PapersOnLine* 53 (2020), pp. 2582–2587 (cit. on p. 6).

[45] K. Paarporn, C. Eksin, J. S. Weitz, and J. S. Shamma. «Networked SIS epidemics with awareness». In: *IEEE Transactions on Computational Social Systems* 4.3 (2017), pp. 93–103 (cit. on p. 6).

[46] B. D. O. Anderson and M. Ye. «Equilibria Analysis of a Networked Bivirus Epidemic Model Using Poincaré–Hopf and Manifold Theory». In: *SIAM Journal on Applied Dynamical Systems* 22.4 (2023), pp. 2856–2889 (cit. on p. 6).

[47] J. Liu, P. E. Paré, A. Nedić, C. Tang, C. L. Beck, and T. Başar. «Analysis and Control of a Continuous-Time Bi-Virus Model». In: *IEEE Transactions on Automatic Control* 64.12 (2019), pp. 4891–4906 (cit. on p. 6).

[48] Hyoung Jun Ahn and Babak Hassibi. *Global dynamics of epidemic spread over complex networks*. 2013, pp. 4579–4585. DOI: 10.1109/CDC.2013.6760600 (cit. on p. 6).

[49] Ali Khanafer, Tamer Başar, and Bahman Gharesifard. «Stability of epidemic models over directed graphs: A positive systems approach». In: *Automatica* 74 (2016), pp. 126–134 (cit. on p. 6).

[50] V. Capasso and G. Serio. «A generalization of the Kermack-McKendrick deterministic epidemic model». In: *Mathematical Biosciences* 42.1 (1978), pp. 43–61. ISSN: 0025-5564. DOI: https://doi.org/10.1016/0025-5564(78)90006-8 (cit. on p. 6).

[51] R. Pastor-Satorras, C. Castellano, P. Van Mieghem, and A. Vespignani. «Epidemic Processes in Complex Networks». In: *Reviews of Modern Physics* 87 (2015), pp. 925–979 (cit. on p. 6).

[52] P. E. Paré, C. L. Beck, and T. Başar. «Modeling, Estimation, and Analysis of Epidemics over Networks: An Overview». In: *Annual Reviews in Control* 50 (2020), pp. 345–360 (cit. on p. 6).

[53] L. Zino and M. Cao. «Analysis, Prediction, and Control of Epidemics: A Survey from Scalar to Dynamic Network Models». In: *IEEE Circuits and Systems Magazine* 21.4 (2021), pp. 4–23. DOI: 10.1109/MCAS.2021.3118100 (cit. on p. 6).

[54] H. W Hethcote. «An immunization model for a heterogeneous population». In: *Theoretical population biology* 14.3 (1978), pp. 338–349 (cit. on p. 6).

[55] C. Nowzari, V. M. Preciado, and G. J. Pappas. «Analysis and Control of Epidemics: A Survey of Spreading Processes on Complex Networks». In: *IEEE Control Systems Magazine* 36.1 (2016), pp. 26–46 (cit. on p. 6).

[56] W. Mei, S. Mohagheghi, S. Zampieri, and F. Bullo. «On the dynamics of deterministic epidemic propagation over networks». In: *Annual Reviews in Control* 44 (2017), pp. 116–128 (cit. on pp. 6, 33).

[57] M. Ogura and V. M. Preciado. «Stability of Spreading Processes over Time-Varying Large-Scale Networks». In: *IEEE Transactions on Network Science and Engineering* 3 (2016), pp. 44–57 (cit. on p. 6).

[58] Martina Alutto, Leonardo Cianfanelli, Giacomo Como, and Fabio Fagnani. «On the dynamic behavior of the network sir epidemic model». In: *IEEE Transactions on Control of Network Systems* (2024) (cit. on p. 6).

[59] Wei-min Liu, Simon A Levin, and Yoh Iwasa. «Influence of nonlinear incidence rates upon the behavior of SIRS epidemiological models». In: *Journal of mathematical biology* 23.2 (1986), pp. 187–204 (cit. on pp. 7, 14).

[60] Y. Jin, W. Wang, and S. Xiao. «An SIRS model with a nonlinear incidence rate». In: *Chaos, Solitons & Fractals* 34 (Dec. 2007), pp. 1482–1497. DOI: 10.1016/j.chaos.2006.04.022 (cit. on pp. 7, 14).

[61] A. Korobeinikov and G.C. Wake. «Lyapunov functions and global stability for SIR, SIRS, and SIS epidemiological models». In: *Applied Mathematics Letters* 15.8 (2002), pp. 955–960. ISSN: 0893-9659. DOI: https://doi.org/10.1016/S0893-9659(02)00069-1. URL: https://www.sciencedirect.com/science/article/pii/S0893965902000691 (cit. on pp. 7, 14).

[62] Cruz Vargas-De-León. «Constructions of Lyapunov functions for classic SIS, SIR and SIRS epidemic models with variable population size». In: *Foro-Red-Mat: Revista electrónica de contenido matemático* 26.5 (2009), pp. 1–12 (cit. on p. 7).

[63] C. Li, C. Tsai, and S. Yang. «Analysis of epidemic spreading of an SIRS model in complex heterogeneous networks». In: *Communications in Nonlinear Science and Numerical Simulations* 19 (2014), pp. 1042–1054. DOI: 10.1016/j.cnsns.2013.08.033 (cit. on pp. 7, 8, 77, 95).

[64] Lijuan Chen and Jitao Sun. «Global stability and optimal control of an SIRS epidemic model on heterogeneous networks». In: *Physica A: Statistical Mechanics and its Applications* 410 (2014), pp. 196–204 (cit. on pp. 7–9).

[65] Yuexia Zhang and Dawei Pan. «Layered SIRS model of information spread in complex networks». In: *Applied Mathematics and Computation* 411 (2021), p. 126524 (cit. on p. 7).

[66] M Ali Saif. «Epidemic threshold for the SIRS model on the networks». In: *Physica A: Statistical Mechanics and its Applications* 535 (2019), p. 122251 (cit. on p. 8).

[67] Lijun Liu, Xiaodan Wei, and Naimin Zhang. «Global stability of a network-based SIRS epidemic model with nonmonotone incidence rate». In: *Physica A* 515 (2019), pp. 587–599. DOI: 10.1016/j.physa.2018.09.161 (cit. on p. 8).

[68] Herbert Hethcote and James Yorke. *Gonorrhea Transmission Dynamics and Control*. Vol. 56. Jan. 1984. Chap. 3.2, pp. 29–31. ISBN: 978-3-540-13870-9. DOI: 10.1007/978-3-662-07544-9 (cit. on p. 8).

[69] Fred Brauer, Carlos Castillo-Chavez, and Carlos Castillo-Chavez. *Mathematical models in population biology and epidemiology*. Vol. 2. 10. Springer, 2012 (cit. on p. 12).

[70] H. W. Hethcote. «The Mathematics of Infectious Diseases». In: *SIAM Review* 42 (2000), pp. 599–653 (cit. on p. 13).

[71] Jianhong Wu Fred Brauer Pauline Driessche. *Mathematical Epidemiology*. Springer Berlin, Heidelberg, 2008 (cit. on p. 14).

[72] Steven H. Strogatz. *Nonlinear Dynamics and Chaos: With Applications to Physics, Biology, Chemistry, and Engineering*. 3rd. Chapman and Hall/CRC, 2024. DOI: 10.1201/9780429398490. URL: https://doi.org/10.1201/9780429398490 (cit. on p. 21).

[73] Abraham Berman and Robert J. Plemmons. *Nonnegative Matrices in the Mathematical Sciences*. Classics in Applied Mathematics. Philadelphia: SIAM, 1994. ISBN: 9780898713217 (cit. on pp. 30–32).

[74] A. Fall, A. Iggidr, G. Sallet, and J. J. Tewa. «Epidemiological Models and Lyapunov Functions». In: *Mathematical Modelling of Natural Phenomena* 2.1 (2007), pp. 62–83. DOI: 10.1051/mmnp:2008011 (cit. on p. 67).

[75] Roger A. Horn and Charles R. Johnson. *Matrix Analysis*. 2nd. Cambridge, New York, Melbourne, Madrid, Cape Town, Singapore, São Paulo, Delhi, Mexico City: Cambridge University Press, 2013. ISBN: 978-0-521-83940-2 (cit. on p. 97).